Scientific Excellence • Resource Protection & Conservation • Benefits for Canadians
Excellence scientifique • Protection et conservation des ressources • Bénéfices aux Canadiens

Flow Dynamics of the Campbell River Estuary

A.B. Ages
A.L. Woollard

Institute of Ocean Sciences
Department of Fisheries and Oceans
Sidney, B.C.

1991

Canadian Technical Report of Hydrography and Ocean Sciences No. 130

Fisheries and Oceans Pêches et Océans

Canada

Canadian Technical Report of Hydrography and Ocean Sciences

These reports contain scientific and technical information of a type that represents a contribution to existing knowledge but which is not normally found in the primary literature. The subject matter is generally related to programs and interests of the Ocean Science and Surveys (OSS) sector of the Department of Fisheries and Oceans.

Technical Reports may be cited as full publications. The correct citation appears above the abstract of each report. Each report will be abstracted in Aquatic Sciences and Fisheries Abstracts. Reports are also listed in the Department's annual index to scientific and technical publications.

Technical Reports are produced regionally but are numbered and indexed nationally. Requests for individual reports will be fulfilled by the issuing establishment listed on the front cover and title page. Out of stock reports will be supplied for a fee by commercial agents.

Regional and headquarters establishments of Ocean Science and Surveys ceased publication of their various report series as of December 1981. A complete listing of these publications and the last number issued under each title are published in the *Canadian Journal of Fisheries and Aquatic Sciences,* Volume 38: Index to Publications 1981. The current series began with Report Number 1 in January 1982.

Rapport technique canadien sur l'hydrographie et les sciences océaniques

Ces rapports contiennent des renseignements scientifiques et techniques qui constituent une contribution aux connaissances actuelles mais que l'on ne trouve pas normalement dans les revues scientifiques. Le sujet est généralement rattaché aux programmes et intérêts du service des Sciences et Levés océaniques (SLO) du ministère des Pêches et des Océans.

Les rapports techniques peuvent être considérés comme des publications à part entière. Le titre exact figure au-dessus du résumé du chaque rapport. Les résumés des rapports seront publiés dans la revue Résumés des sciences aquatiques et halieutiques et les titres figureront dans l'index annuel des publications scientifiques et techniques du Ministère.

Les rapports techniques sont produits à l'échelon régional mais sont numérotés et placés dans l'index à l'échelon national. Les demandes de rapports seront satisfaites par l'établissement auteur dont le nom figure sur la couverture et la page de titre. Les rapports épuisés seront fournis contre rétribution par des agents commerciaux.

Les établissements des Sciences et Levés océaniques dans les régions et à l'administration centrale ont cessé de publier leurs diverses séries de rapports depuis décembre 1981. Vous trouverez dans l'index des publications du volume 38 du *Journal canadien des sciences halieutiques et aquatiques,* la liste de ces publications ainsi que le dernier numéro paru dans chaque catégorie. La nouvelle série a commencé avec la publication du Rapport n° 1 en janvier 1982.

Canadian Technical Report of
Hydrography and Ocean Sciences No. 130
1991

FLOW DYNAMICS OF THE CAMPBELL RIVER ESTUARY

A.B. Ages
A.L. Woollard

Institute of Ocean Sciences
Department of Fisheries and Oceans
Sidney, B.C.

Cat. No. FS 97-18/130 ISSN 0711-6764

Correct citation for this publication:

Ages, A.B. and A.L. Woollard, 1991. Flow Dynamics of the Campbell River Estuary. Can. Tech. Rep. Hydrog. Ocean Sci. No. 130: 97 pp.

CONTENTS

ACKNOWLEDGEMENTS

The large number of data required for this analysis was collected jointly with the staff of the Pacific Biological Station in Nanaimo. We acknowledge their generous help and, in particular, appreciate the guidance of Dr. Carey McAllister. We also thank Alexandra Dobbs for her able assistance in the field and for her artistic interpretation of the salinity and current distribution in the main channel of the Campbell River Estuary in Appendix A.

Dr. Rick Thomson spent much of his valuable time reviewing the report and we appreciate his professional scrutiny and his constructive criticism.

We are indebted to Rosalie Rutka for the compilation and TEX-setting of the report and for her sketches, as well as to Joan Cahill for her contribution in illustrating both this report and the preceding technical report.

Egalement, nous remercions Diane Masson pour le temps qu'elle a bien voulu nous consacrer en corrigeant notre version française du résumé.

Finally, our thanks to Sharon Thomson, who did the proof-reading and assisted in the publication.

ABSTRACT

Ages, A.B. and A.L. Woollard, 1991. Flow Dynamics of the Campbell River Estuary. Can. Tech. Rep. Hydrogr. Ocean Sci. No. 130: 97 pp.

An analysis of the physical oceanography in the Campbell River estuary was carried out to support a habitat assessment for juvenile salmon. In this report, we discuss the interaction between tides and discharges and their effect upon the movement of the salt wedge, and examine conditions which would generate mixing across the halocline. Other aspects of the salinity intrusion such as its upstream limit and the effect of the topography upon the salinity distribution are discussed. Finally, we present a method to compute volume transport of salt water by combining a split one-dimensional numerical model with observed salinity profiles.

Keywords: Campbell River estuary, salinity intrusion, volume transport.

RESUME

Ages, A.B. and A.L. Woollard, 1991. Flow Dynamics of the Campbell River Estuary. Can. Tech. Rep. Hydrogr. Ocean Sci. No. 130: 97 pp.

Une analyse de l'océanographie physique de l'estuaire de la rivière Campbell a été entreprise afin de soutenir une évaluation de l'habitat des saumons juvéniles. Ce rapport examine l'interaction entre les marées et les débits et leur effet sur le mouvement du coin salé, et ensuite les conditions qui produisent le mélange vertical à travers l'halocline. D'autres aspects de l'intrusion saline sont décrits, comme la pénétration maximale en amont, et l'effet de la topographie sur la distribution de la salinité. Enfin, nous soumettons une méthode de calcul du transport de volume d'eau salée qui combine un modèle mathématique unidimensional divisé en deux avec des profils observés de la salinité.

Mot-Clés: estuaire de la rivière Campbell, intrusion saline, transport de volume.

THIS PAGE IS BLANK

INTRODUCTION

Since it was first logged in 1900, the Campbell River estuary on the east coast of Vancouver Island, has provided the forest industry with a large and protected basin for log storage, leading to the establishment of several lumber mills in the area. However, the seaward reaches of the river are also the spawning grounds for chinook salmon, making the Campbell River one of the most popular centres for sport fishermen along the coast. Farther upstream, the Quinsam tributary is the site of a large hatchery which annually produces several million chinook, coho and pink salmon. Logging and fisheries are equal in their support of the local economy, and the environmental impact of the logging industry in this sensitive area has been of concern to a variety of government agencies.

British Columbia Forest Products (now Fletcher Challenge) carried out an environmental enhancement project in the early 1980s, building a dry log sorting area and creating an adjoining storage basin. Upon the completion of the project, the Pacific Biological Station (PBS) in Nanaimo examined the effects of these changes and approached the Institute of Ocean Sciences (IOS) in Patricia Bay to assist with a study of the tides and currents in the estuary. Particular interest was on the salinity intrusion. PBS and IOS staff measured currents, tides, salinities, temperatures and wind velocities at regular intervals from 1984 to 1986. In 1986, the Canadian Hydrographic Service at IOS surveyed the area, not only to update their chart but also to provide a numerical model incorporating a detailed bottom profile.

This report discusses the hydrodynamic aspects of the Campbell River study, *viz.* the interaction between river discharge and tides; the upstream limit of the salt wedge and its velocity of intrusion; the stability of the saline-freshwater interface: and the volume transport of salt and fresh water at sections representative of the two different flow regimes in the estuary. The volume transport was estimated by combining conventional one-dimensional tidal computations with observed salinity profiles over a variety of tidal heights at normal, controlled discharges.

THE ESTUARY

This section covers some general features of the Campbell River estuary and the recent changes in topography which prompted the study.

The seaward boundary consists of a low sandspit ending at Tyee Point and a large drying shoal (Fig. 1). The tidal influence ends in the river rapids below the Highway 19 bridge, 2.5 km upstream from Tyee Point. The surface area of the estuary covers about 0.7 km^2 at high tide, the drying flats (exposed at a very low tide) about 0.3 km^2. At low tides, only small boats with draughts of a few decimetres can navigate across a shallow bar south of Tyee Point. Figure 2 is a sketch of the tidal prism.

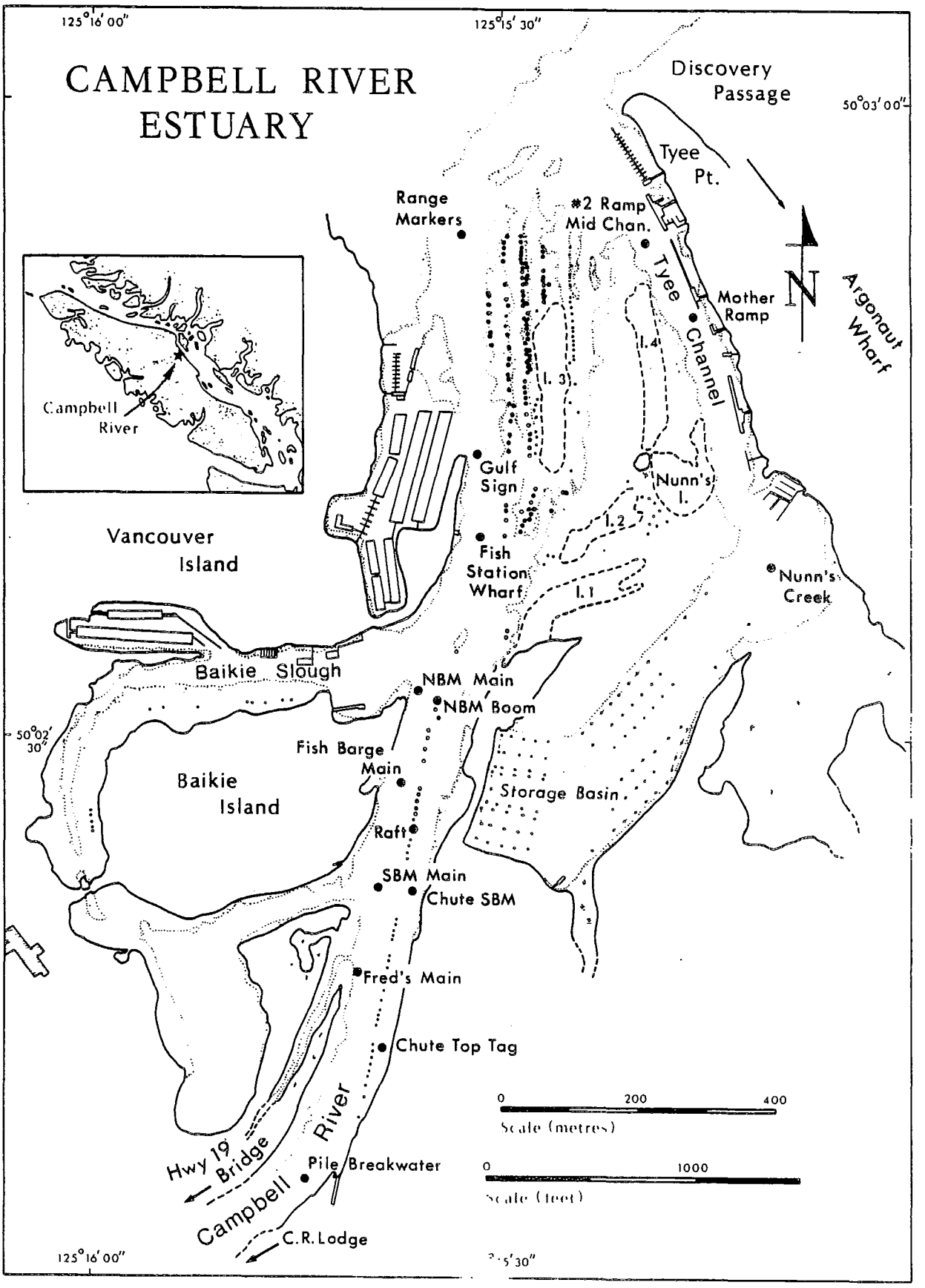

Fig. 1 The study area, the main channel. sloughs and log storage area.

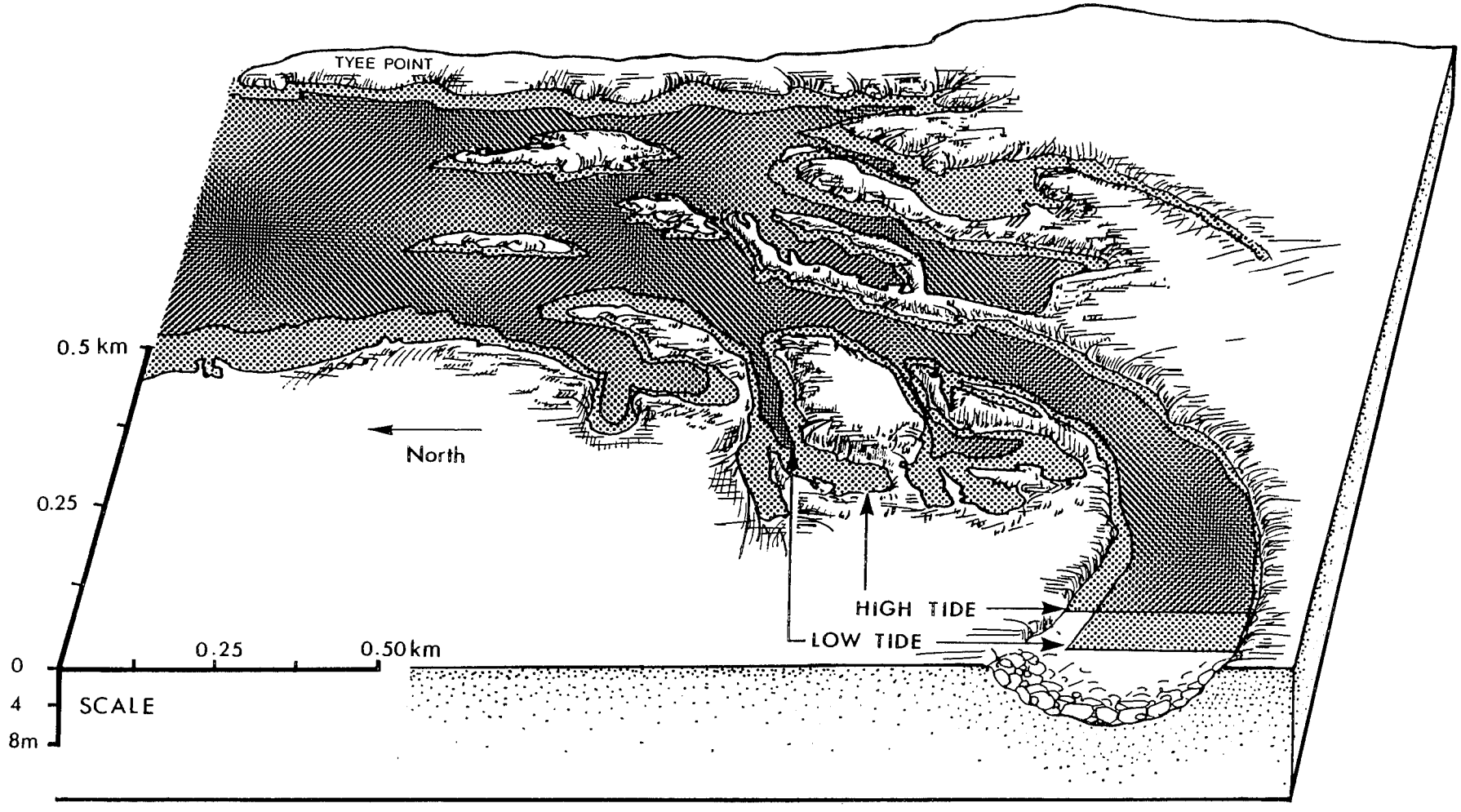

Fig. 2 Tidal prism of the Campbell River estuary (looking east).

The river flow into the estuary is regulated by the John Hart Power Generating Station which is located about 5 km upstream from the mouth. The river drains into the strong tidal currents of Discovery Passage and mixes almost immediately with the sea water, making this estuary unique by the absence of a characteristic freshwater plume. Details of the estuary dynamics will be discussed later.

Most of the estuary is used by the logging industry for the storage of logs. The eastern part is a storage area for logs trucked in by Fletcher Challenge from the nearby timber leases, to be transported to various mills along the coast. A local mill, operated by Raven Ltd., stores its logs in Baikie Slough. Two large freshwater marinas open into the river and Tyee Point shelters a busy float plane base.

To improve their log handling, B.C. Forest Products (Fletcher Challenge) changed the traditional method of receiving logs in the waters of the estuary and instead built a dryland log sorting area in 1982. From an operational point of view, the dryland alternative facilitated the entire process of unloading trucks, log-grading, sorting and watering. Environmentally, it reduced damage to the estuary bottom caused by logs grounding at low tides and by periodic dredging to remove the debris. After being processed on land, the logs enter the water in a deep storage basin, to be towed out at high tide.

One of the conditions set by the Department of Fisheries and Oceans to allow B.C. Forest Products to proceed with the dryland sorting facilities was the construction of four intertidal islands planted with marsh. The purpose of this construction was to increase the intertidal area. So far, the islands have remained stable, even at a very high river discharge of 450 m^3/sec, which was well above the design discharge of 350 m^3/sec released from the John Hart Dam in 1981 to assess the erodibility of the construction materials (Brownlee, Mattice and Levings, 1984).

Even though the rehabilitation site was located away from the main channel and was selected after extensive biological and engineering studies, the possible long-term effect of this man-made "adjustment" upon such features as sedimentation and erosion in other parts of the estuary may not be identifiable for some time.

OBSERVATIONS

Between July 18, 1984 and June 10. 1986. salinities, temperatures and currents were recorded at various tidal phases and. with some exceptions, at average discharges. A total of forty-one stations was occupied throughout the estuary intermittently for a total of 28 days. A few time series were included for a closer examination of the current pattern near the interface between fresh and salt water. Profiles were generally measured at one-metre intervals, using a General Oceanics impeller and a Hydrolab salinometer deployed from a Zodiac semi-inflatable boat. The intervals were often reduced to 0.5 m or even to 0.1 m when there was a need for more detail.

The absence of turbidity during normal flow conditions made it possible to measure current profiles with a small impeller without having to risk inaccurate readings due to bearings clogged by suspended sediment. Moreover, there was no need for a directional unit with a deck read-out to locate flow reversals near the halocline because the probe could be tracked visually from the surface as it was being lowered. Thus it was possible to determine the depth of flow reversal within a few centimetres. These measurements coincided with salinity measurements carried out with an equally small probe. The results will be discussed in the following section on the dynamics of the estuary.

In addition to the current, salinity and temperature measurements, three pressure tide gauges were installed and maintained for a few months, partly to calibrate a numerical model and partly to provide hydrographers with a reference level for their soundings. Figure 3 shows the locations of the gauges, and recording anemometer which was installed in July 1984 to record wind conditions. These and other data relevant to the study are published in the data record (Ages, Dobbs, and McAllister, 1990).

DYNAMICS

Although a considerable amount of biological data has been collected in the Campbell River estuary in the past, there has been little information on the physical characteristics associated with biological processes. Much of the previous field work focussed on the presence of zooplankton, an important food source for juvenile salmon, in sea water. The sea water intrusion depends on the interaction between tides and river discharges, and on the topography of the estuary. Therefore, to establish some sort of predictive capability to estimate the volume of sea water penetrating the estuary during a tidal cycle, tides, river discharges, bottom topography and stratification have to be considered.

a) River Discharges

The discharge of the Campbell River is regulated by the John Hart Generating Station, approximately 4 km above the upstream boundary of the estuary. To operate the power plant, B.C. Hydro requires a minimum flow of 13 m^3/sec but maintains a flow of at least 25 m^3/sec to protect the spawning grounds in the lower reaches (Bell and Thompson, 1977). The capacity of the turbines allows a maximum discharge of 124 m^3/sec. During a rain-storm, the Campbell River's discharge was observed to reach 857 m^3/sec (November 16, 1939). In more recent years, a maximum of 381 m^3/sec was observed on December 6, 1989, and a minimum of 36 m^3/sec on September 9, 1986. Data records provided by B.C. Hydro for the period between January 1982 and December 1989 indicate an average daily discharge of 93.5 m^3/sec at the dam. Figure 4 is a histogram of the daily discharges at the Hart Dam for the year 1989, based on B.C. Hydro data.

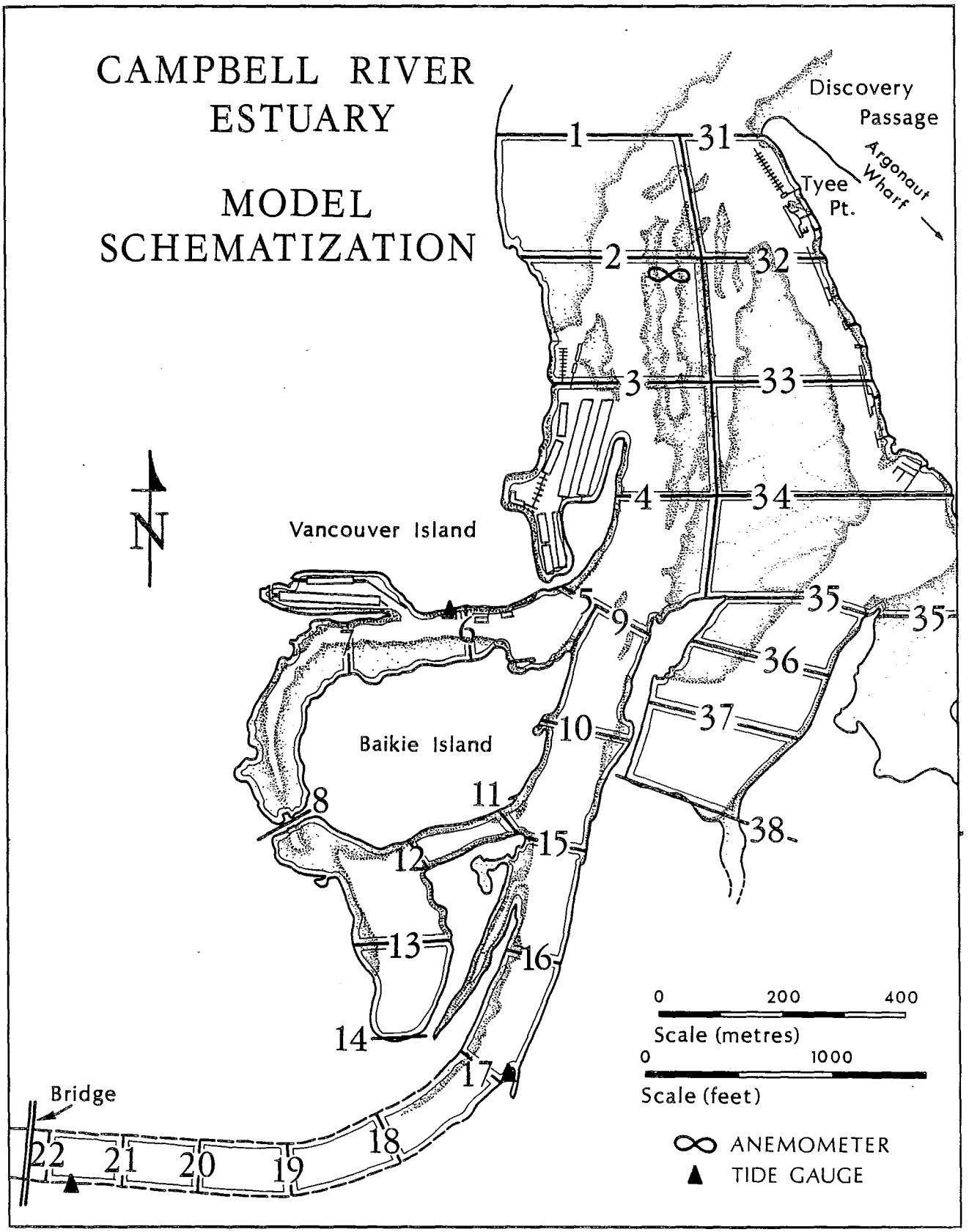

Fig. 3 Locations of tide gauges and anemometer in the Campbell River estuary, and the model segments.

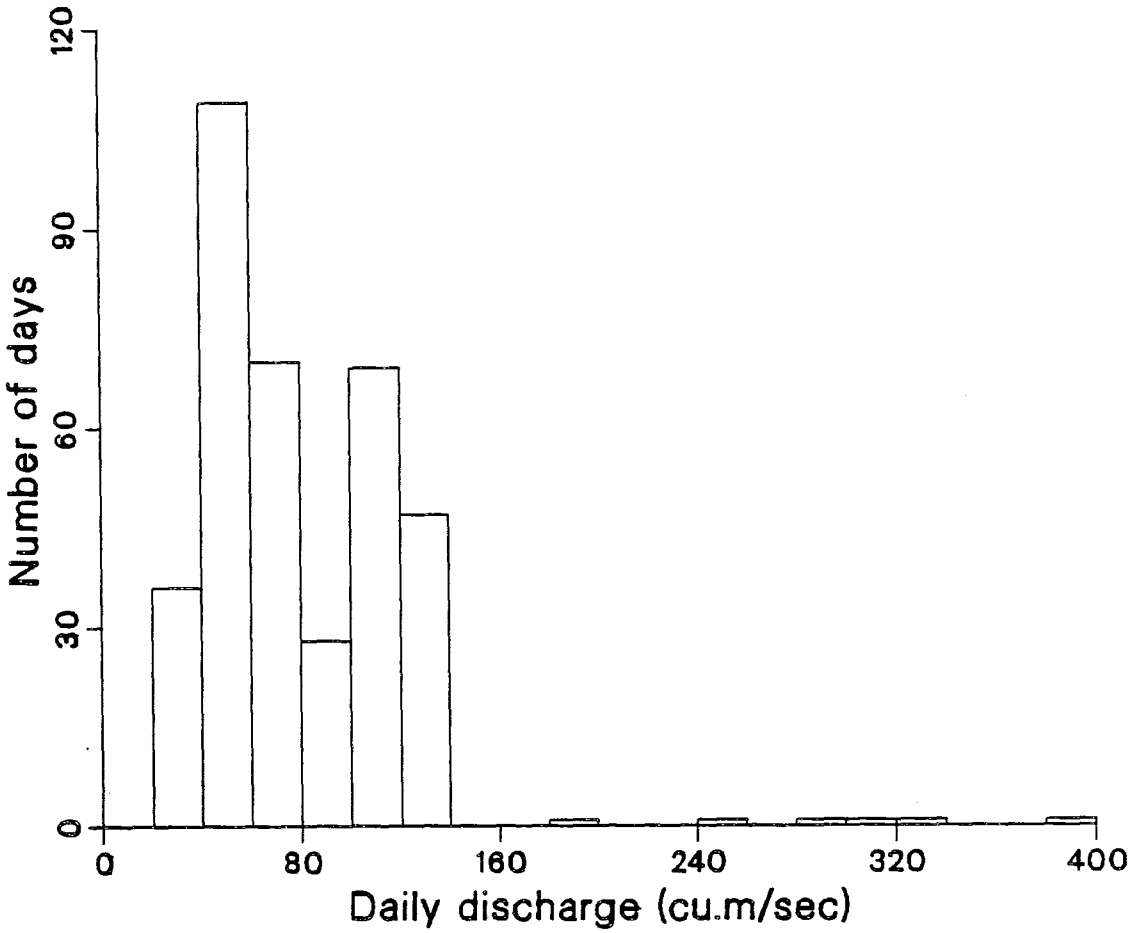

Fig. 4 Histogram of daily discharges at the Hart Dam in 1989.

Farther downstream, the river is joined by the Quinsam River (a mean annual flow of 9 m^3/sec), resulting in a total average daily inflow at the upstream estuary boundary of slightly over 100 m^3/sec.

b) Tides

The tides at the seaward entrance of the estuary are mixed, mainly semi-diurnal, characterized by two complete tidal oscillations per day with inequalities in heights as well as in times of successive high and low waters. According to the tide tables of the Canadian Hydrographic Service, the range for a large tide is 4.6 m, and for a mean tide 2.9 m. The tidal amplitudes in the nearby waters of Discovery Passage reach a minimum at Campbell River (Crean, Murty and Stronach, 1988). Daily extrema in Owen Bay, only 33 km north of Campbell River, precede those at Campbell River by about two hours. The hydraulic gradient associated with this phase difference generates very high tidal velocities in both directions in the vicinity of Campbell River, sweeping away any form of river plume entering the passage.

In the river itself, the tidal influence virtually ends at the Highway 19 bridge. According to our tidal records, daily high waters at the bridge are normally about 10 cm higher than those at the entrance. Their phase lag is about 10 min, which corresponds with the progression of a shallow water wave at the average depth of the river. Height differences between low waters at the bridge and entrance vary anywhere between 0.5 and 4 m, depending on the heights at the entrance. At a falling tide, the river flow near the bridge rapidly becomes critical, resulting in virtually constant water surface elevations at that section. The phase lag of the low tides is impossible to establish because of the absence of a distinct minimum.

Figure 5 compares representative daily tidal records at the bridge and at the Argonaut Wharf near the seaward entrance. The comparison suggests that at normal tides and discharges, even a higher high water at the entrance does not generate a reversal of surface flow anywhere in the lower reaches because the hydraulic gradient remains positive (*i.e.* the water surface everywhere slopes down toward the entrance). This inference is consistent with our data. During our observations, the surface flow in the river itself did not turn to flood at any time although there were some brief periods of flooding in the eastern basin away from the river's influence.

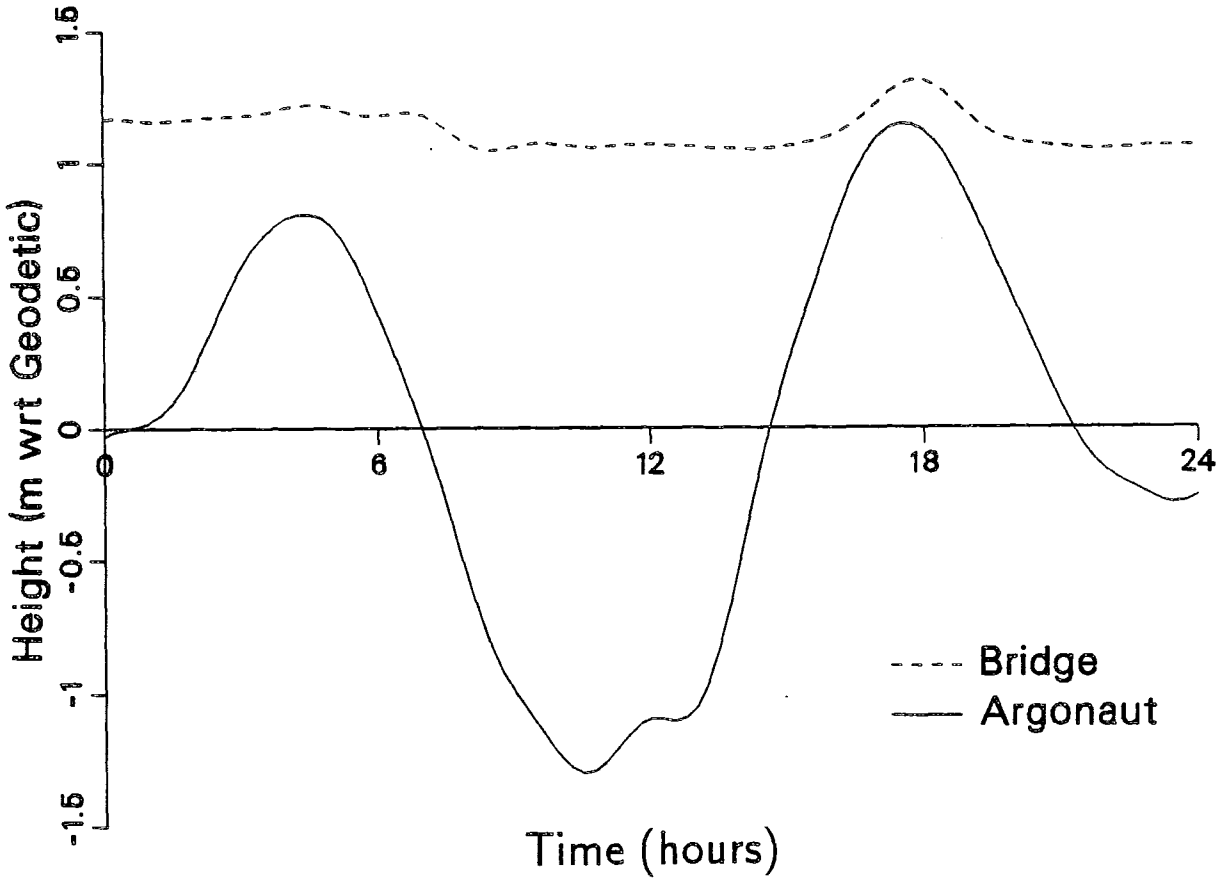

Fig. 5 Tides at upstream and downstream boundaries for a 24-h period, September 10, 1984.

The absence of surface flow reversal is due mainly to the slope of the river bottom which drops 4 m over a distance of 2.5 km between the bridge and Tyee Point. In comparison, flow reversals in the Fraser River have been observed at very low discharges as far as Mission, 80 km upstream from the entrance at Sandheads. The bottom of the lower Fraser rises only 3 m over that distance. Comparing their geomorphology, the Fraser is a much more mature river than the Campbell. This difference becomes evident not only from the bottom slope but also from the sediment deposition in the lower reaches, which is predominantly sand and mud in the Fraser delta and gravel in the Campbell River estuary (B. Bornhold, pers. comm.).

Weather affects the tides both in and outside the estuary. For instance, the tidal records of October 12, 1984 show a rise of 0.6 m above the predicted low and 0.4 m above the predicted high waters at the entrance, and a rise of about 0.2 m above normal for both high and low waters at the bridge. On that day, our anemometer recorded an extreme wind velocity of 9.22 m/s towards the NNW (Fig. 6). In addition, the heavy rain (44 mm of a monthly total of 249 mm) made the discharge twice as high, delaying the arrival of both low and high waters at the bridge by several hours.

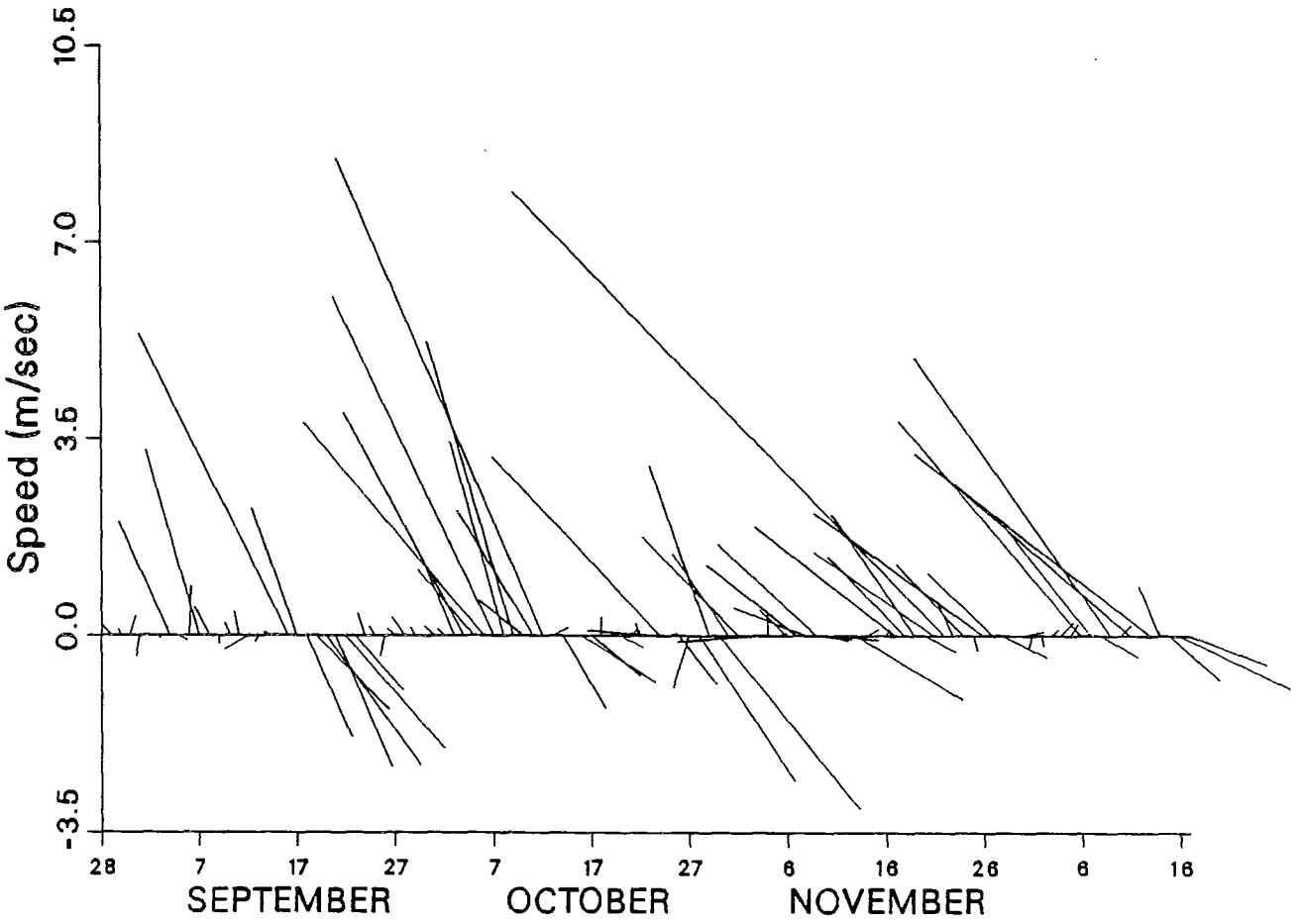

Fig. 6 Daily averaged wind velocities at the entrance of the Campbell River estuary for 1984.

c) The Salinity Intrusion

To introduce this section, it might be useful to briefly review the concepts of barotropic and baroclinic flows, as applied to estuaries.

By definition, barotropic flow is generated by a longitudinal pressure gradient due to the surface slope only. The hydrostatic pressure difference associated with this gradient would accelerate the flow at the same rate from surface to bottom, and in the same direction. Baroclinic flow is caused by a horizontal pressure gradient due to density differences (salinity and temperature). This pressure gradient varies with depth.

If the flow were uniform, (*i.e.* the density is homogeneous) the driving force would simply be the hydrostatic pressure difference

$$\frac{\partial p}{\partial x} = \rho g \frac{\partial h}{\partial x},$$

where we differentiate pressure p and depth h in the x-direction (downstream) and assume uniform density ρ (Fig. 7a).

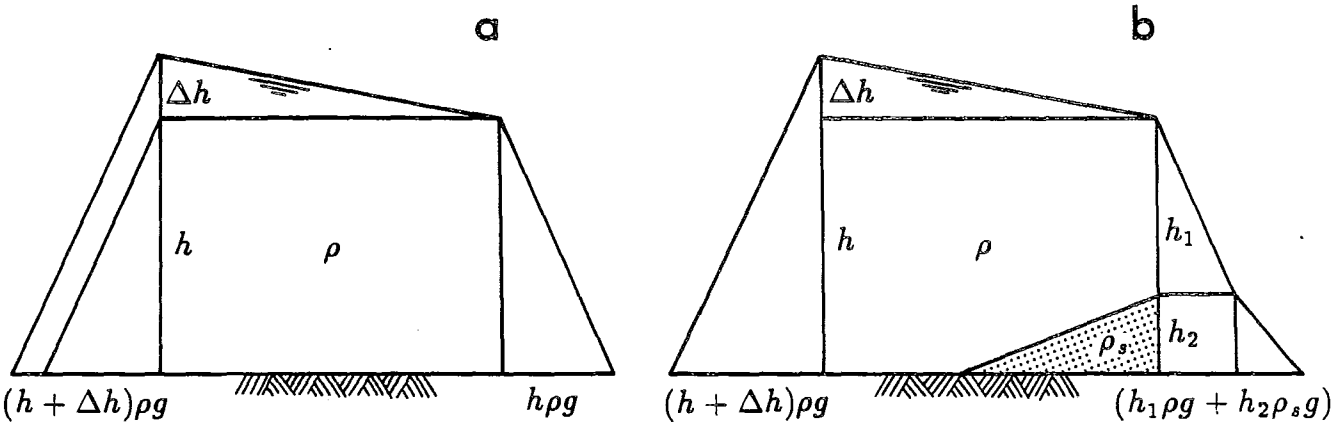

Fig. 7 (a) Barotropic pressure gradient. (b) Baroclinic pressure gradient.

In an estuary the density is not homogeneous during much of the tidal cycle. At a rising tide, the denser sea water advances upstream below the freshwater outflow and generates bottom currents opposing the surface flow.

Figure 7b illustrates the effect of the salinity intrusion upon the pressure distribution. In this sketch, ρ_s is the density of the sea water. The additional pressure due to the density gradient in the lower layers forces the salt water upstream near the bottom, in the form of a wedge. In mathematical terms, including the density effect, we write

$$\frac{\partial p}{\partial x} = \rho g \frac{\partial h}{\partial x} + (h - z) g \frac{\partial \rho}{\partial x}.$$

The second term, added to our earlier expression for uniform flow, accounts for the difference in pressure at level z due to the density gradient in the x-direction.

When a rising tide at the mouth of a river becomes sufficiently high to reverse the surface slope, the two gradients combine to force both salt and fresh water in the same, upstream direction. For instance, in the gently sloping lower reaches of the Fraser River, the salinity wedge may migrate upstream as far as 34 km at a low discharge and a high tide. When the tide at the mouth of that river subsequently falls, the surface gradient changes sign, the flow turns and accelerates, often disintegrating the interface as both fresh and salt water are swept downstream. As we discussed earlier (page 8) the much larger surface gradient of the Campbell River does not allow a reversal of the surface freshwater outflow.

Appendix A shows velocity vectors and salinity contours for the centre transect of the main channel, compiled from our data report (Ages, Dobbs, and McAllister, 1990). Although sketches of isopycnals (contours of equal density) would perhaps be somewhat more appropriate for a study of the dynamics of an estuary, isohalines (contours of equal salinity) were selected for the benefit of a biological analysis in the near future. Individual profiles of salinities, temperatures and currents in the channel as well as in the adjoining sloughs and basins can be found in the data report. It should be noted that a few of these profiles listed in the data report fall below the bottom contour because they were taken in deeper spots nearby.

Because of the absence of major seasonal variations in the regulated river flow, the limit of the salt intrusion in essence depends on the tidal amplitude, and is fairly constant. A mean high tide of 4.1 m moves the salt wedge 1.8 km upstream from the entrance at Tyee Point, against a normal inflow of 100 m^3/sec. These conditions are typified by our data of September 10, 1984, perhaps the most complete set of observations of the progress of an advancing wedge in the main channel (see Appendix A). The sketches show a strong, horizontal salinity gradient of approximately $20^0/_{00}$ per 100 m maintained in the front of the advancing salt wedge. Behind the front, the salinity contours spread out as the wedge advances against the river flow. Finally, at high water, the wedge's progress is arrested when the barotropic pressure gradient of the increasing river velocity equals the baroclinic pressure gradient of the salt intrusion.

At a high tide, on that same date, we measured a bottom salinity of $29.7^0/_{00}$ at Tyee Point and one of $21.4^0/_{00}$ at the upstream limit, station Pile Breakwater. Both measurements were taken at depths of 5 m.

At the same tidal amplitude and bottom salinity near the entrance, a lower inflow of 64 m^3/sec on September 24, 1984 did not seem to change the intrusion limit but was associated with a bottom salinity of $27.6^0/_{00}$ at the limit.

The obvious influence of the river inflow upon the bottom salinity at the intrusion limit is perhaps less likely associated with mixing than with the topography of the channel. A relatively shallow reach downstream from the intrusion limit might have blocked the deeper and more saline part of the advancing salt wedge at an inflow of 100 m^3/sec. On the other hand, a low inflow of 60 m^3/sec would interfere less with the

stratification and allow the deeper water to move across the sill, resulting in a higher bottom salinity at the limit.

The salinity contours for the high tides at the two dates (September 10, 1984 (1710–1806 h) and September 24, 1984 (1703–1755 h)), respectively, are sketched in Appendix A. A more detailed comparison between the two sets of data is provided by the salinity profiles in Figs. 8 and 9. One aspect to be considered in this comparison was the timing of the two observations with respect to high water. On September 10 and 24, profiles at the limit were measured at 0014 and 0120 h, respectively, after high water at the entrance. Time series at a nearby station on September 24 (Chute SMB) indicated that the salinity profile deeper than 2 m had remained unchanged 0124 h after high tide and similarly, on August 2, 1985 (discharge 49 m^3/sec), the salinity profile below 2 m at another nearby station (Chute Top Tag) had fluctuated less than $0.6^0/_{00}$ two hours after high water, to decrease rapidly shortly afterwards. At higher discharges of about 100 m^3/sec (*e.g.* July 30, 1984; August 13, 1984; September 10, 1984), our data (Ages, Dobbs, and McAllister, 1990) showed that the salt wedge reaches its limit about 15 min past the time of high water. Therefore, it seems reasonable to assume that the two sets of salinity profiles taken at the intrusion limit on September 10 and 24 represented comparable conditions.

We have attempted to examine these data somewhat more closely by computing the interfacial Froude number

$$F_i = \frac{u}{\sqrt{\frac{\Delta\rho}{\rho} g D}},$$

where u is the velocity of the upper layer, $\Delta\rho$ the density difference between the two layers, ρ the density of the lower layer and D the depth of the upper layer.*

The interfacial Froude number takes into account density differences in the vertical and is used as an indicator of the stability of the interface in stratified flow. When $F_i > 1$, the interface between layers of different density becomes unstable, the internal waves at this interface are unable to propagate against the flow, become steeper and are partly entrained in the upper layer.*

We applied F_i to our data of September 10 and 24. estimating the depth of the interface in the shallow area at 2.5 m (stations Fred's Main and SBM Main) and converting salinities into densities (Dietrich and Kalle, 1975). Values of F_i varied between 0.6 and 0.8 for September 10, and 0.4 and 0.5 for September 24, an indication that the

---

* In its original form, the Froude number $F=u/\sqrt{gh}$ is applied to the design of hydraulic structures and ships. If F exceeds unity for motions in an open channel with flow velocity u, a tidal wave front with velocity $\sqrt{gh}$ is prevented from propagating upstream (supercritical flow). In the Campbell River, this condition exists most of the time near the highway bridge. Records of our tide gauge 100 m below the bridge show small periodic fluctuations only at a high tide when the river flow has decreased and the water depth has increased for a short time. Normally, the flow near the bridge is supercritical.

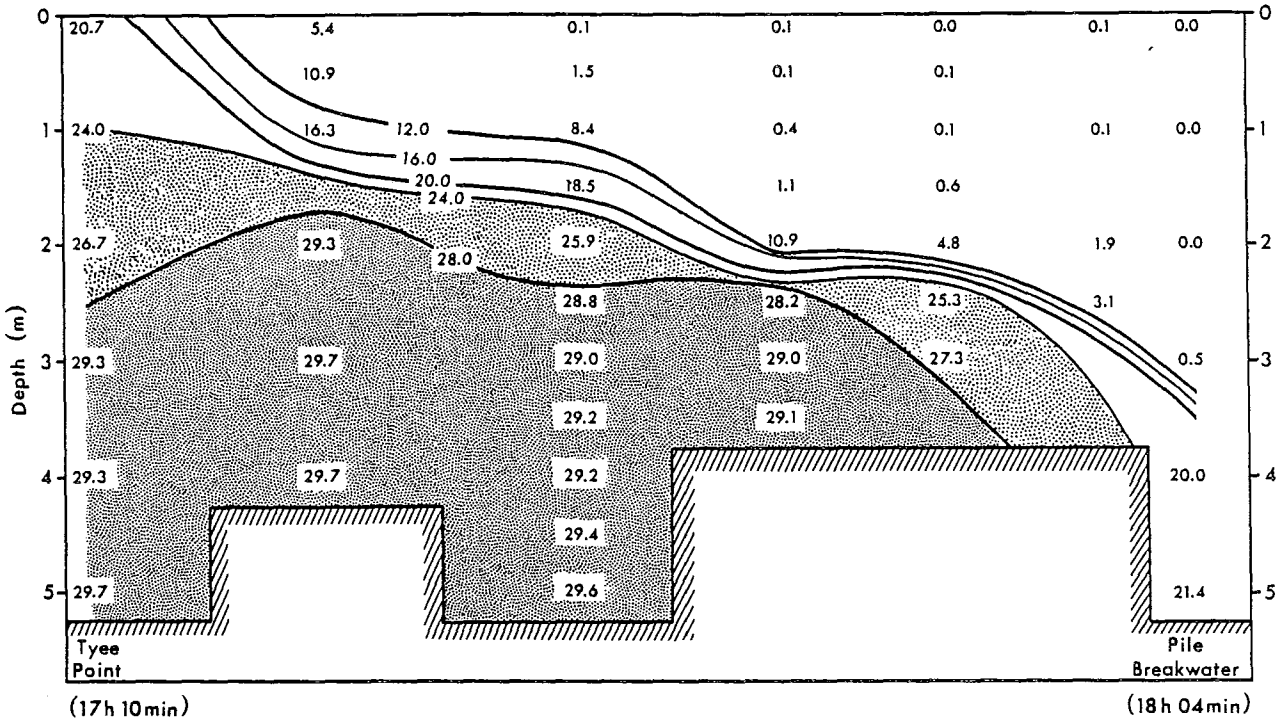

Fig. 8 Salinity distribution in mid-channel at high tide, September 10, 1984. Units are in $^{0}/_{00}$.

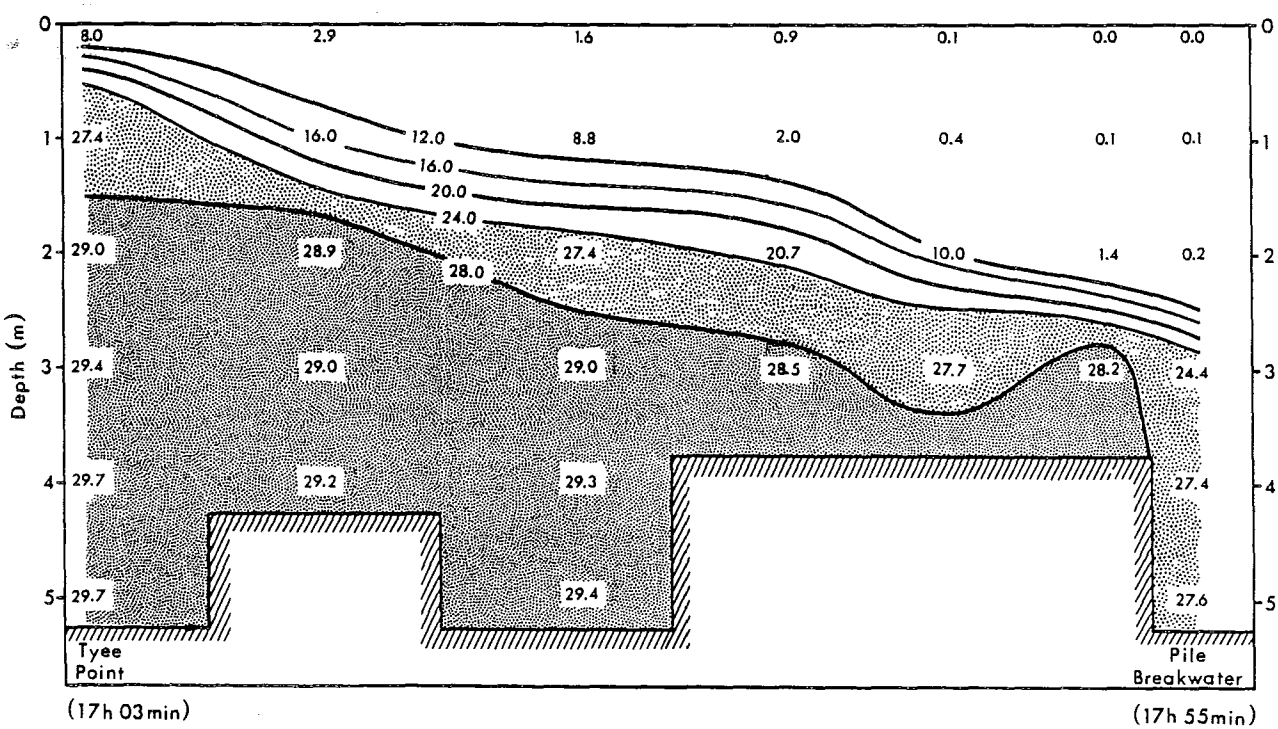

Fig. 9 Salinity distribution in mid-channel at high tide, September 24, 1984. Units are in $^{0}/_{00}$.

stratification above this extended sill was more stable on September 24 (low discharge) than on September 10 (normal discharge) and might have made it possible for the high salinity layer near the bottom to cascade into the deeper water at the intrusion limit. However, because of the rather uncertain variables involved (*e.g.* the exact location of the interface, in other words, D), an interfacial Froude number is still subject to some wishful manipulation of the data, and should be verified by more observations at different discharges.

Entrainment due to an unstable density interface ($F_i > 1$) would set up a vertical movement of saline water into the more turbulent fresh upper layer and thus transport marine foods to juvenile salmon commonly residing in the upper layer and halocline. Since this aspect would be of interest to the marine biologists involved in the study, we computed interfacial Froude numbers for several profiles in the main channel at rising and falling tides and concluded that, at a rising tide, there is very little mixing by entrainment, except near the tip of the wedge. (At station Fish Barge Main, 1602 h, August 27, 1984, $F_i = 1$ near an abrupt flow reversal in the halocline while behind this front F_i was much lower.) At a falling tide our computations of F_i suggested significant mixing over a short period as the salt wedge is swept out.

Another indicator of the stability of the interface in stratified flow is the Richardson number:

$$Ri = \frac{-g}{\rho} \frac{\partial \rho / \partial z}{(\partial u / \partial z)^2}, \qquad z \text{ positive upwards.}$$

This dimensionless number originally was introduced to study the suppression of turbulence in the air by a strong density gradient but in more recent years has found application in hydrodynamics (Richardson, 1920). The interfacial Froude number and Richardson number consist of the same variables but are derived in a different way and examine different aspects of mixing. Where F_i considers mixing by entrainment, Ri gives us an indicator of conditions under which we can expect turbulence to exist in stratified flow. Turbulent eddies are responsible for vertical transport of substances or fluids, in other words, for vertical mixing by eddy diffusion. In a rather crude way, we might explain the role of turbulent eddies in vertical transport by visualizing an eddy with its horizontal axis perpendicular to the flow; one part of the eddy lifts a heavier fluid to a lighter layer and the other part, moving in an opposite direction, pushes lighter fluid to a heavier layer. This process brings about an increase in potential energy.

Using Prandtl's mixing length l over which the exchange takes place, we write $\Delta \text{PE} = \left[g \frac{\partial \rho}{\partial z} l \right] l$ per unit volume for the gain in potential energy. The increase in potential energy must be balanced by a loss of kinetic energy in the eddy field, which in turn has to be extracted from the mean flow in order to maintain turbulence. We can express the decrease in kinetic energy as $\Delta \text{KE} = -\left(\frac{\partial u}{\partial z} l^2 \right) \rho$ per unit volume, u being the mean velocity. Since some of this energy is lost in friction, ΔKE must exceed ΔPE, which leads to the Richardson number

$$Ri = \frac{-g}{\rho} \frac{\partial \rho / \partial z}{(\partial u / \partial z)^2} < \text{“some fraction”}.$$

This fraction, estimated theoretically by Miles (1961) at $\frac{1}{4}$, is considered a necessary condition to maintain vertical mixing by turbulent eddies. Other attempts to evaluate Ri are reviewed by Schlichting (1960), who also discusses a laboratory experiment by Prandtl and Reichardt supporting the theoretical results.

It would be unrealistic to apply this threshold value rigidly to mixing processes in the Campbell estuary with its very shallow and irregular topography. Moreover, even though our current meters were small enough to operate within the scale of the shear layers, any discrepancies in the data would be magnified in the mean-shear-squared term $(\frac{\partial u}{\partial z})^2$ and affect the computed Richardson numbers well beyond the precision of the critical value. However, comparison of instantaneous Richardson numbers computed for several transects and time series provided us with a reasonable indication where and when we might expect mixing to occur.

The computations were based on instantaneous data and not on tidal averages as in some other estuary studies. The periods of observations were too short and too scattered to allow averaging. Even partial averaging would have masked the considerable short-term variations in stratification and flow fields.

Because of their continuity and detail, the data collected in the main channel on August 27, 28 and September 10, 11, 1984 appeared most suitable for the computations of the Richardson numbers. The figures in Appendix A illustrate the distribution of salinities and velocities during these periods. In most cases the computations used a vertical scale between shear layers of 0.5 m in the halocline within a density gradient of about 10 g/cm^3.

Throughout our transects at an increasing tide on August 27 and September 10, the Richardson numbers exceeded 0.5 at various points in the halocline, except near the advancing head of the wedge, where values occasionally dropped to 0.25 (*e.g.* 1602 h, August 27, 1984, station Fish Barge Main) and where the interfacial Froude numbers hovered around unity, indicating a possible instability. At falling tides (August 28, September 11), the Richardson numbers in the halocline were significantly lower, as could be expected from the rapidly increasing $(\frac{\partial u}{\partial z})^2$ term. However, they rarely fell below the theoretical threshold value even though the Froude numbers at the same locations suggested supercritical conditions (*e.g.* 0741 h, September 11, 1984, station NBM Main, $Ri = 0.5$, $F_i = 2.0$).

More detailed information on the vertical distribution of salinities and currents in the advancing salt wedge was provided by time series in three locations. Two stations, Raft and NBM Boom were simultaneously occupied on June 9, 1986 during the first hours of the passage of the salt wedge. Station Raft was located 192 m upstream from station NBM Boom and at a (normal) discharge of 102 m^3/sec and a depth of 4 m, the salt wedge moved at a speed of 7 cm/sec in that reach, about 1 km from the entrance. Figure 10 plots the salinity and current observations for that date. These and other time series marked the arrival of the wedge by a sudden increase in salinity up to $25^0/_{00}$ in the bottom half-metre, accompanied by a current reversal near the bottom of the order of 0.1 m/sec. At Raft, the salt wedge disappeared altogether about one-half hour after its arrival, to reappear 20 min later. The bottom current also switched direction

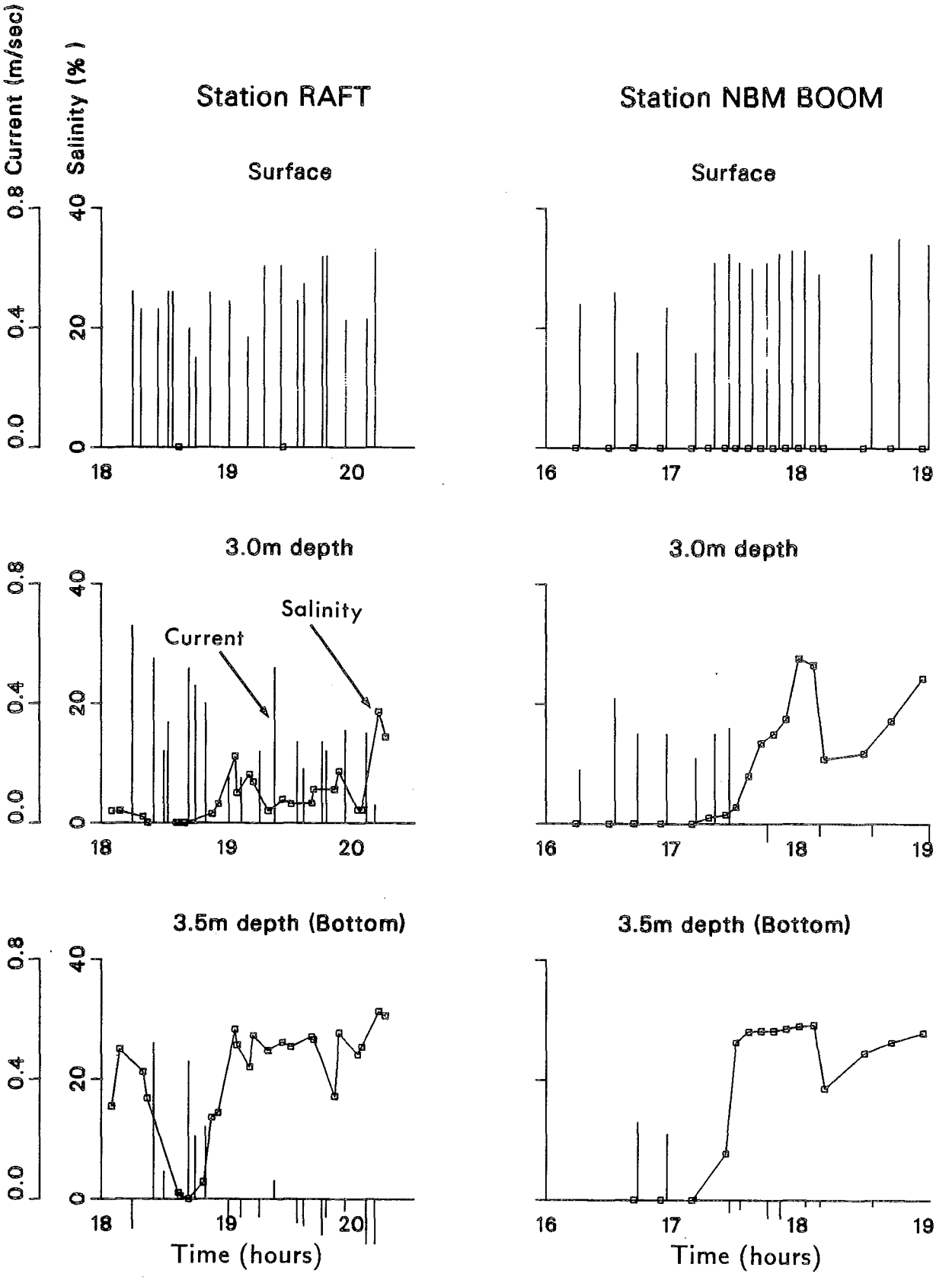

Fig. 10 Simultaneous time series of the arrival of the salt wedge at two locations in the Campbell River, June 9, 1986 (ebb velocities positive).

twice. An explanation of this behaviour might be the approach of a towboat with a log bundle moving upstream shortly after the arrival of the salt wedge. The tow decreased the cross-sectional area of the shallow reach, forcing an acceleration of the river flow which in turn pushed the head of the wedge back until the boom had left the channel. Downstream, at NBM Boom, this temporary constriction only seemed to lower but not eliminate the salinities, perhaps because the salt wedge had been well established before the passage of the tow.

Figures 11 and 12 sketch the haloclines, current profiles and points of zero flow (or null points, *i.e.* the points of flow reversals in or near the halocline) of these two stations. Both time series show evidence of an internal wave behind the head of the wedge. The abrupt decrease in high salinities at about 1810 h at NBM Boom (Fig. 11) was obviously due to mixing caused by the propeller wash of the tug boat passing the station at that time. Similarly, the gap in salinities between 1825 h and 1850 h at Raft (Fig. 12) was likely due to the same tow, as was suggested above. Richardson numbers were calculated near the points of zero flow and showed occasional instabilities near the head but a fairly stable shear interface behind the head.

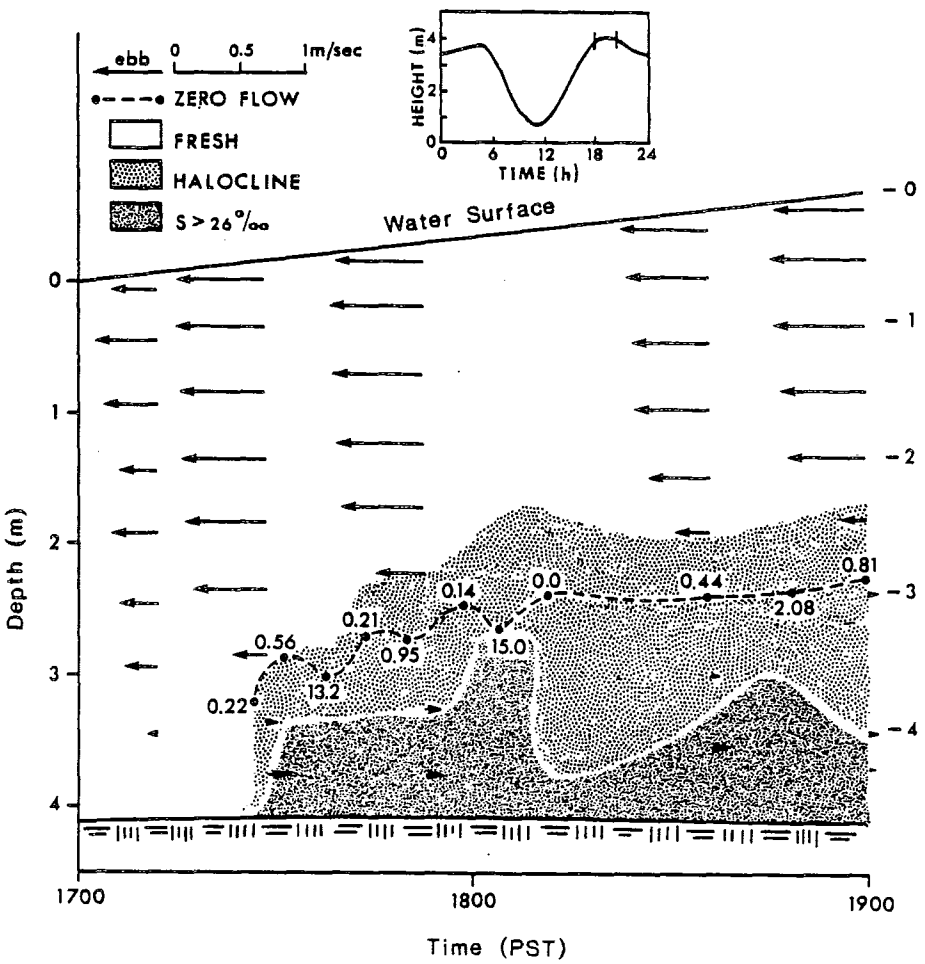

Fig. 11 The salt wedge, null points and Richardson numbers at NBM Boom, June 9, 1986.

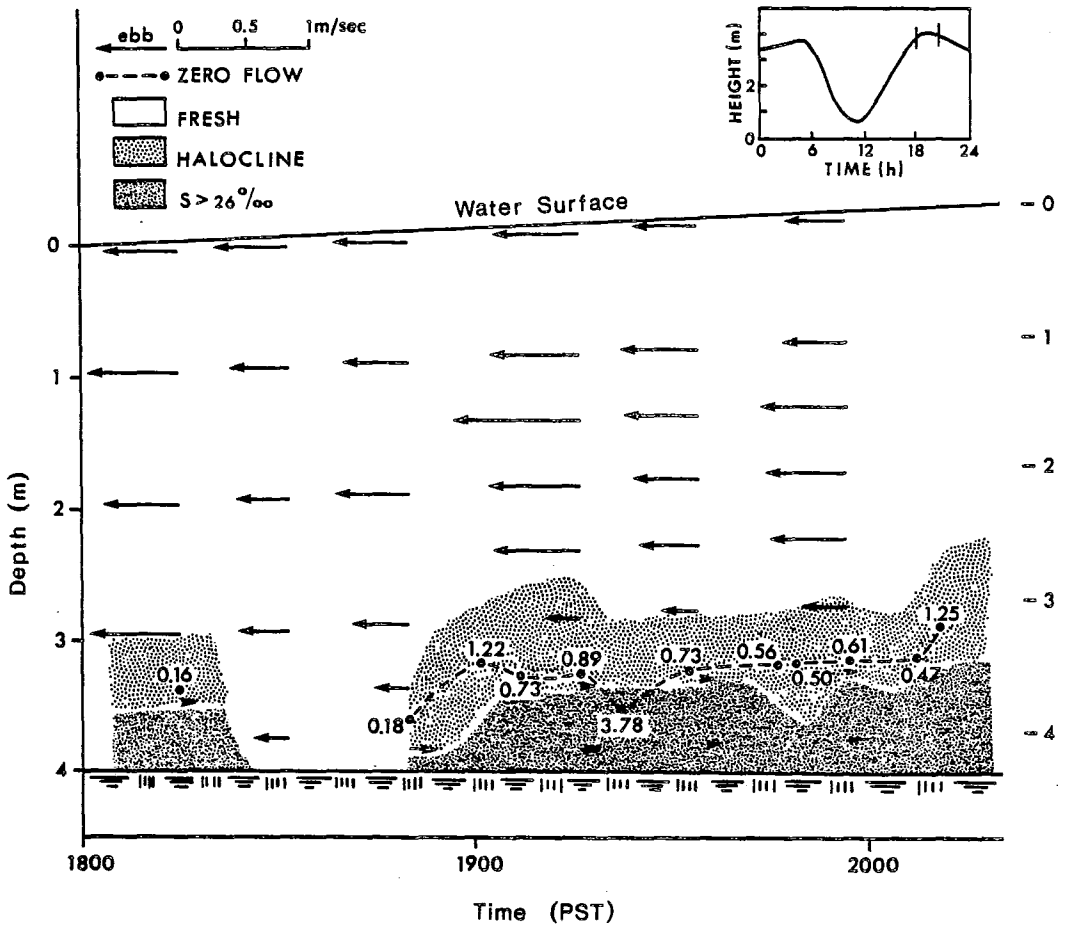

Fig. 12 The salt wedge, null points and Richardson numbers at Raft, June 9, 1986.

Time series were also carried out at a nearby station (Chute SBM) during the upstream passage of the salt wedge, the first series at a low discharge of 58 m^3/sec (September 24, 1984) and the second at a discharge of 102 m^3/sec (November 6, 1985). Figures 13 and 14 illustrate the data. The low discharge on September 24, 1984 clearly had a significant effect upon the stability of the stratification, as demonstrated by the very high Richardson numbers in Fig. 13.

A short time series on August 2, 1985 covered the retreat of the wedge during a discharge rate of 45 m^3/sec. The observations during the early morning at station Chute Top Tag (Ages, Dobbs, and McAllister, 1990) showed an increase in salinity towards the surface, until the stratification completely disappeared shortly before the salt was flushed out to sea as a well-mixed mass. Initially, the river current accelerated above the salt wedge by about 60% shortly after the tide started to fall, subsequently decreased by 25% when the interface disintegrated (creating a larger cross-sectional area), and finally accelerated again to adjust to the diminishing cross-sectional area brought about by the falling water surface in the river. The same fluctuation in flow was partly observed during the retreat of the salt wedge in a time series closer to the entrance (Fish Station Wharf, September 25, 1984). The final phase (flow acceleration after the wedge had retreated) was not detected at this station, possibly because of its

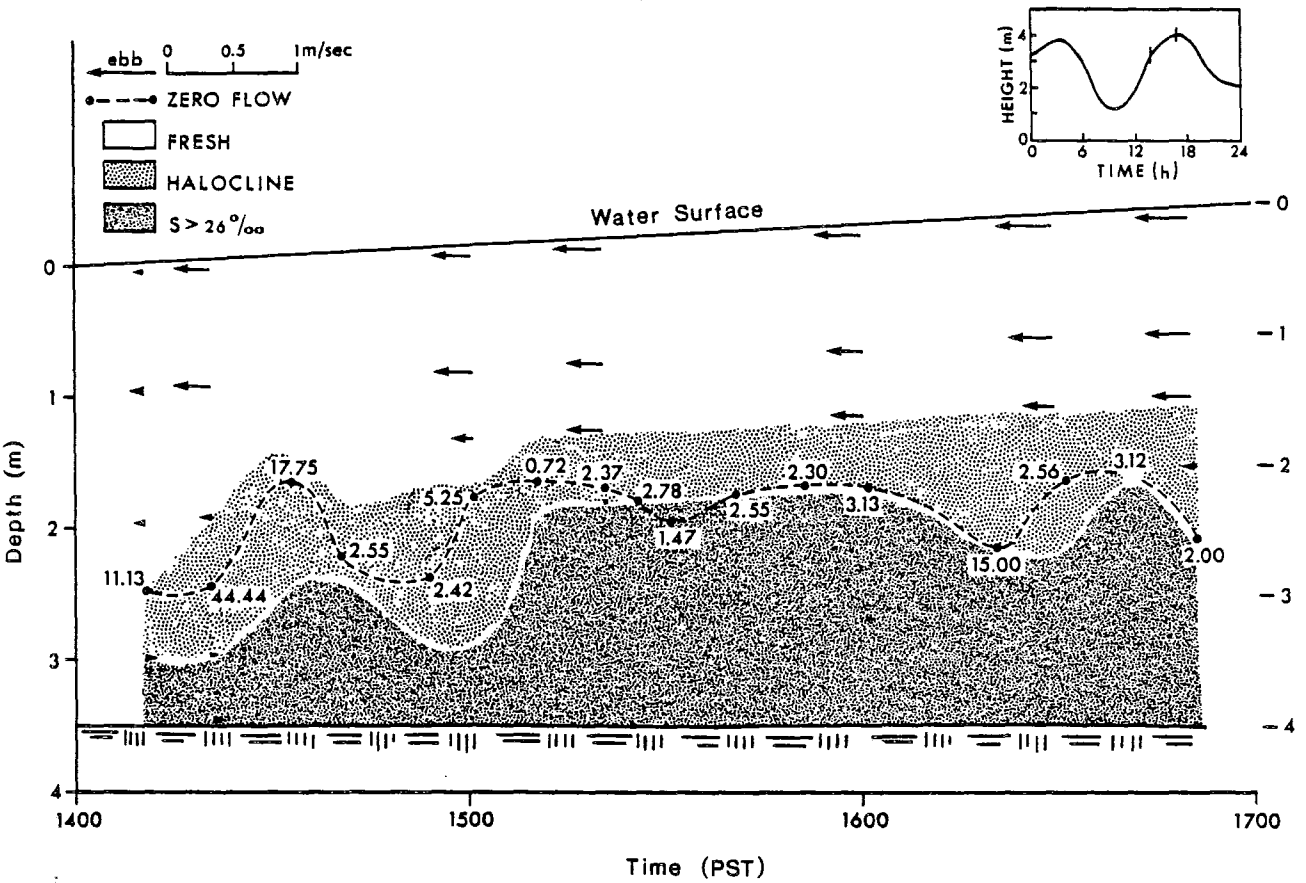

Fig. 13 The salt wedge, null points and Richardson numbers at Chute SBM at low discharge (September 24, 1984).

much larger water depth. A falling tide here would have had a relatively smaller effect upon the cross-sectional area.

In general terms, we may summarize our observations and computations of the movement of the salt wedge as follows.

At a mean high tide of 4.1 m and a normal, controlled freshwater inflow of 100 m^3/sec, the salt wedge moves upstream to just 0.3 km below the highway bridge, in other words, about 1.8 km from the entrance at Tyee Point. Because of the abrupt shallowing beyond the observed limit, low discharges would not allow the salinity intrusion farther upstream. High discharges would reduce the intrusion, but because of their rare occurrence in this estuary. we do not have sufficient information to relate the intrusion limit to the discharge. Deviations from the mean high tide of 4.1 m remain within 10% of that mean value most of the time; their effect on the limit should be minimal.

The wedge was observed to move into the estuary at a tidal height of 2.3 m at the entrance, about 3 to 4 h after low water (depending on the low-water height), and it started to retreat from its limit about one hour after high water at the entrance. We estimated the speed of the wedge at anywhere between 7 and 21 cm/sec in both directions, as it varied with the depth.

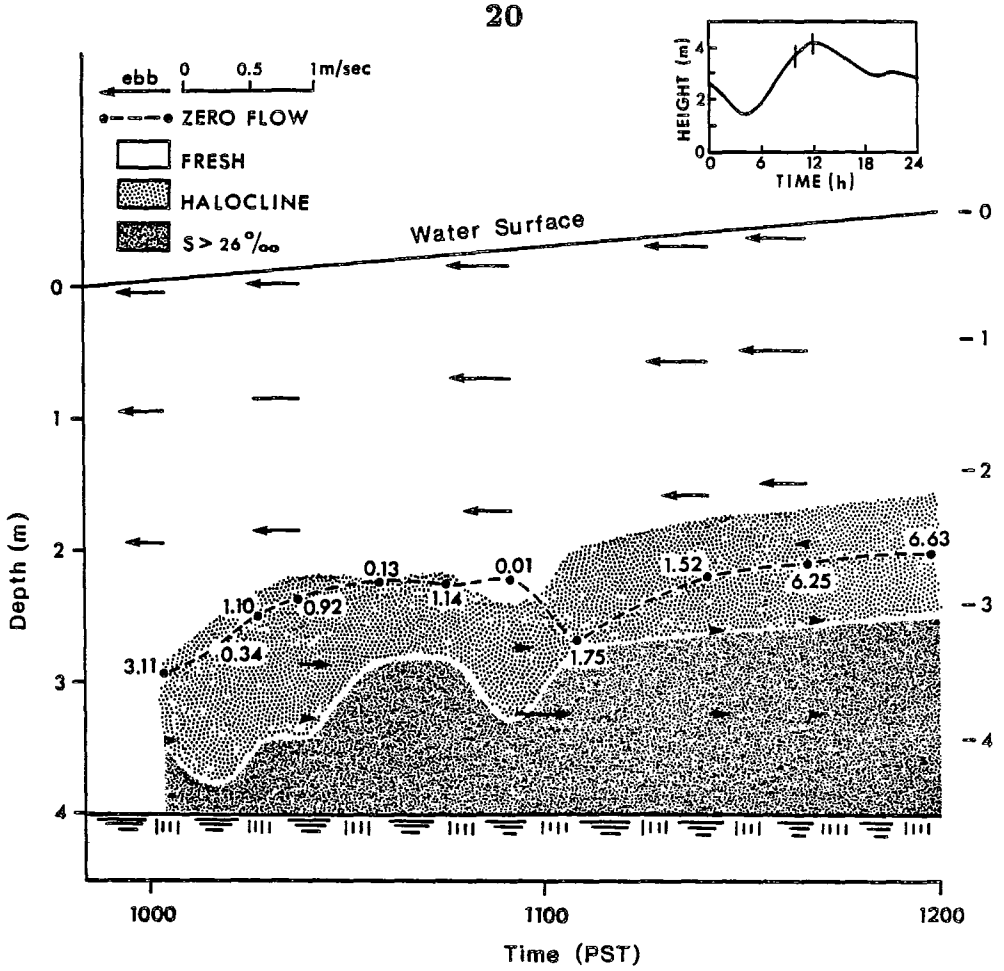

Fig. 14 The salt wedge, null points and Richardson numbers at Chute SBM at a mean discharge (November 6, 1985).

In the main channel, any significant transport of salt water into the fresh upper layer can be expected at the head of an advancing wedge and during the last stages of the wedge's retreat when the interface disintegrates. At low tide, all salt in the main channel is completely flushed out. Some salt usually remains trapped in Baikie Slough and in the deep log basin east of the channel. For instance, the salinity in Baikie Slough was still $1^0/_{00}$ at low water on May 12, 1986 while in the main channel outside the slough all salt had been swept out (Gulf Sign, 1606 h). On May 26, 1986 the bottom salinity in the log basin (Nunn's Creek) was still $29.5^0/_{00}$ at lower low water while farther north along the much shallower Tyee Channel the salinity did not exceed $6^0/_{00}$ (#2 Ramp, 1558 h).

d) Temperatures

Observed temperatures of the surface water at Tyee Point ranged from 3.2°C in the winter to 16.8°C in the summer. The minimum was measured on January 9, 1985 during a falling tide and exceeded the surface temperature in the upstream reaches by 0.6°C. Since the corresponding surface salinities at Tyee Point and at the upstream end (Pile Breakwater) were $3.3^0/_{00}$ and $0.0^0/_{00}$, respectively, the difference in these surface

temperatures was obviously due to mixing of the freshwater layer with the retreating salt wedge which had a temperature of 6.7°C near the interface. The maximum of 16.8°C at Tyee Point was measured on August 27, 1984 at a rising tide and a surface salinity of $0.9^0/_{00}$. The freshwater inflow had a temperature of 15.5°C (*vid.* the profile at 1720 h in our data record) and should have decreased near Tyee Point because of the colder temperature of 10.5°C at the salt wedge interface. We suspect that our observations were inadvertently taken too close to the shore where the water temperatures were higher than in mid-channel.

Outside the channel, the maximum observed surface temperature was 18.5°C on July 30, 1984; the minimum 2.8°C on January 9, 1985; both extrema occurred in the log basin.

COMPUTATIONS

Since zooplankton entering the estuary via the salt wedge are an important food source for juvenile salmon using the estuary, we had to develop a method to compute the volume transport of sea water per tidal cycle in selected locations.

The most detailed approach would be a three-dimensional model solving the equations of motion, continuity and salinity distribution with tides and salinity profiles as downstream boundary conditions and river discharges as upstream boundary conditions. Theoretically, a model should provide us with the upstream limit of the salt wedge as well as with the horizontal and vertical distribution of salinities and currents, including the local vertical velocities needed to estimate volume transport across the halocline.

The complex topography of this estuary with its drying flats and shallow braided channels would make a three-dimensional or even a two-dimensional, laterally averaged (x-z) model prohibitively expensive. Its calibration would require instrumentation (*e.g.* an acoustic Doppler system) which has yet to be tested for very shallow waters. In particular, the vertical velocities would be almost impossible to verify with some confidence. Their order of magnitude becomes evident when we apply the equation of continuity to a short reach where measurements were taken at a few minutes' interval (*e.g.* Gulf Sign—Fish Station Wharf, 1725–1729 h, September 10, 1984). Assuming constant width and depth above the halocline, we write

$$\frac{\partial \overline{u}}{\partial x} + \frac{\partial \overline{w}}{\partial z} = 0,$$

where $\overline{u}$ is the horizontal velocity averaged over a measured vertical profile at each station, and $\overline{w}$ is the vertical velocity averaged over the distance between surface and halocline. Over a longitudinal distance of 100 m, $\overline{w}$ would be of the order of only 1 mm/sec. Other aspects justifying a less elaborate numerical model were the regulated discharge, which rarely varied significantly, and the shoaling area near the highway bridge, which restricted the hydrodynamic effect upon the extent of the salinity intrusion.

On the basis of these considerations, a vertically integrated model combined with observed salinity profiles appeared to be an acceptable approach to estimate volume transport of sea water at selected locations.

The study area consists of two distinct flow regimes, the river itself and a narrow channel (Tyee Channel) which connects the log storage basin to the river mouth at Tyee Point. At low tide, the two channels are completely separated by tidal flats and although much of the shallow area is flooded at high tide, the presence of densely arrayed piles all along the east bank of the river would still maintain this partition. With the exception of some weak cross-currents over the shoals during tidal transitions, our observations indicated a general one-dimensional flow in both parts of the estuary.

The computations follow a standard one-dimensional technique used in estuary hydrodynamics and are based on the shallow-water wave equations

$$\frac{\partial Q}{\partial x} + W\frac{\partial h}{\partial t} = 0 \qquad \text{(continuity)}$$

and

$$\frac{\partial u}{\partial t} + u\frac{\partial u}{\partial x} = -g\frac{\partial h}{\partial x} - g\frac{u|u|}{C^2 d} \qquad \text{(motion).}$$

The equations are rewritten in finite difference form and solved for discharge Q and height h on a space-time grid, with depth d and width W averaged over the length of each segment. The computed tidal heights are compared with the actual heights recorded by gauges (with respect to geodetic datum), and adjusted with the coefficient C in the friction term. With the river discharge as upstream boundary and the tides at the entrance as downstream boundary, the model produces water surface elevations and flows at alternate sections. A detailed description of the technique can be found in an earlier report on numerical modelling (Ages, 1973) or in the literature, *e.g.* (Dronkers, 1964).

A conventional one-dimensional model schematization covering the entire area would ignore not only the different flow regimes in the two parts (the main channel and the storage basin) but also their distinctly different topographical features. If we lump the two regimes into one model, the term $u\frac{\partial u}{\partial x}$ in the equation of motion as well as the $\frac{\partial u}{\partial t}$ term need a correction coefficient to allow for the cross-sectional variability of the currents caused by the large difference in depth and the resulting difference in bottom resistance. In the equation of motion, both the local derivative $\frac{\partial u}{\partial t}$ and the convective term $u\frac{\partial u}{\partial x}$ assume a mean velocity $\overline{u} = Q/A$ to be uniform throughout a cross-section (of area A), an assumption which does not truly reflect the actual non-uniform flow distribution. This discrepancy is readily demonstrated by considering the kinetic head $\frac{u^2}{2g}$ (in essence an integrated form of $u\frac{\partial u}{\partial x}$) and comparing $\overline{\frac{u^2}{2g}}$ (the correct kinetic head) and $\frac{(\overline{u})^2}{2g}$, the head obtained from assuming uniform distribution; $\overline{u^2}$ would have been obtained from measured velocity profiles and would always be more than $(\overline{u})^2$.

In the development of the equation of motion, the non-uniform flow distribution in the cross-section is normally taken into account by applying correction coefficients to

the two velocity derivations:

$$\alpha_1 \frac{\partial u}{\partial t} \qquad \text{and} \qquad \alpha_2 \left(u \frac{\partial u}{\partial x} \right)$$

where $\alpha_1 = \int \frac{u^2 dA}{\overline{u}^2 A}$; $\alpha_2 = \int \frac{u^3 dA}{\overline{u}^3 A}$; u the local and $\overline{u}$ the mean velocity. The derivation of α_2 can be obtained by equating the integrated transfer of kinetic energy through each element dA, per unit weight of fluid, to the transfer based on the mean velocity. In a similar fashion, α_1 is derived from a transfer of momentum (Chow, 1959).

It can be shown that α_2 must be larger than α_1. Conversely, the term $u\frac{\partial u}{\partial x}$ with which α_2 is associated, is in most cases much smaller than the other terms in the equation of motion, as was demonstrated in an analysis of these terms by McDowell and O'Connor (1977) for a number of tidal rivers. Both coefficients are normally neglected in a smooth single channel.

However, with its irregular bottom topography, the lower part of the Campbell River estuary cannot be characterized as a smooth single channel and the velocity coefficients may be significant. To evaluate these coefficients in each segment, current profiles would have to be taken almost simultaneously from shore to shore, an operation which would be hampered by many obstacles. Although the river discharge is fairly constant, the measurements would still have to be taken at a variety of tidal conditions to account for changes in bottom friction as the tides move in and out.

Separating the estuary into two different but much more uniform flow regimes avoided this need for an elaborate additional field program which would have had little other use than an upgraded estimate of the mean flow in the schematized segments. The area was schematized into two one-dimensional models with the tides as a common downstream boundary condition. The "river model" covered the main channel below the highway bridge and the "storage model" covered the storage basin and Tyee Channel (Fig. 3). The upstream boundary condition of the river model was the discharge measured at the Hart Dam with a 10% increase for the tributary inflow from the Quinsam River. The storage model's upstream boundary condition was the discharge set at zero. A slough around Baikie Island and a freshwater marina were included in the river model. The observed tides at the nearby Argonaut Wharf were the downstream boundary condition shared by both models. This boundary was assumed to be right at the entrance instead of farther south of Tyee Point near the wharf where a permanent tide gauge would have represented the vertical tides somewhat better but where we could not assume the water movement to be one-dimensional. Records of three temporary tide gauges along the river and in Baikie Slough were used to calibrate the river model, *i.e.* to establish the friction coefficients C in the equation of motion. An estimate of the friction coefficient in the storage model was based on the similarity of its bottom with that of Baikie Slough. Table 1 lists the friction coefficients.

The low values of the coefficients compared to those in other estuary models, *e.g.* an average of 50 $m^{1/2}/sec$ in the Fraser River model, (Ages and Woollard, 1976) are not surprising if we keep in mind that the friction coefficients do not merely represent

Table 1 Friction Coefficients, C

Segment	Friction Coefficient ($m^{1/2}/sec$)
1 – 5	30
5 – 8	40
9 – 11	30
11 – 14	40
15 – 22	30
31 – 38	40

the bottom friction but any obstruction which would influence the "tuning" of the model, such as the many piles and stored log booms in these shallow waters. Increasing the friction coefficient relaxed the friction term to the extent that the model's output started to generate unacceptable fluctuations. It became completely unstable at $C = 70\ m^{1/2}/sec$.

Another form of instability in this explicit type of scheme is caused by the progressive amplification of numerical errors introduced by rewriting the differential equations in finite differences. The criterion for unconditional stability has been investigated by several authors, *e.g.* Leendertse (1967), and has been established at $\frac{\Delta x}{\Delta t} \geq c$, where $c = \sqrt{gh}$, the velocity of a tidal wave in shallow water of depth h. To satisfy this condition, the time step and segment length were set at 5 sec and 140 to 200 m, respectively. Calibration curves, comparing the model-produced tidal heights with those recorded at three sections are plotted in Figs. 15 to 17.

In the reaches affected by the salinity intrusions (sections 7 and 17, Fig. 3), the computed and observed high water levels agree closely, while the computed corresponding low waters are higher than the observed ones. This error could not be eliminated by the friction coefficients without detracting from the more important accuracy of the high waters. The inconsistency between the comparisons could perhaps be explained by the type of tide gauges used for the calibration. They were pressure gauges, set at a sea water density of 1.025, and could be expected to be less accurate at low tides when the salt wedge had retreated. More importantly, the readings would also be lower because of the velocity head created by the faster flow. An average negative error of 15 cm throughout a tidal cycle in our computed water levels near the bridge was more difficult to explain but we might speculate that it was due to a nearby freshwater outfall. This location was well outside the limit of the salinity intrusion and a discrepancy in our computations of the tidal heights near the bridge would have little effect upon the estimated transport volumes of sea water. However, to produce accurate tidal predictions in these upstream reaches (for instance, for flood control), the model should be calibrated in more detail with one or two additional tide gauges.

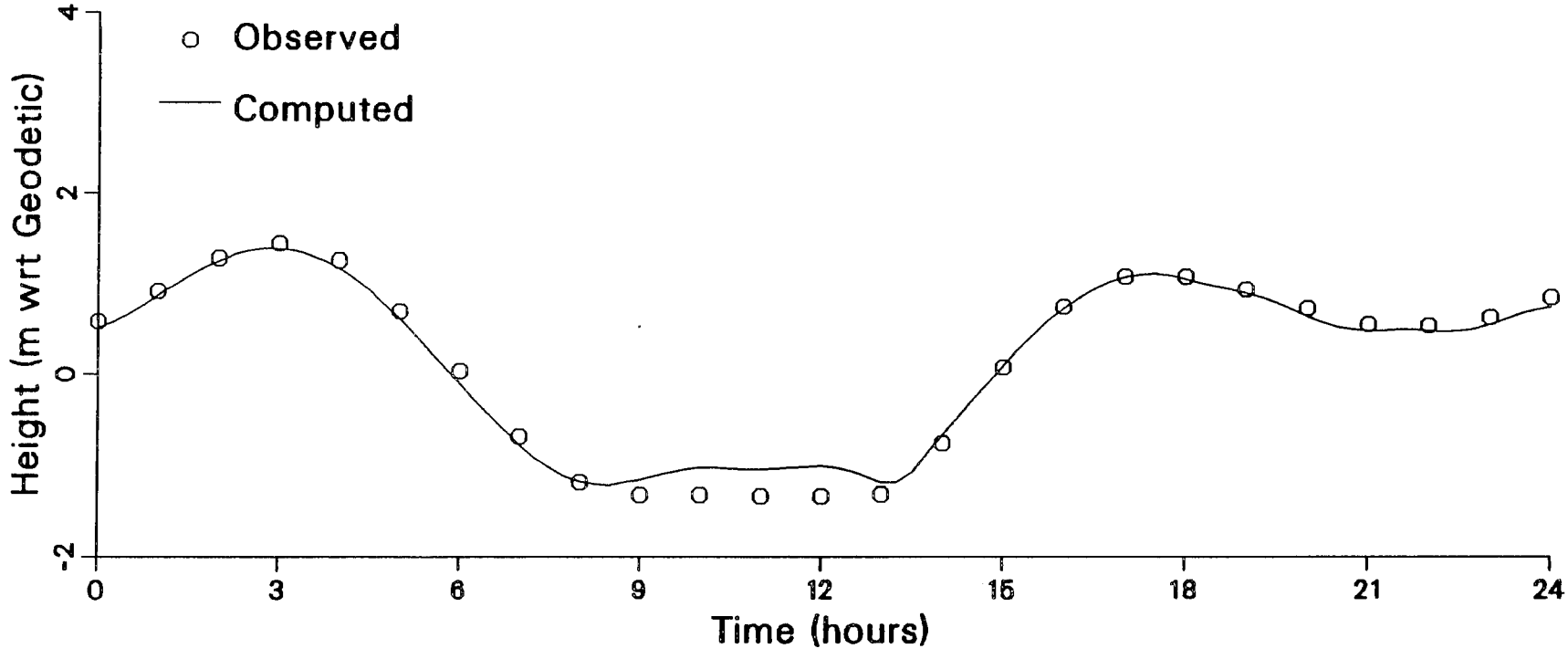

Fig. 15 Calibration of the Campbell River model, Section 7 (see Fig. 3), May 23, 1986. Discharge at the Hart Dam is 101 m^3/sec.

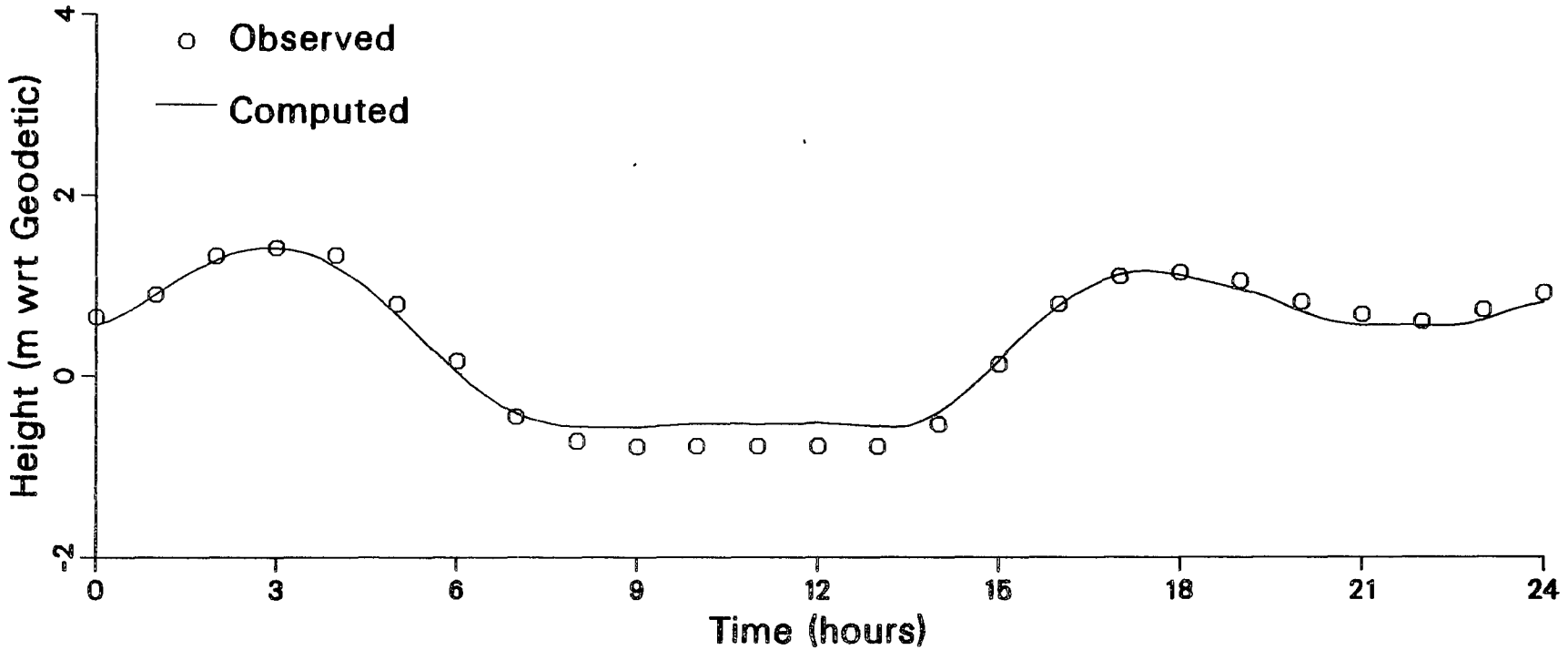

Fig. 16 Calibration of the Campbell River model, Section 17 (see Fig. 3), May 23, 1986. Discharge at the Hart Dam is 101 m^3/sec.

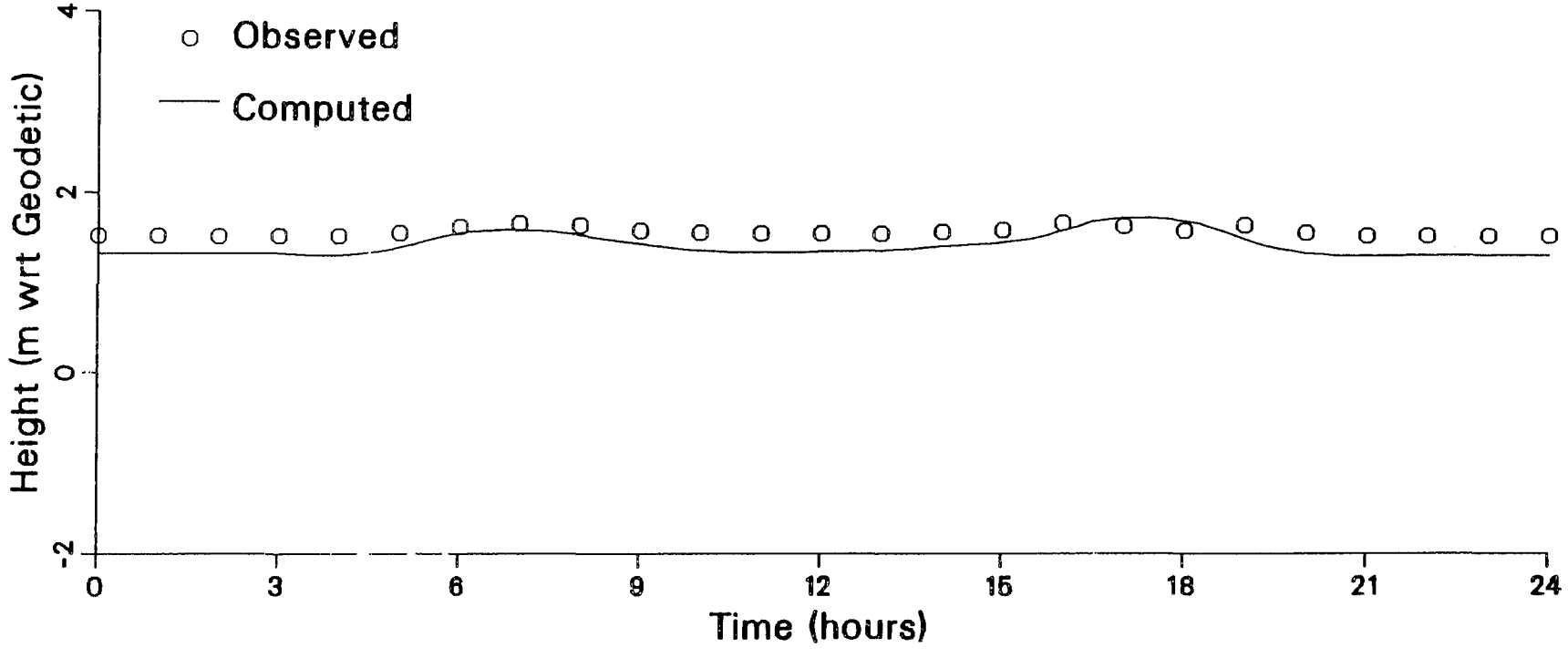

Fig. 17 Calibration of the Campbell River model, Section 21 (see Fig. 3), Oct. 12, 1984. Discharge at the Hart Dam is 166 m^3/sec.

a) Computation of Total Tidal Prism

The tidal prism of the entire estuary is the summation of volumes between low and high water in each schematized segment as obtained from the model:

$$\text{tidal prism} = (\Delta h)(B)(L) + \frac{1}{2}(\Delta h - y)\left\{BW + \frac{D_{\max} + y - \Delta h}{D_{\max}} BW\right\}(L) + (y)(BW)(L);$$

where (Fig. 18)

Δh = distance between high and low waters as computed by the model,
B = channel width, from schema,
L = segment length, from schema,
BW = bank width, from schema,
$D_{\max}$ = bank height, from schema,
y = $h + CD - D_{\max}$, where h is obtained from the model output, CD is the distance between geodetic and local chart datum.

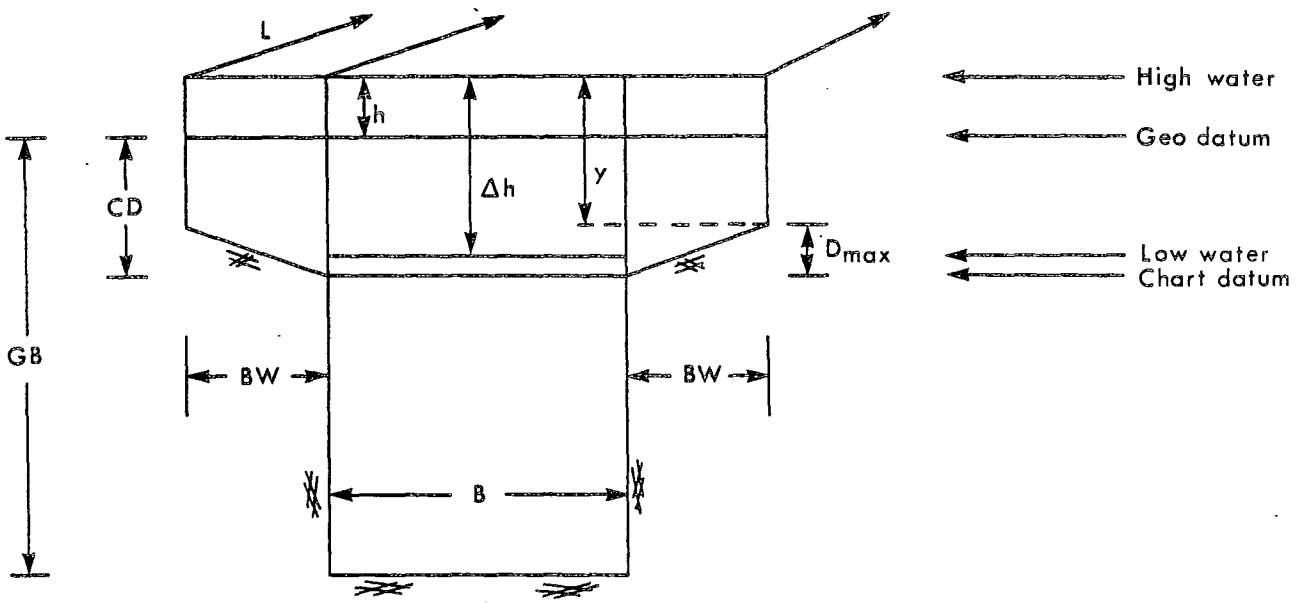

Fig. 18 Schematization of a cross-section for the computation of the tidal prism.

Since only y and Δh vary from day to day, the calculations are facilitated by writing:

$$\text{tidal prism per segment} = \underline{(B \cdot L)}\Delta h + \frac{L \cdot BW}{\underline{2D_{\max}}}(\Delta h - y)(2D_{\max} - (\Delta h - y)) + \underline{(BW)(L)}(y),$$

where the underlined terms are fixed for each segment.

Maximum and minimum water surface elevations throughout the estuary were calculated by the model for four dates, with an input of representative observed discharges and tides. The computer plots in Appendix B were used to obtain the term Δh in our equation for the tidal prism.

Table 2 lists the total tidal prisms for these dates, *i.e.* the tidal prisms between Tyee Point and the highway bridge, including Baikie Slough and the storage basin.

Table 2 Total Tidal Prism

Date	Q_{Dam} (m^3/sec)	High/Low Waters at Argonaut Wharf (m)	Tidal Prism ($\times 10^3$ m^3)
Sept. 10, 1984	90	4.04/1.66	1753.9
June 12, 1986	142	4.34/0.28	1813.0
July 8, 1982	113	3.81/1.05	1834.4
Aug. 13, 1986	58	4.15/1.36	1915.1

The relatively limited effect of the boundary conditions upon the volume changes shown by the table should be due mainly to the absence of flow reversals that would trap the freshwater inflow and hence increase the influence of the discharge on the tidal prism.

The computed tidal prism provided a general estimate of the volume of sea water entering the estuary per tidal cycle as required by the biological component of this study.

For most estuaries, the tidal prism would be a rather poor estimate of the accumulation of sea water during a tidal cycle because the salt wedge rarely retreats completely before the next high tide at the entrance. Moreover, the river usually backs up with the increasing tide for several hours, making it very difficult to evaluate the salt/fresh water of the total volume at high tide.

However, apart from a few deep persistent saline pockets in the storage basin, all sea water in the Campbell estuary is flushed out at an ebb tide and the river does not back up at a rising tide. Observations at various locations along the channel confirmed that the volume of fresh water leaving the estuary was very close to that of the discharge entering the upstream boundary near the bridge even at a high tide. For instance, using the cross-section at NBM Main and the flow profile of August 27, 1984 at 1816 h, we computed a freshwater outflow of 108 m^3/sec at high tide while the upstream discharge at the bridge was 112 m^3/sec. Similarly, at 1459 h, May 14, 1985, the freshwater outflow

at this station came to 50 m^3/sec at high tide, compared with a steady upstream discharge at the bridge of 52 m^3/sec. At a falling tide, the computed freshwater outflow at NBM Main at 0748 h, September 25, 1984, was 66 m^3/sec, versus a discharge of 64 m^3/sec at the bridge. NBM Main was chosen for most of the comparisons because of its regular cross-section which made the observed current profiles representative of the total flow. Computations at other downstream stations confirmed the results at NBM Main.

b) Variations in Local Seawater Transport

In addition to a volume estimate of the salinity intrusion in the entire estuary, the study of food availability needed a more detailed evaluation of the variation in local seawater transport during a tidal cycle.

NBM Main and Mother Ramp were selected not only because they represented the two flow regimes (the river and the storage basin, respectively) but also because of the large number of data collected at these stations.

Computations of the seawater volume at each cross-section per unit length of reach required the following information:

1.) the bottom contour obtained from a hydrographic survey,
2.) the water surface elevation at each observation, from the model,
3.) the salinity profile, from our observations,
4.) the tidal height at the entrance, from the permanent tide gauge at Argonaut Wharf.

With the salinity profile and cross-sectional area, the freshwater portion was computed and subtracted from the entire cross-sectional area to give the salt water volume per one metre length.

Computing the salt water portion directly from the cross-sectional area below the measured interface would have been less accurate because during our observations, the salinity probe was suspended about 20 cm above a lead weight and rarely reached the bottom. The freshwater portion was better defined by the measured distance between water surface and interface.

Resulting salinity volumes were plotted against corresponding tidal heights observed at the entrance (Figs. 19 to 21). A least-squares best-fit approximation was applied to the data points. Low and average discharges were considered separately for NBM Main. Only one data point was available for an extremely high discharge of 370 m^3/sec and was not included in the best-fit equation.

Finally, the variation of seawater volume per one metre segment length (obtained from these equations) was plotted against the observed tide at the entrance for both stations at 15-min intervals and at an average river discharge (Fig. 22). If required, volume variations at other stations can be computed in a similar fashion.

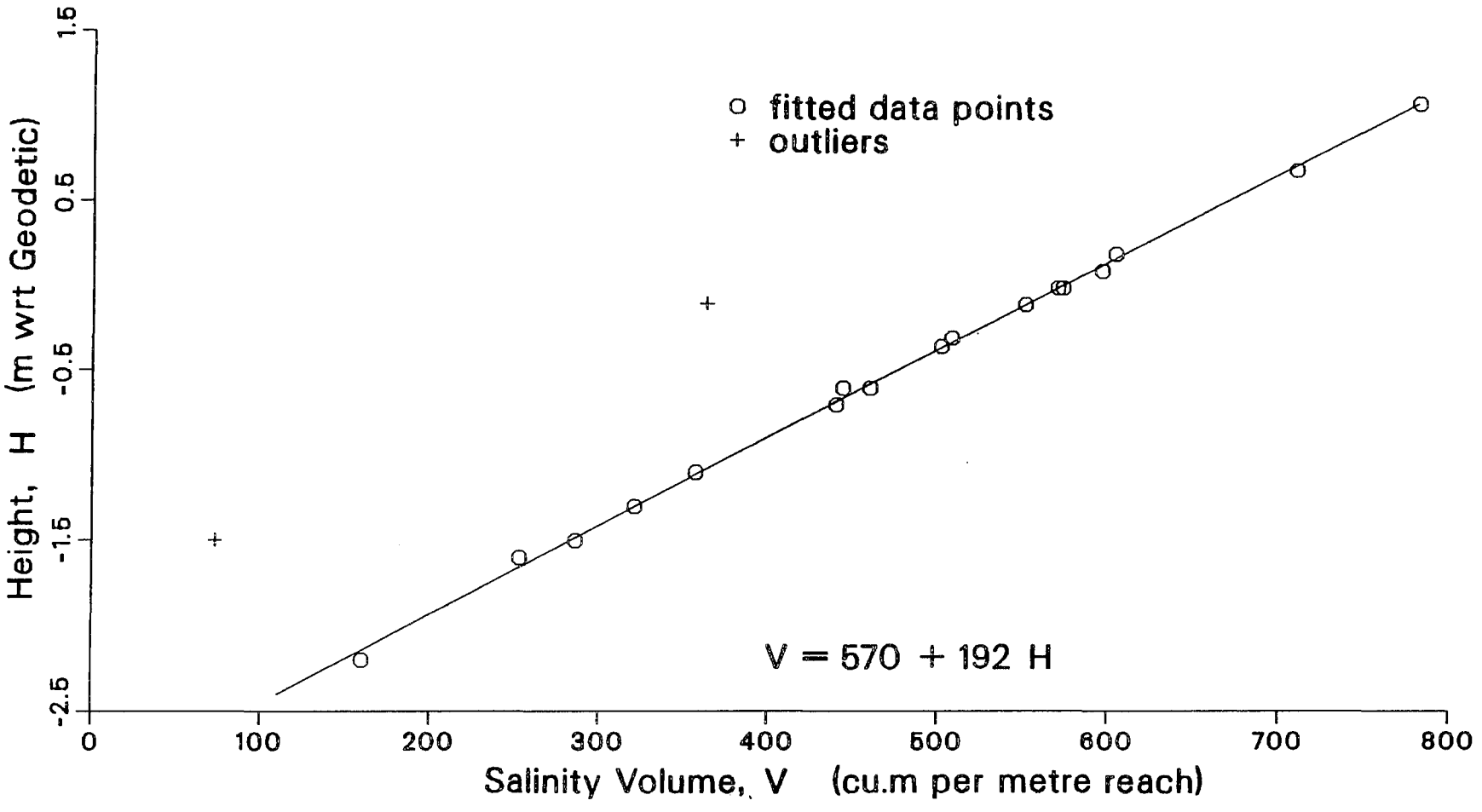

Fig. 19 Salinity volume, measured at station Mother Ramp, versus the tidal height at the mouth of the Campbell River.

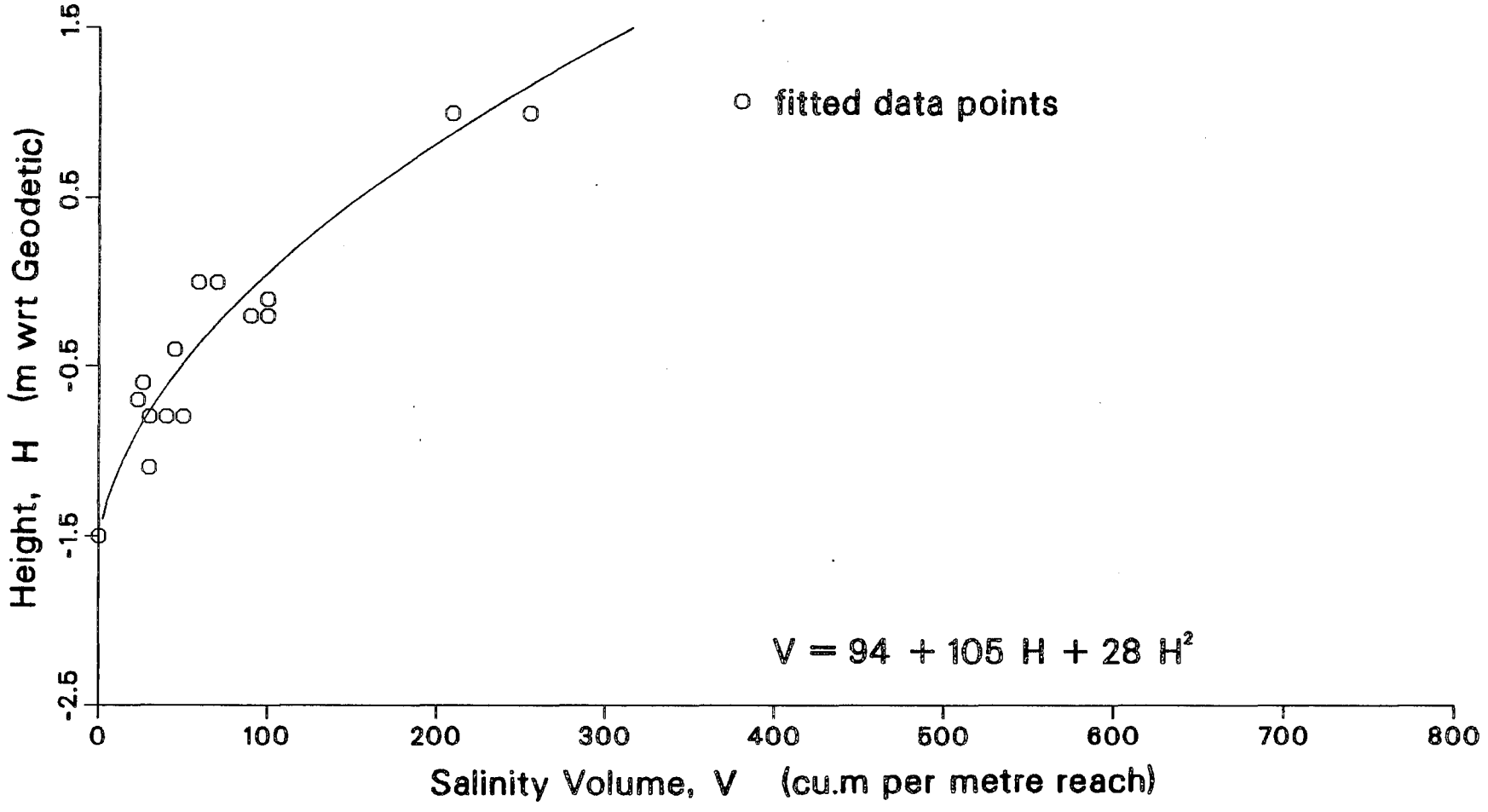

Fig. 20 Salinity volume, measured at station NBM Main during low discharge (40–70 m^3/sec), versus the tidal height at the mouth of the Campbell River.

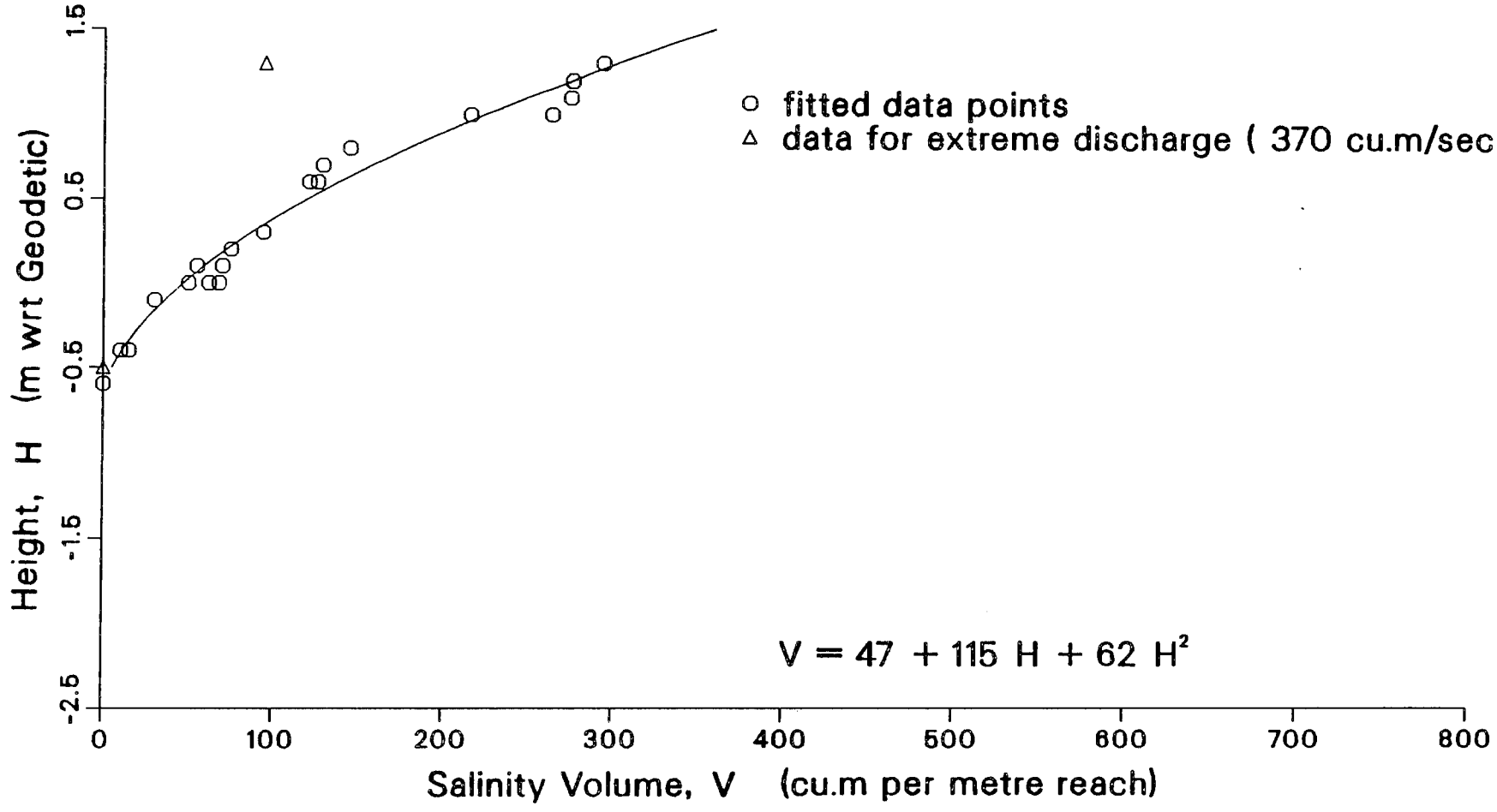

Fig. 21 Salinity volume, measured at station NBM Main during average discharge of 90–100 m^3/sec, versus the tidal height at the mouth of the Campbell River.

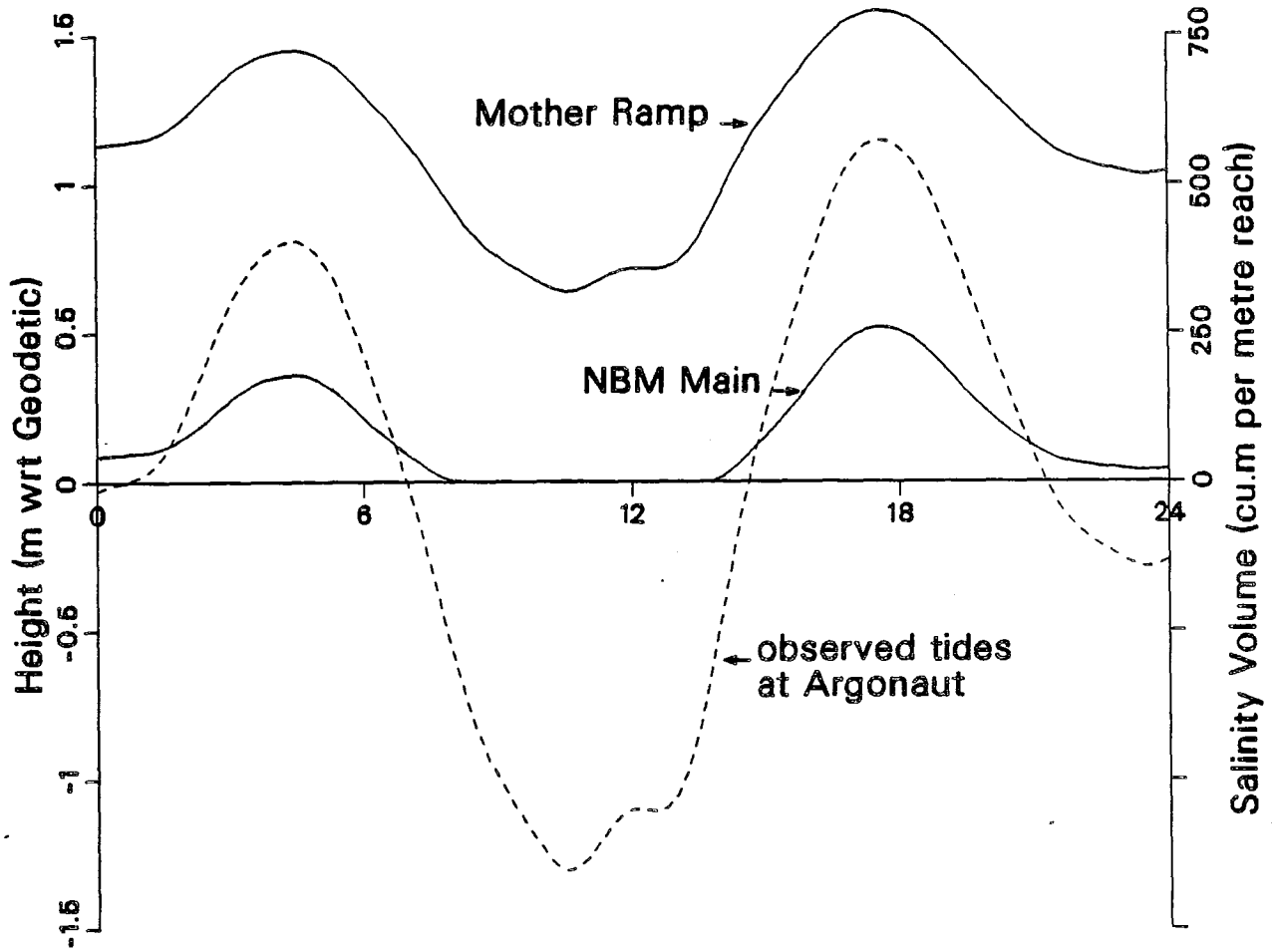

Fig. 22 Sea water volume per metre reach at two stations in the Campbell River for a 24-h period September 10, 1984.

SUMMARY AND RECOMMENDATIONS

To support a biological study of the Campbell River estuary, much of the hydrodynamic analysis discussed in this report focussed on the salinity intrusion as a source of marine food for juvenile salmon. Related aspects such as tidal propagation, flow distribution, temperatures and winds were also covered.

In a somewhat condensed form, the main objectives of this analysis were:

1.) to examine the conditions under which vertical transport across the halocline could be expected;
2.) to estimate the volume of sea water entering the system during a tidal cycle,
   a) throughout the entire estuary,
   b) at selected locations.

Conditions inducing vertical transport (*i.e.* mixing) depend largely on the stability of the interface between fresh and salt water. Using both Richardson and interfacial

Froude numbers as indicators of this stability, we concluded that significant vertical mixing across the halocline in the main channel could only be expected near the head of an advancing salt wedge and, for a short time, during the retreat of the wedge when the interface disintegrates. Even without computing the two dimensionless numbers, one could readily arrive at the same conclusion by a cursory inspection of the salinity contours and velocity vectors in Appendix A.

Away from the influence of the river flow, the traditional use of Richardson and Froude numbers as criteria for mixing would be meaningless because of the absence of any measurable currents in either the storage basin or Baikie Slough, the main bodies of water adjacent to the river. Most of the time, our data records indicate some salt in the surface layers of the strongly stratified storage basin, and low salinities from surface to bottom in the very shallow Baikie Slough.

To estimate the volume of sea water entering the estuary during a full tidal cycle, a model was developed which computed the tidal prism of the entire study area at representative discharges and tides. The model had to take into account two distinct flow regimes (the river and the storage basin) and was therefore split into two coupled one-dimensional schematizations (*i.e.* parallel models with shared downstream boundary conditions).

Mainly because of the controlled discharge and the absence of flow reversals at a flood tide, the tidal prism was found to remain relatively constant at approximately 1.8×10^6 m^3. It was shown that in this particular estuary, the tidal prism was a reasonably accurate estimate of the volume of sea water entering during a tidal cycle.

Computations of sea water volumes at selected locations followed a different approach. Here, an empirical relationship between local salt water volumes and tidal heights at the entrance had to be established, using observed salinity profiles, model-produced local water surface elevations and recorded tidal heights near the entrance. As an example of this procedure, a computer plot demonstrated the variation of sea water volumes during a tidal cycle for two stations at an average discharge. Volume variations at other locations can be treated in a similar fashion.

Sea water volume computations assumed salinities of at least $1^0/_{00}$. If a higher threshold salinity is required (*e.g.* to account for the survival of certain zooplankton species) the salinity profiles have to be reviewed and the computations modified accordingly.

The model was calibrated for average discharges. High discharges rarely occur. They imply substantial releases of water at the Hart Dam which would result in extensive flooding of the surrounding community.

The abundance of field data facilitated the computations by allowing the use of a modified version of a one-dimensional model. combined with observed salinity profiles. It would be a worthwhile but much more costly project to compare our results with a two- or three-dimensional model using the same topography and boundary conditions. A proposed dredging operation at the estuary entrance in the near future may necessitate re-calibration of the model and a review of our field data. Increasing the depth at the

entrance is unlikely to move the limit of the salt wedge farther upstream because this limit is restricted by the supercritical flow at the bridge.

Because of its clear and shallow water and its predictable, controlled river flow, the Campbell River estuary presented us with a unique opportunity to monitor the salinity intrusion with unsophisticated instrumentation. The depth of the interface between salt and fresh water, as well as that of the abrupt current reversal, could be measured within centimetres and the movement of the head of the wedge could be followed by visually tracking suspended particles advancing with the wedge along the bottom. This very small and accessible estuary seems to be an excellent site for any future research for a variety of aspects pertinent to the salinity intrusion, for instance, a critical re-evaluation of the Richardson and interfacial Froude numbers as indicators of the stability of the interface between salt and fresh water.

REFERENCES

Ages, A.B., 1973. A Numerical Model of Victoria Harbour to Predict Tidal Response to Proposed Hydraulic Structures. Pacific Marine Science Report, **73-3**.

Ages, A.B., F.A. Dobbs and C. McAllister, 1990. The Salinity Intrusion in the Campbell River Estuary. Canadian Data Report of Hydrography and Ocean Sciences, **83(1,2)**.

Ages, A.B. and A.L. Woollard, 1976. The Tides in the Fraser Estuary. Pacific Marine Science Report, **76-5**.

Bell, L. and J. Thompson, 1977. The Campbell River Estuary. Special Estuary Series, **7**, Fisheries and Environment Canada.

Bornhold, B.D., 1990. Pacific Geoscience Centre, personal communication.

Brownlee, M.J., E.R. Mattice and C.D. Levings, 1984. The Campbell River Estuary: A Report on the Design, Construction and Preliminary Follow-up Study Findings of Intertidal Marsh Islands Created for Purposes of Estuarine Rehabilitation. Canadian Manuscript Report of Fisheries and Aquatic Sciences, **1789**.

Chow, V.T., 1959. Open-Channel Hydraulics. McGraw-Hill, N.Y.

Crean, P.B., T.S. Murty and J.A. Stronach, 1988. Mathematical Modelling of Tides and Estuarine Circulation. Springer-Verlag, N.Y.

Dietrich, G. and K. Kalle, 1975. Allgemeine Meereskunde. Bornträger, Berlin.

Dronkers, J.J., 1964. Tidal Computations in Rivers and Coastal Waters. Noord Holland Publ. Co., Amsterdam.

Leendertse, J., 1967. Aspects of a Computational Model for Long-Period Water-Wave Propagation. Memorandum RM–5294–PR, Rand Corp.

McDowell, D.M. and B.C. O'Connor, 1977. Hydraulic Behaviour of Estuaries. Wiley, N.Y.

Miles, J.W., 1961. On the stability of heterogeneous shear flows. *J. Fluid Mech.*, **10**: 496–512.

Richardson, L.F., 1920. The supply of energy from and to atmospheric eddies. *Proc. Roy. Soc.*, **A97**: 354–373.

Schlichting, H., 1960. Boundary Layer Theory. McGraw Hill Book Co., N.Y.

THIS PAGE IS BLANK

APPENDIX A

THIS PAGE IS BLANK

SALINITY AND CURRENT DISTRIBUTION
CAMPBELL RIVER ESTUARY

JULY 30, 1984 : 1503 - 1521 hrs

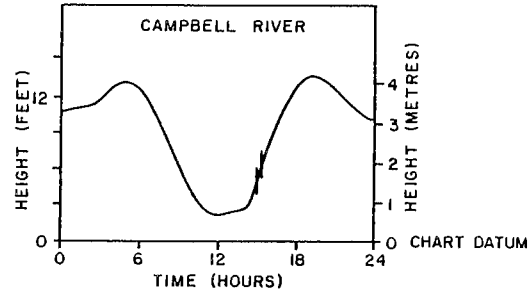

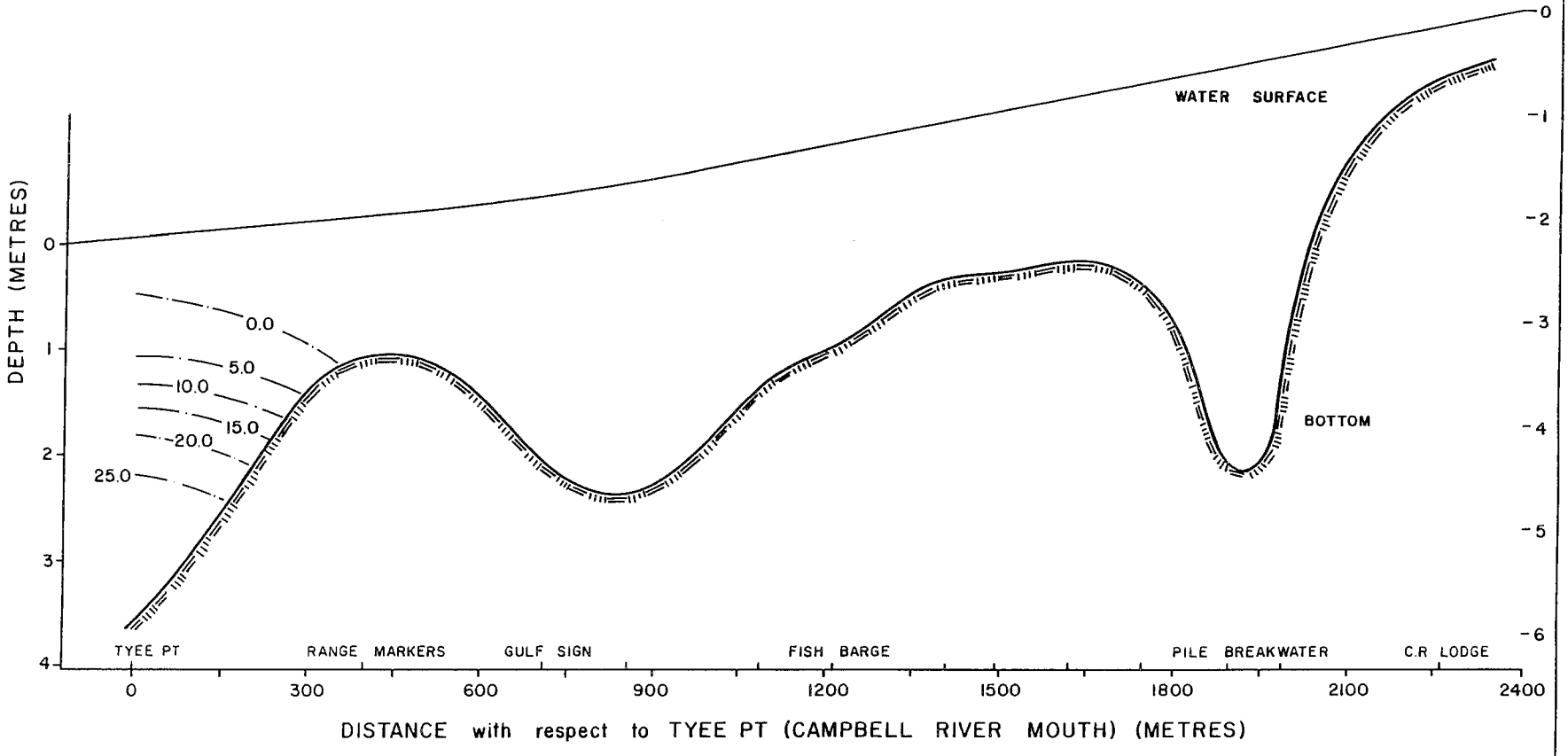

SALINITY AND CURRENT DISTRIBUTION
CAMPBELL RIVER ESTUARY

JULY 30 1984 : 1840 - 1943 hrs

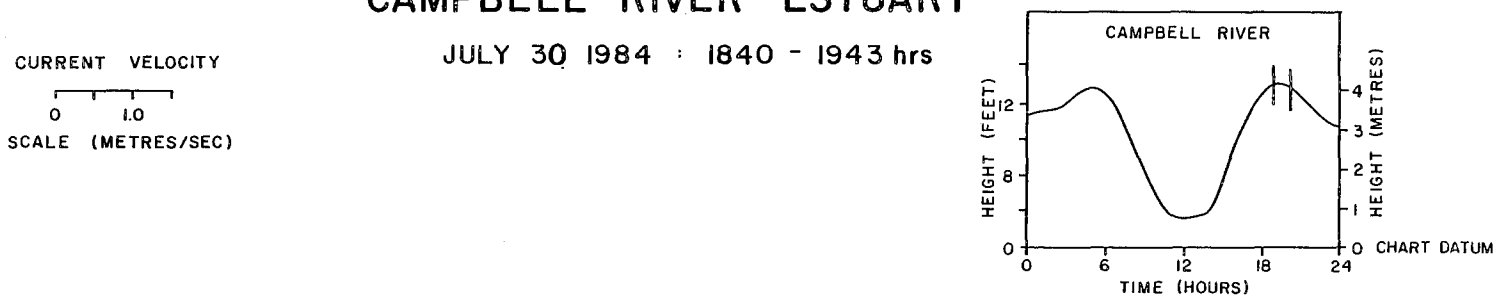

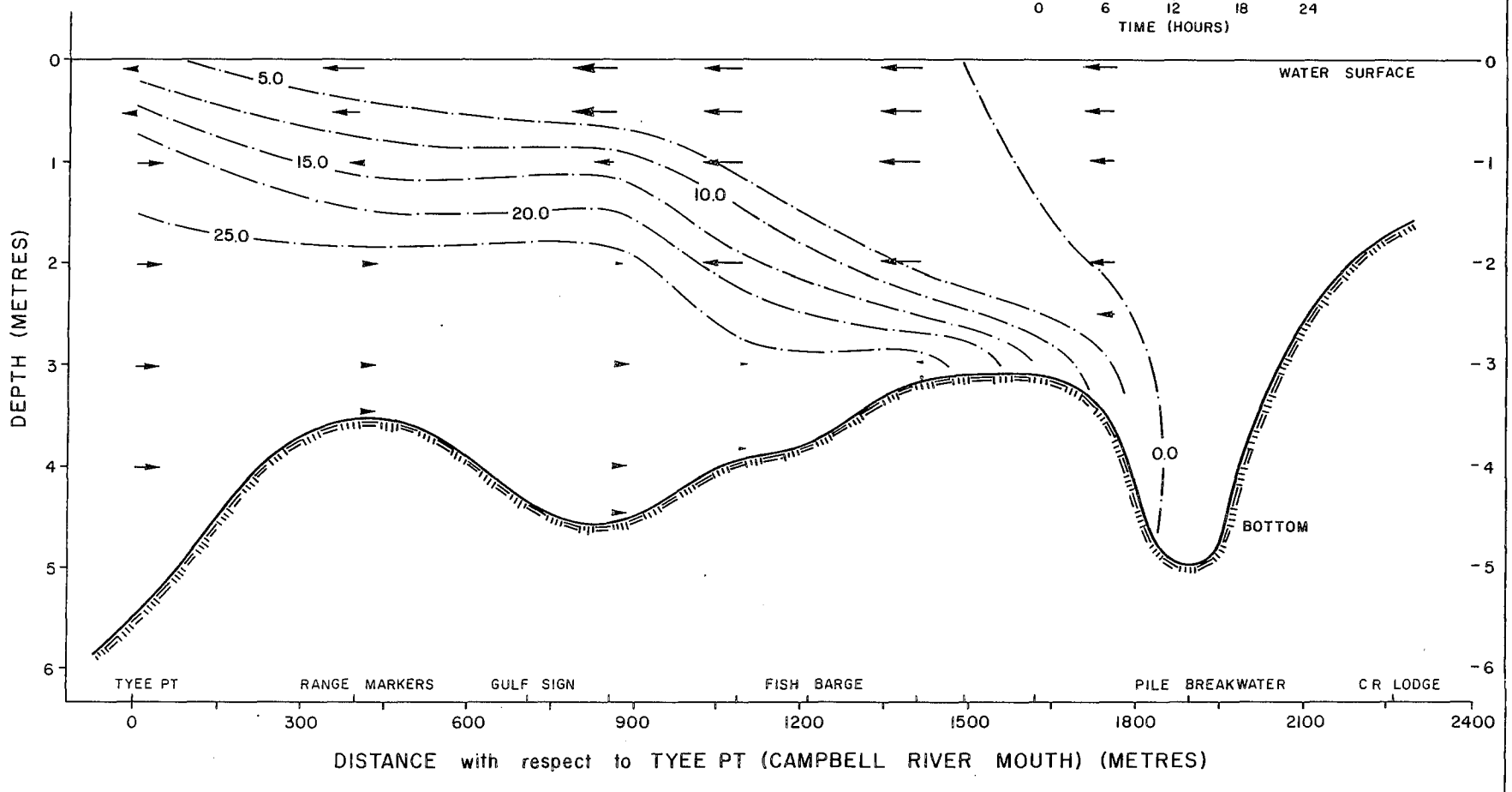

SALINITY AND CURRENT DISTRIBUTION
CAMPBELL RIVER ESTUARY

JULY 30, 1984 : 1955 - 2027 hrs

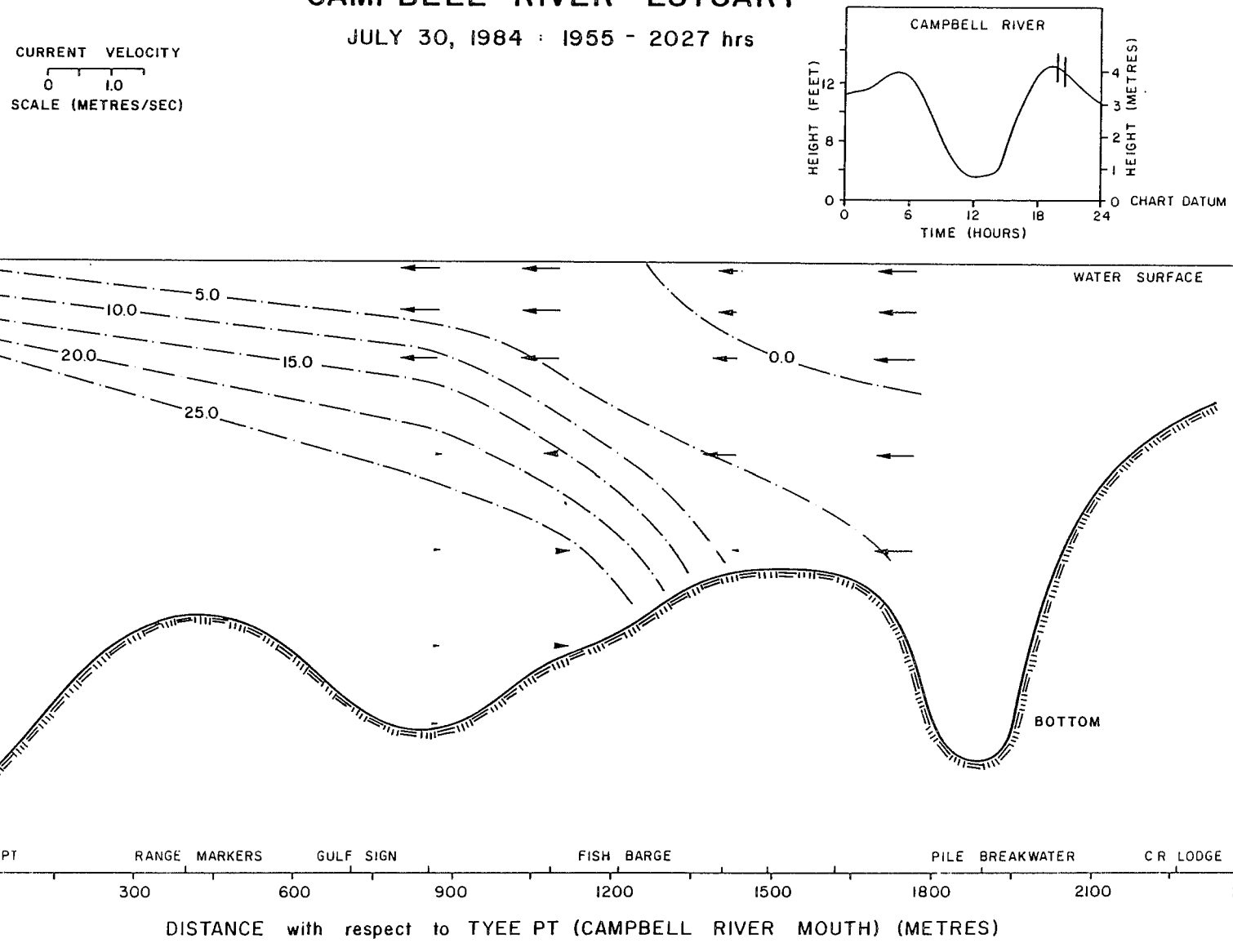

SALINITY AND CURRENT DISTRIBUTION
CAMPBELL RIVER ESTUARY

JULY 31, 1984 : 0708 - 0756 hrs

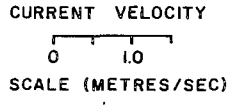

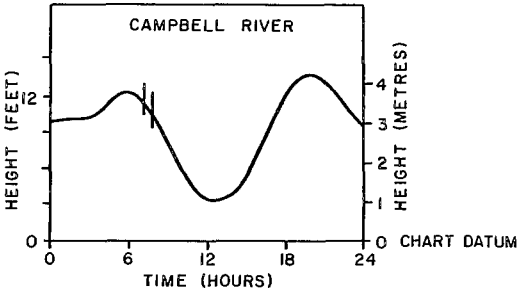

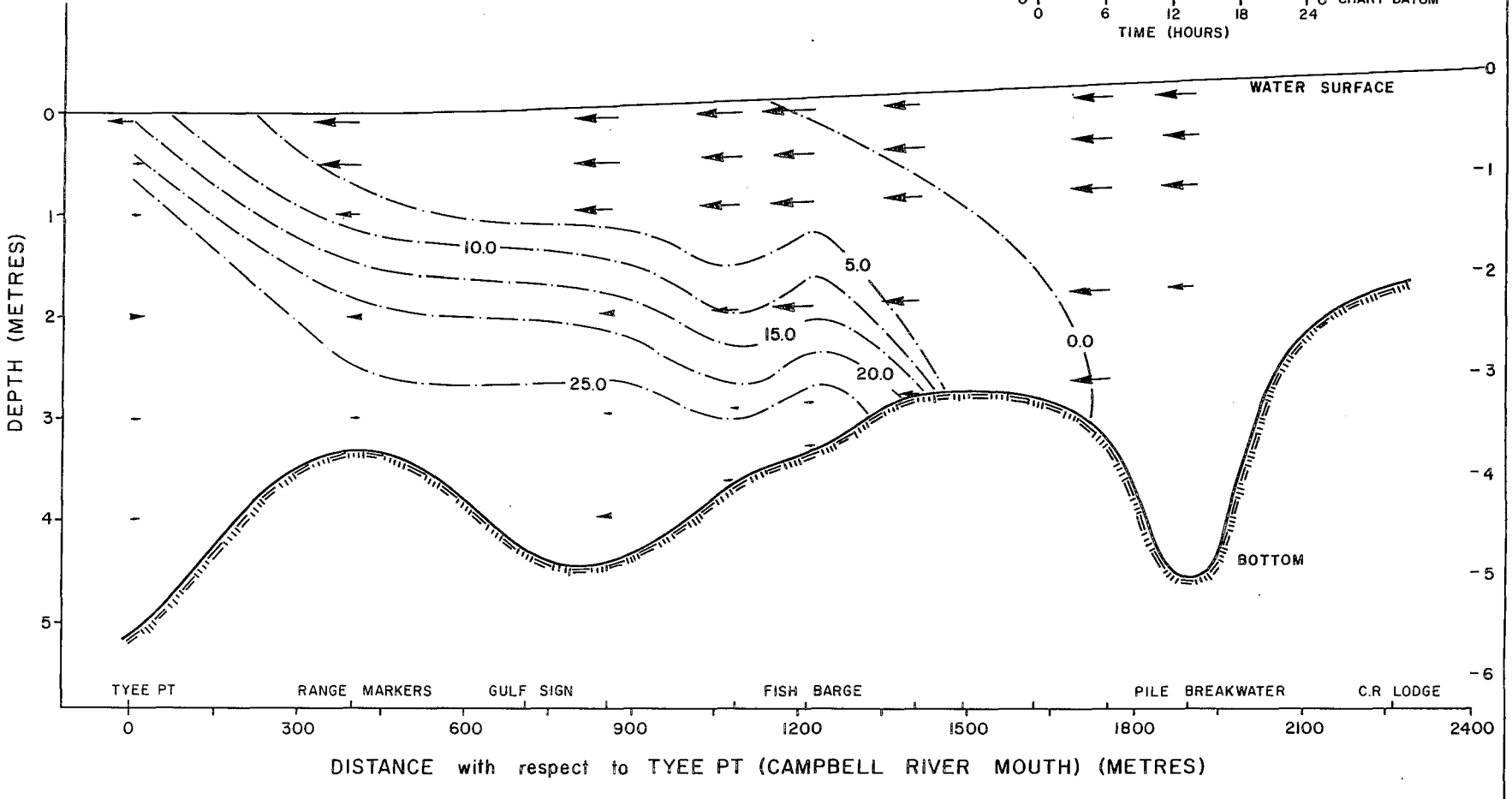

SALINITY AND CURRENT DISTRIBUTION
CAMPBELL RIVER ESTUARY

JULY 31, 1984 : 0851 - 0930 hrs

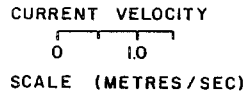

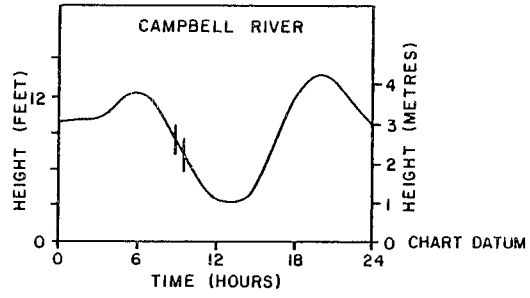

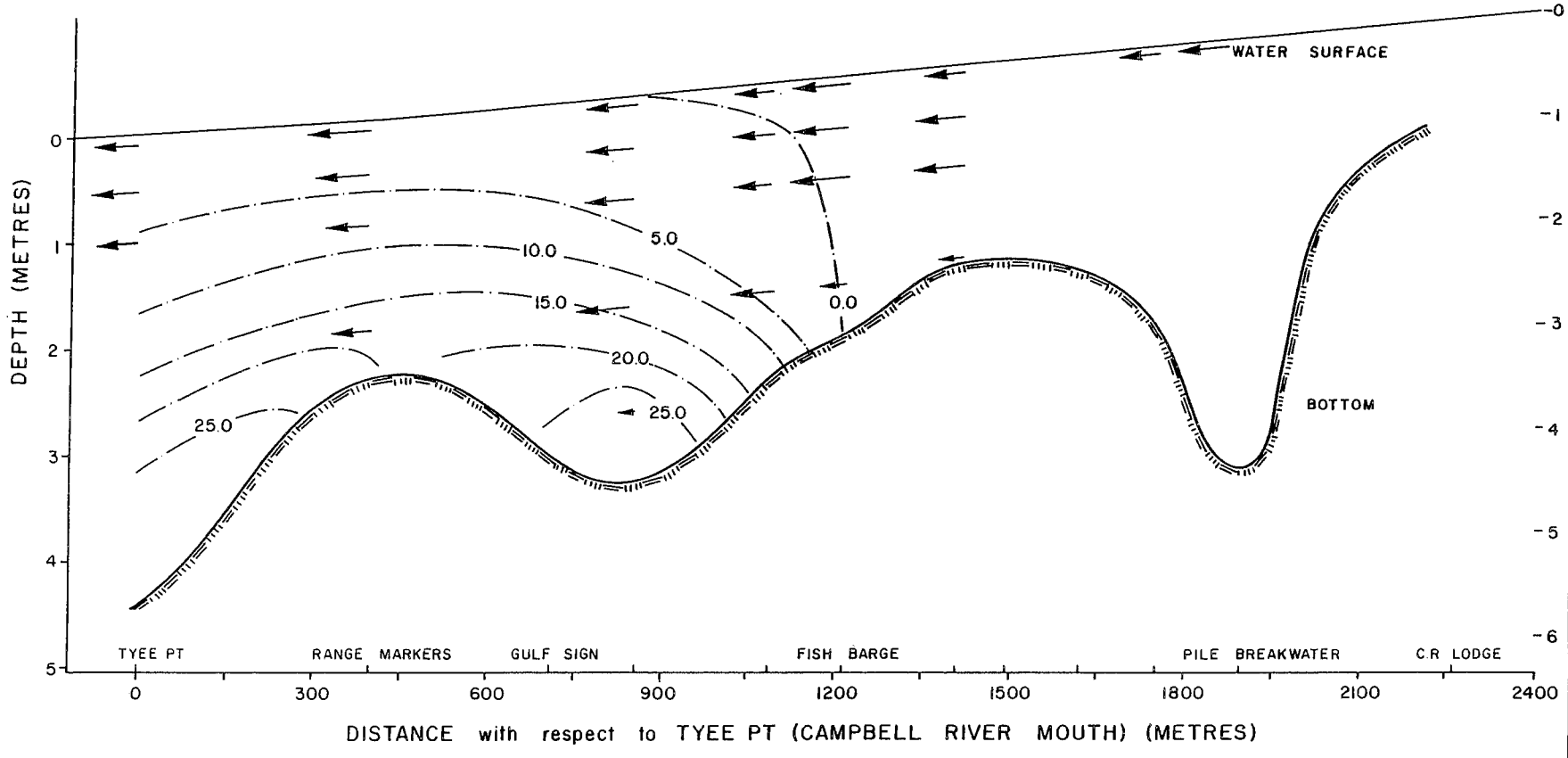

SALINITY AND CURRENT DISTRIBUTION
CAMPBELL RIVER ESTUARY

JULY 31, 1984 : 1020 - 1047 hrs

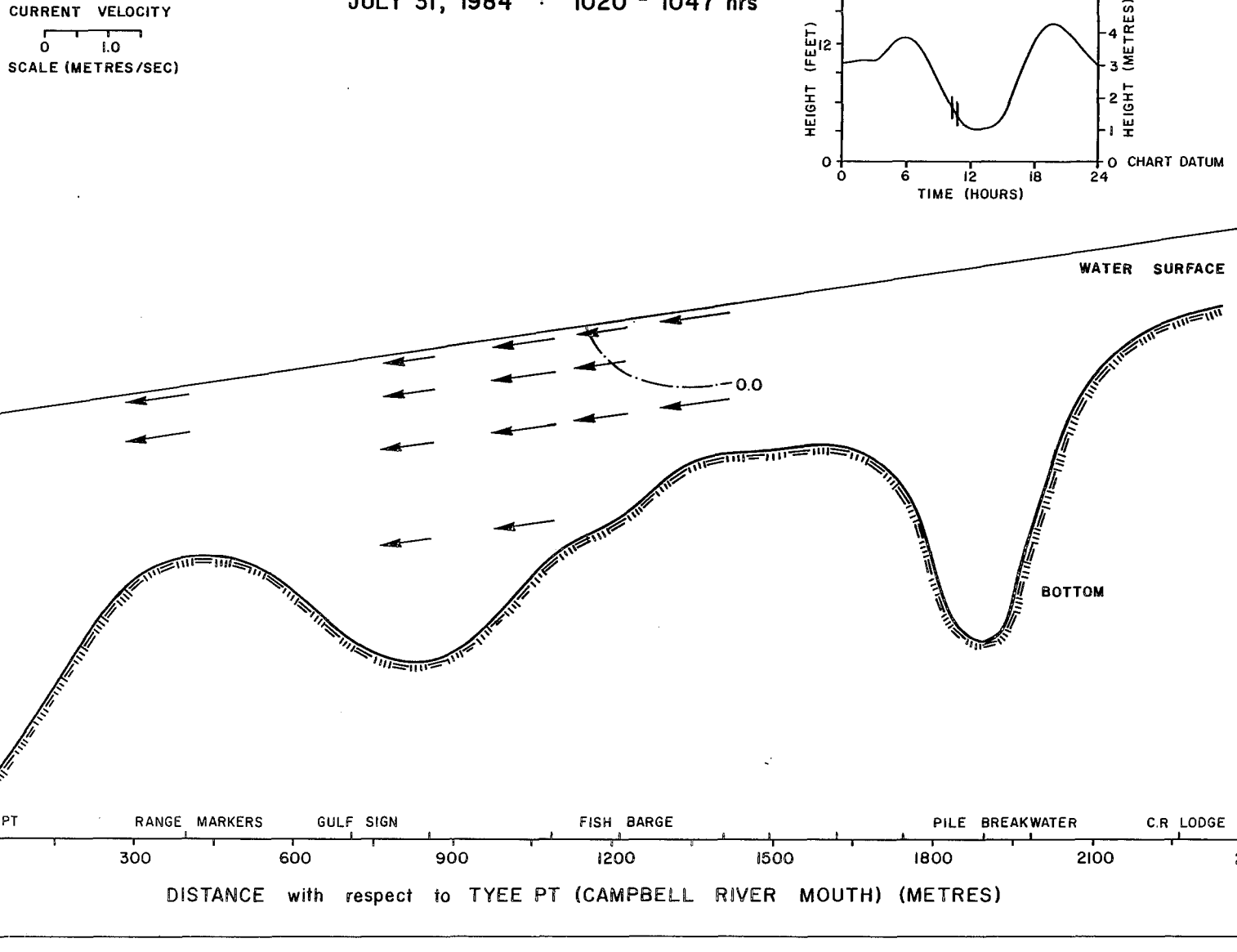

SALINITY AND CURRENT DISTRIBUTION
CAMPBELL RIVER ESTUARY

AUGUST 13, 1984 : 1237 - 1314 hrs

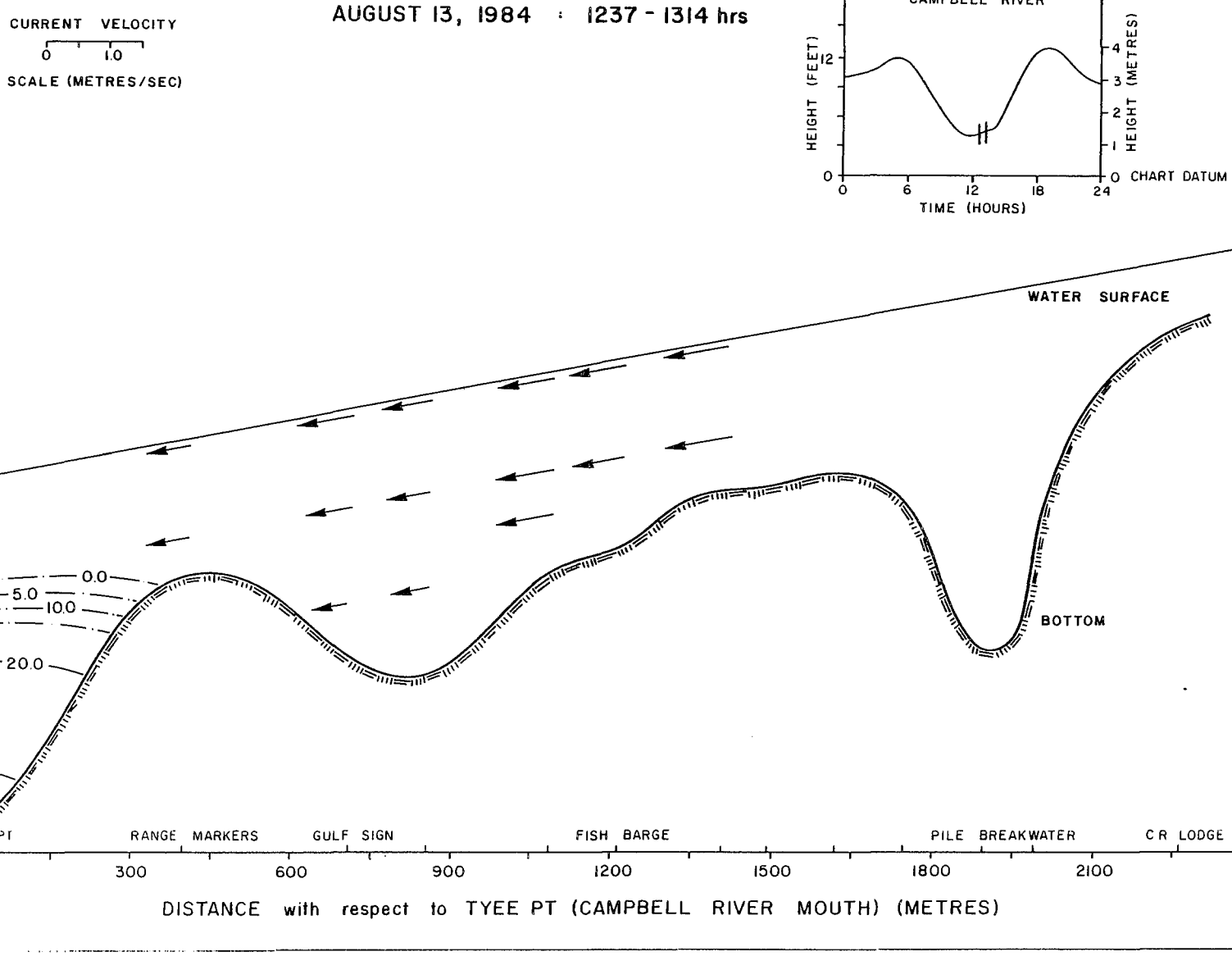

SALINITY AND CURRENT DISTRIBUTION
CAMPBELL RIVER ESTUARY

AUGUST 13, 1984 : 1408 - 1416 hrs

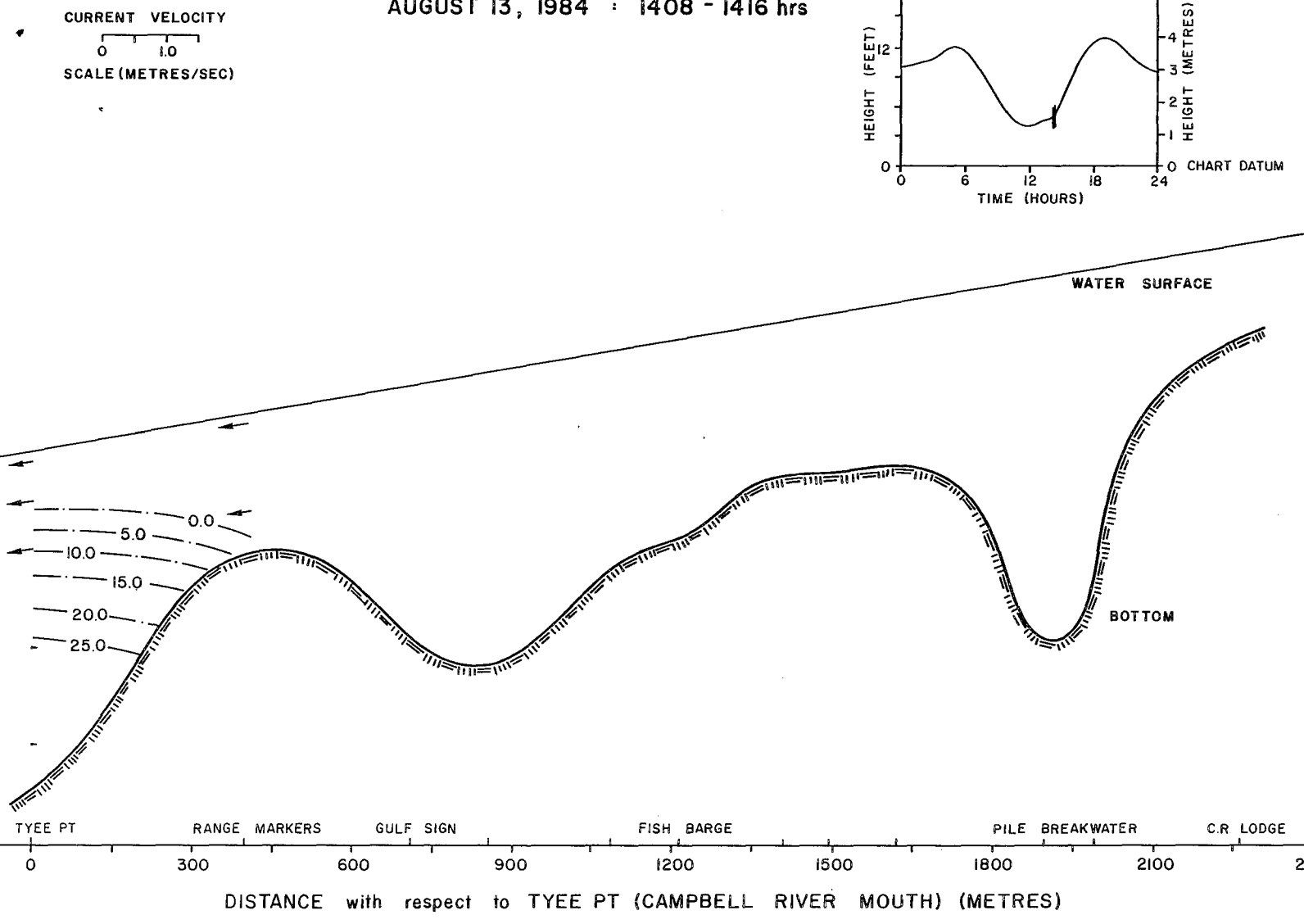

SALINITY AND CURRENT DISTRIBUTION
CAMPBELL RIVER ESTUARY
AUGUST 13, 1984 : 1514 - 1533 hrs

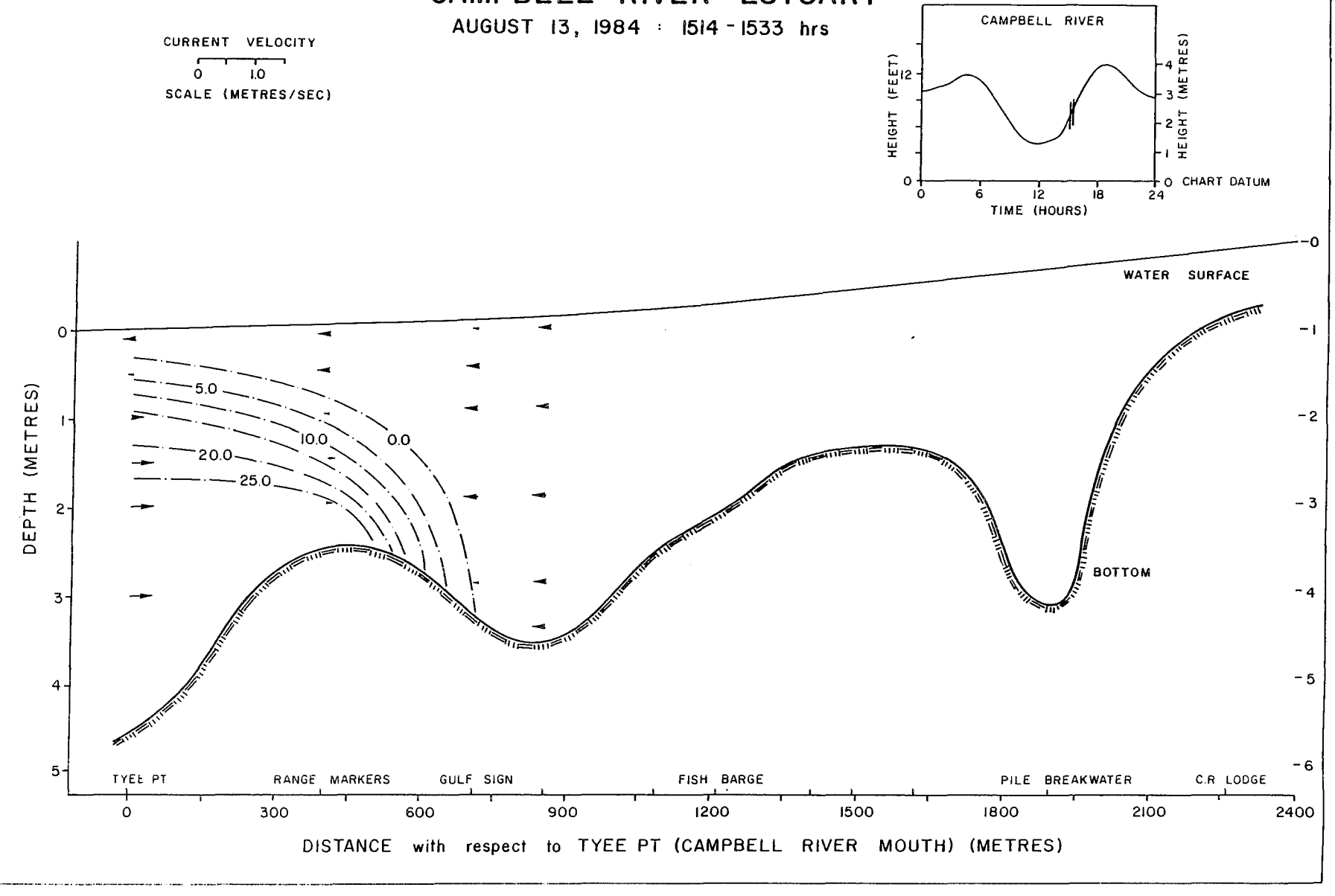

SALINITY AND CURRENT DISTRIBUTION
CAMPBELL RIVER ESTUARY

AUGUST 13, 1984 : 1550 - 1632 hrs

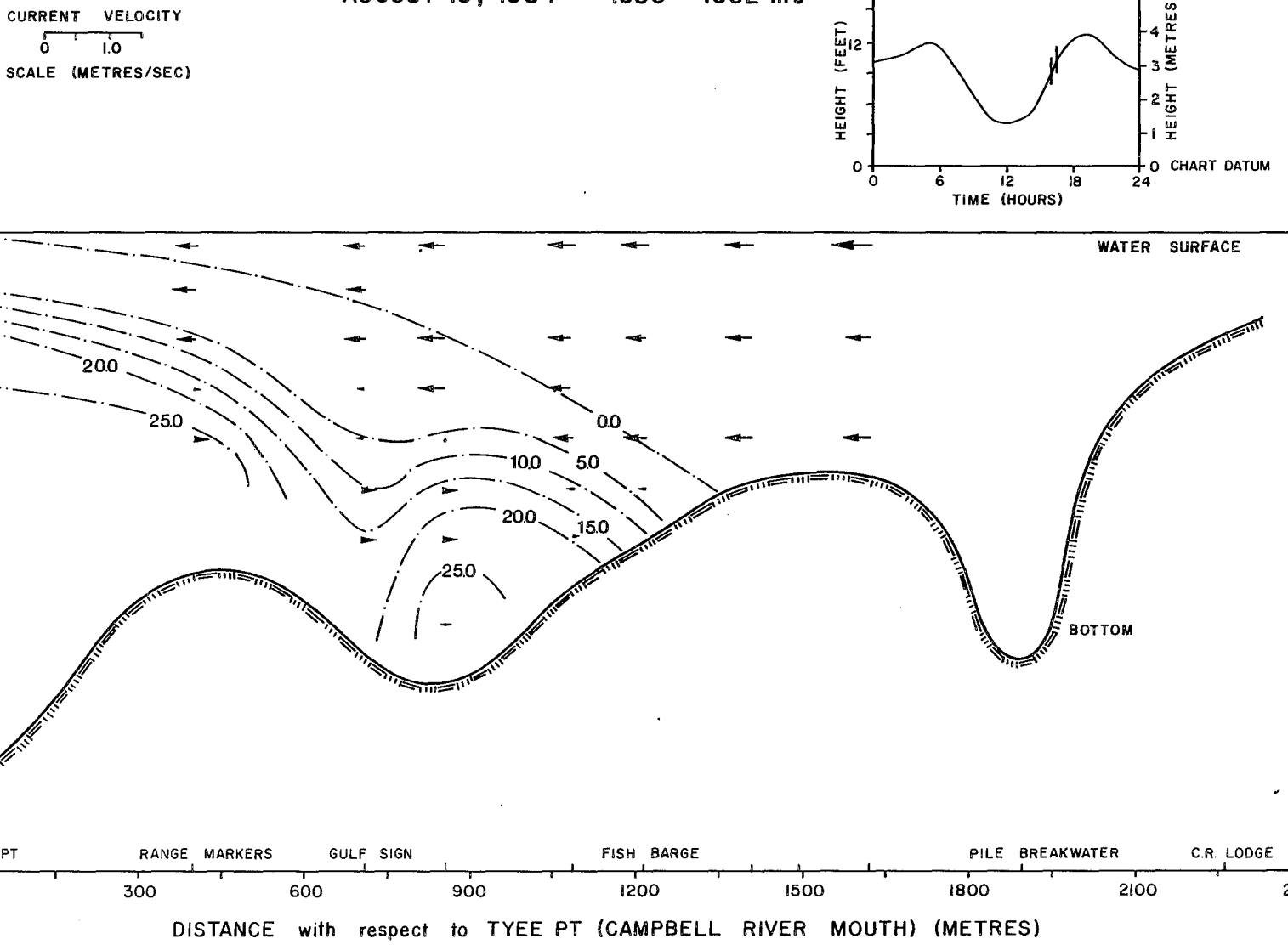

SALINITY AND CURRENT DISTRIBUTION
CAMPBELL RIVER ESTUARY

AUGUST 13, 1984 1642 : 1802 hrs

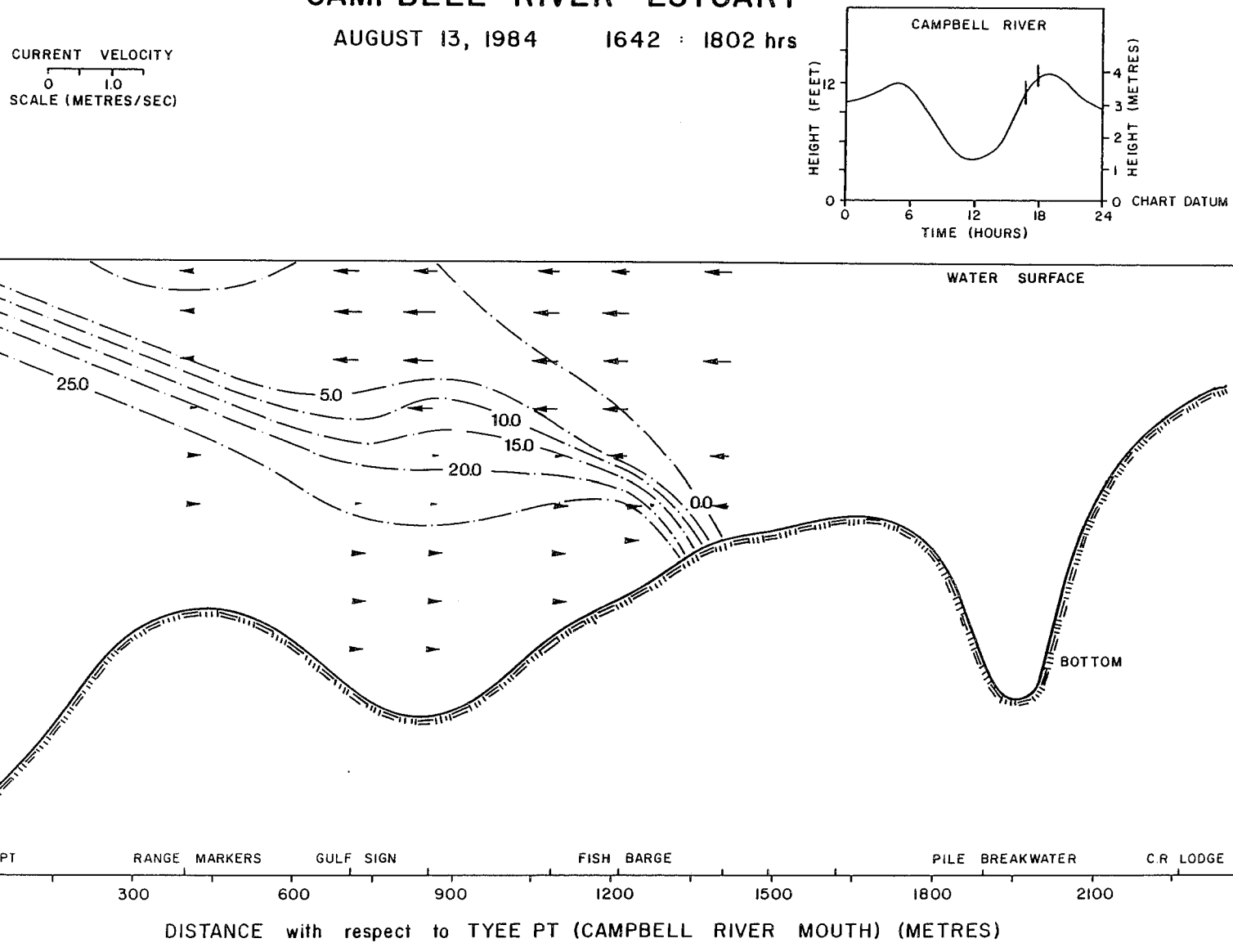

SALINITY AND CURRENT DISTRIBUTION
CAMPBELL RIVER ESTUARY
AUGUST 13, 1984 : 1820 - 1912 hrs

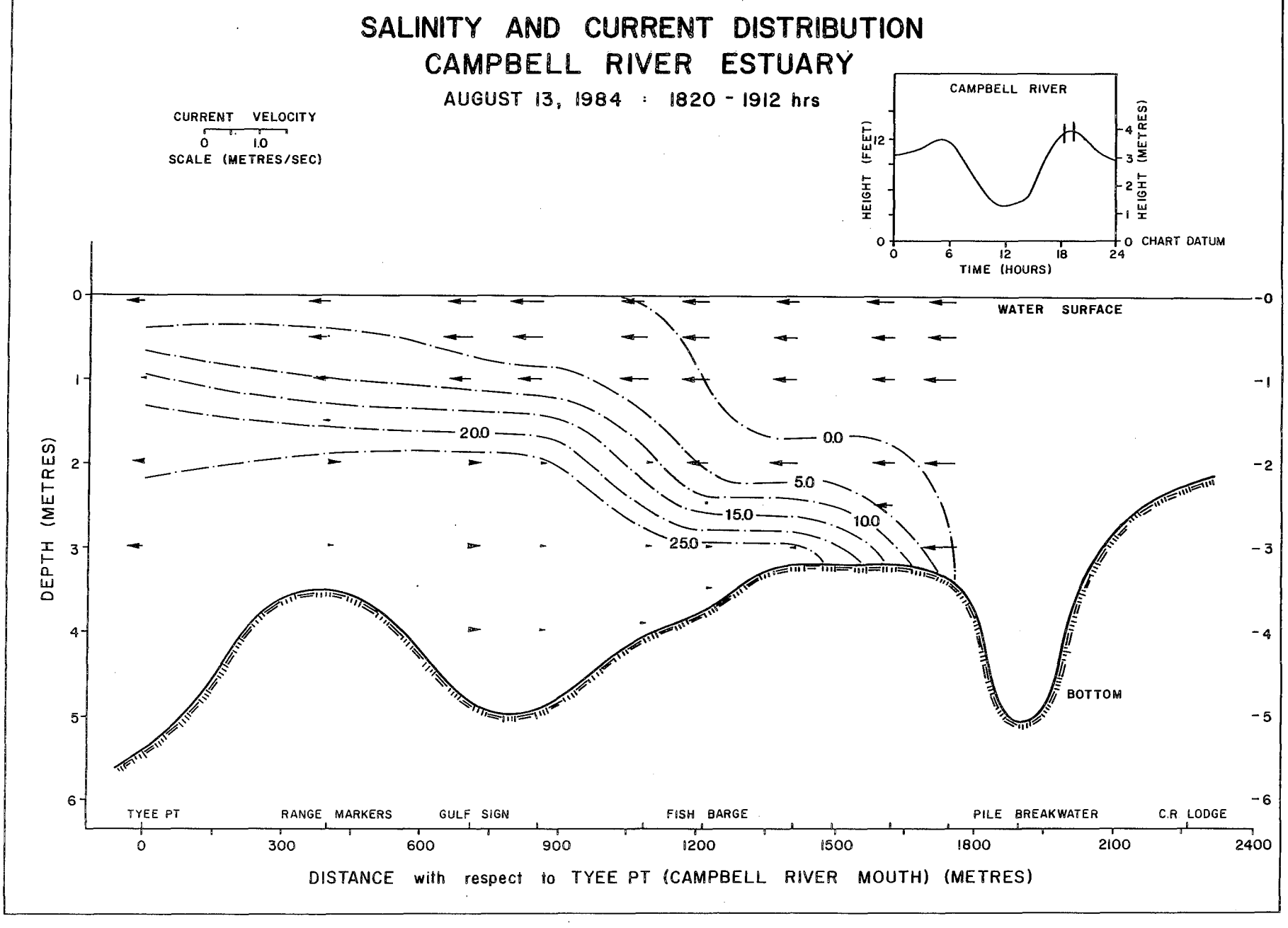

SALINITY AND CURRENT DISTRIBUTION
CAMPBELL RIVER ESTUARY

AUGUST 14, 1984 : 0744 - 0825 hrs

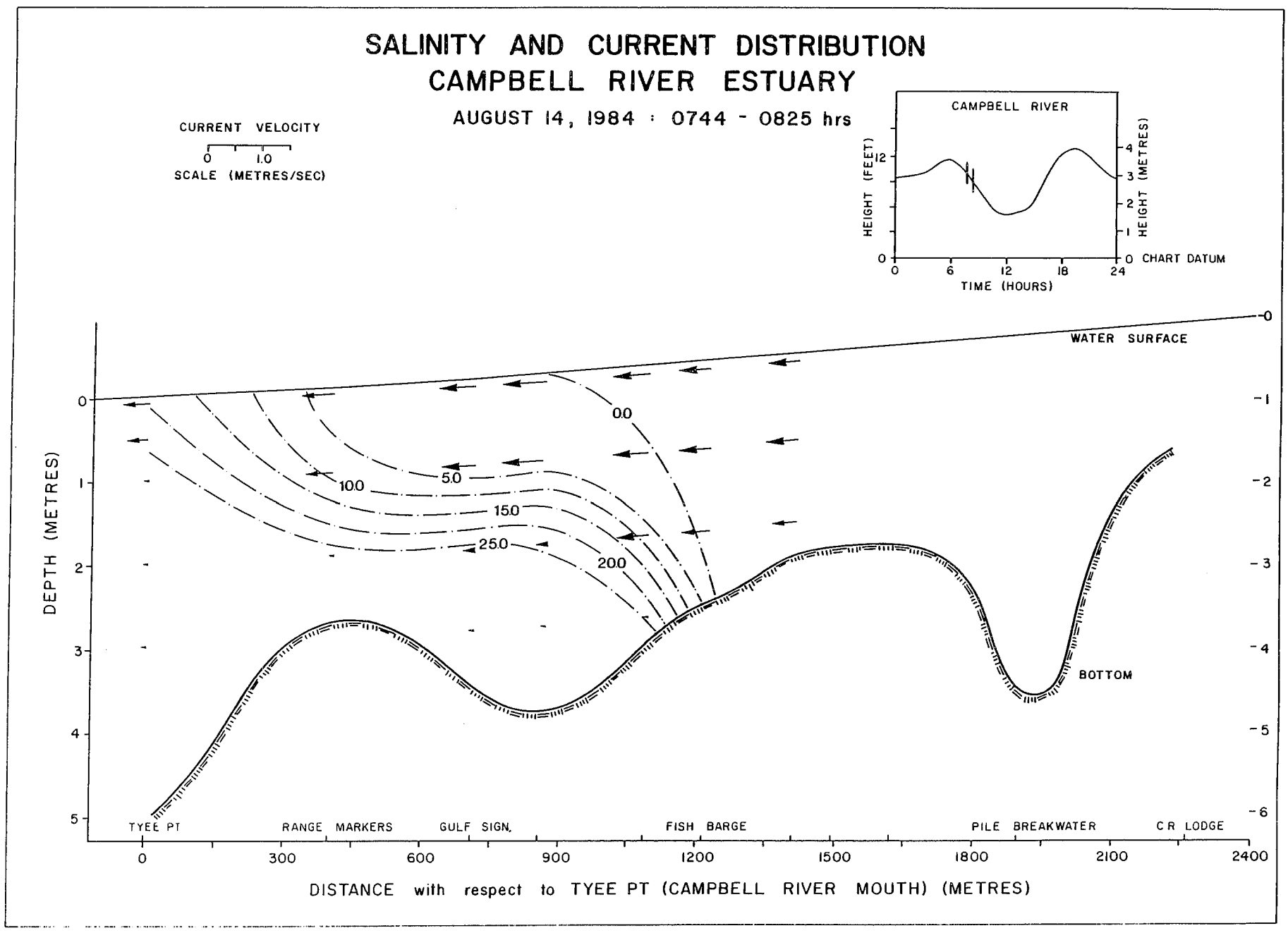

SALINITY AND CURRENT DISTRIBUTION
CAMPBELL RIVER ESTUARY

AUGUST 14, 1984 : 0935 - 1012 hrs

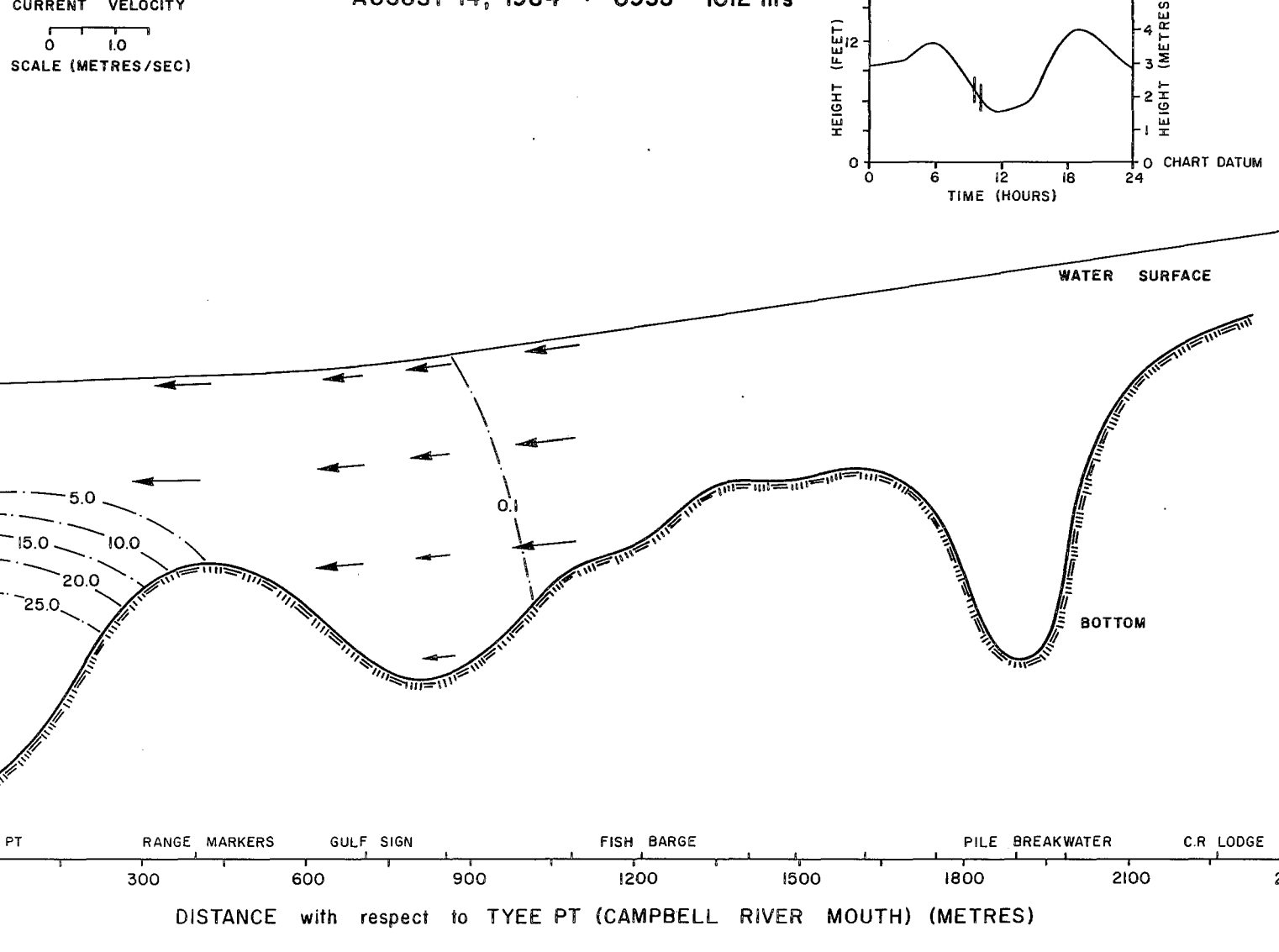

SALINITY AND CURRENT DISTRIBUTION
CAMPBELL RIVER ESTUARY

AUGUST 14, 1984 : 1032 - 1054 hrs

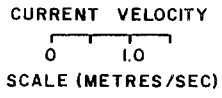

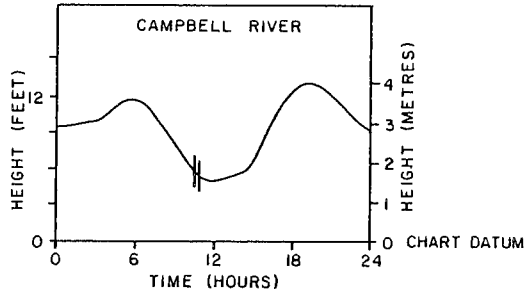

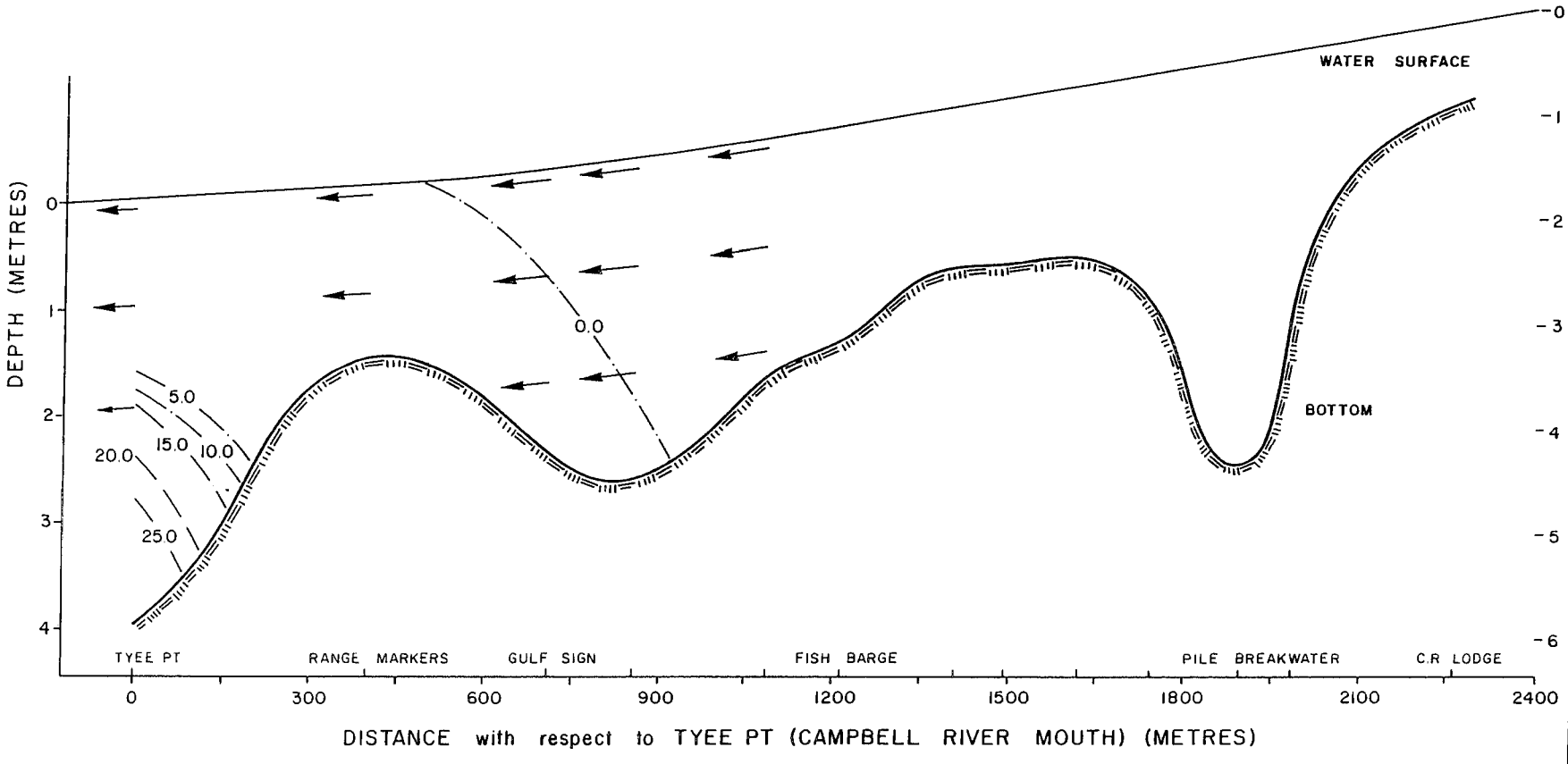

SALINITY AND CURRENT DISTRIBUTION
CAMPBELL RIVER ESTUARY

AUGUST 27, 1984 : 1350 - 1417 hrs

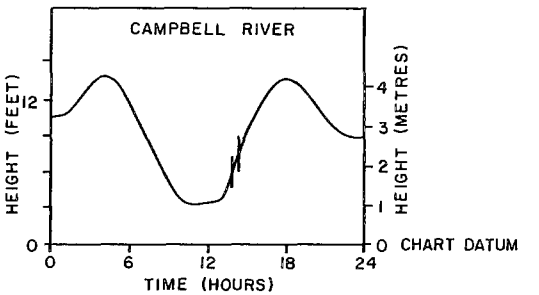

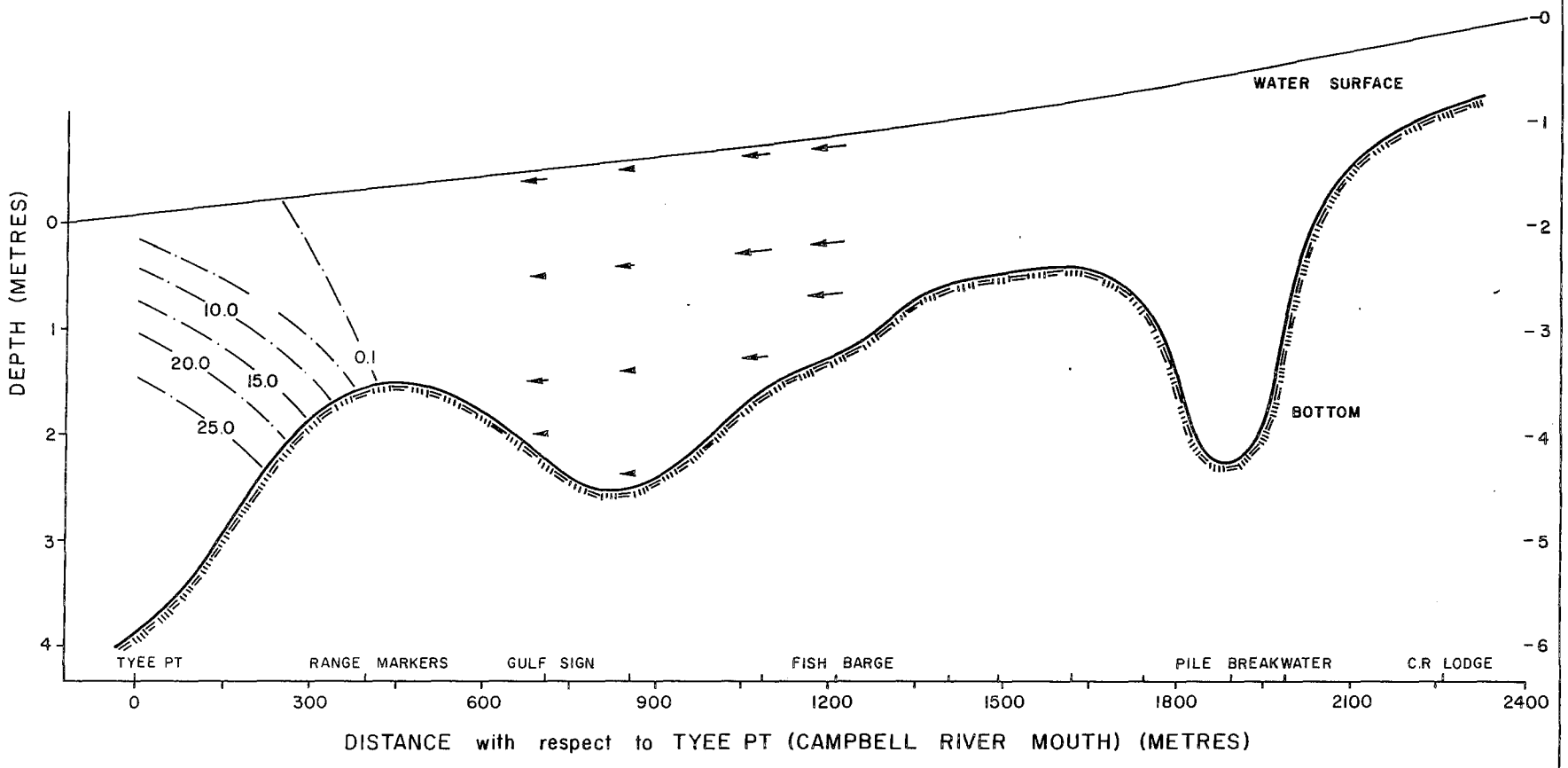

SALINITY AND CURRENT DISTRIBUTION
CAMPBELL RIVER ESTUARY

AUGUST 27, 1984 : 1437 - 1512 hrs

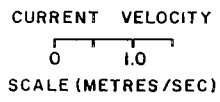

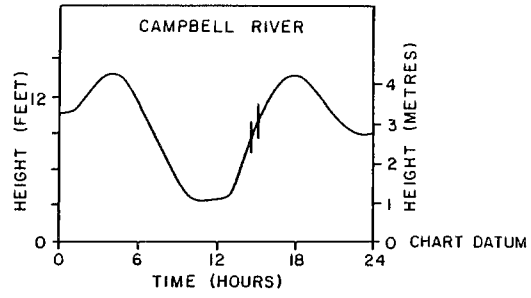

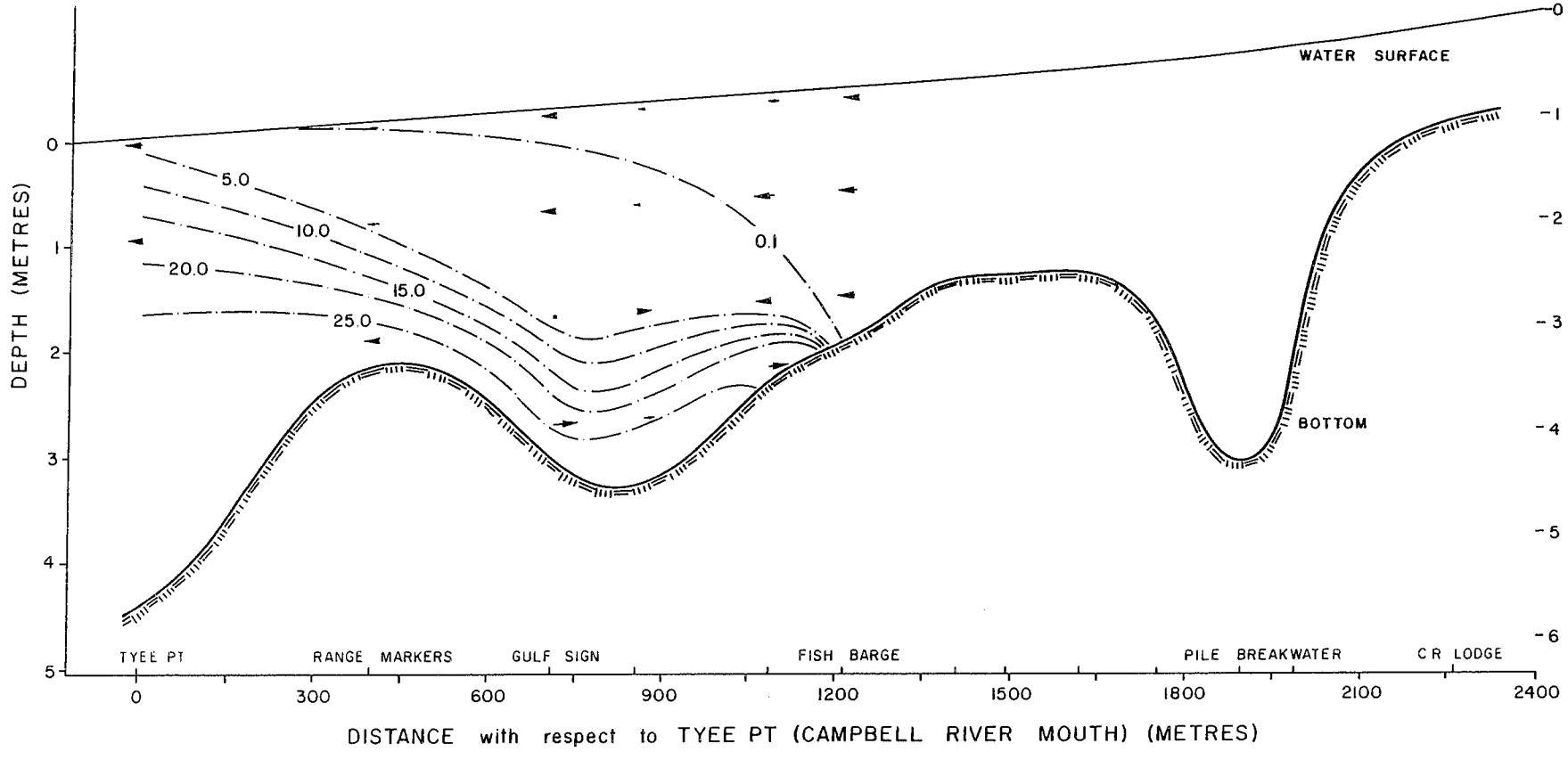

SALINITY AND CURRENT DISTRIBUTION
CAMPBELL RIVER ESTUARY

AUGUST 27, 1984 : 1526 - 1608 hrs

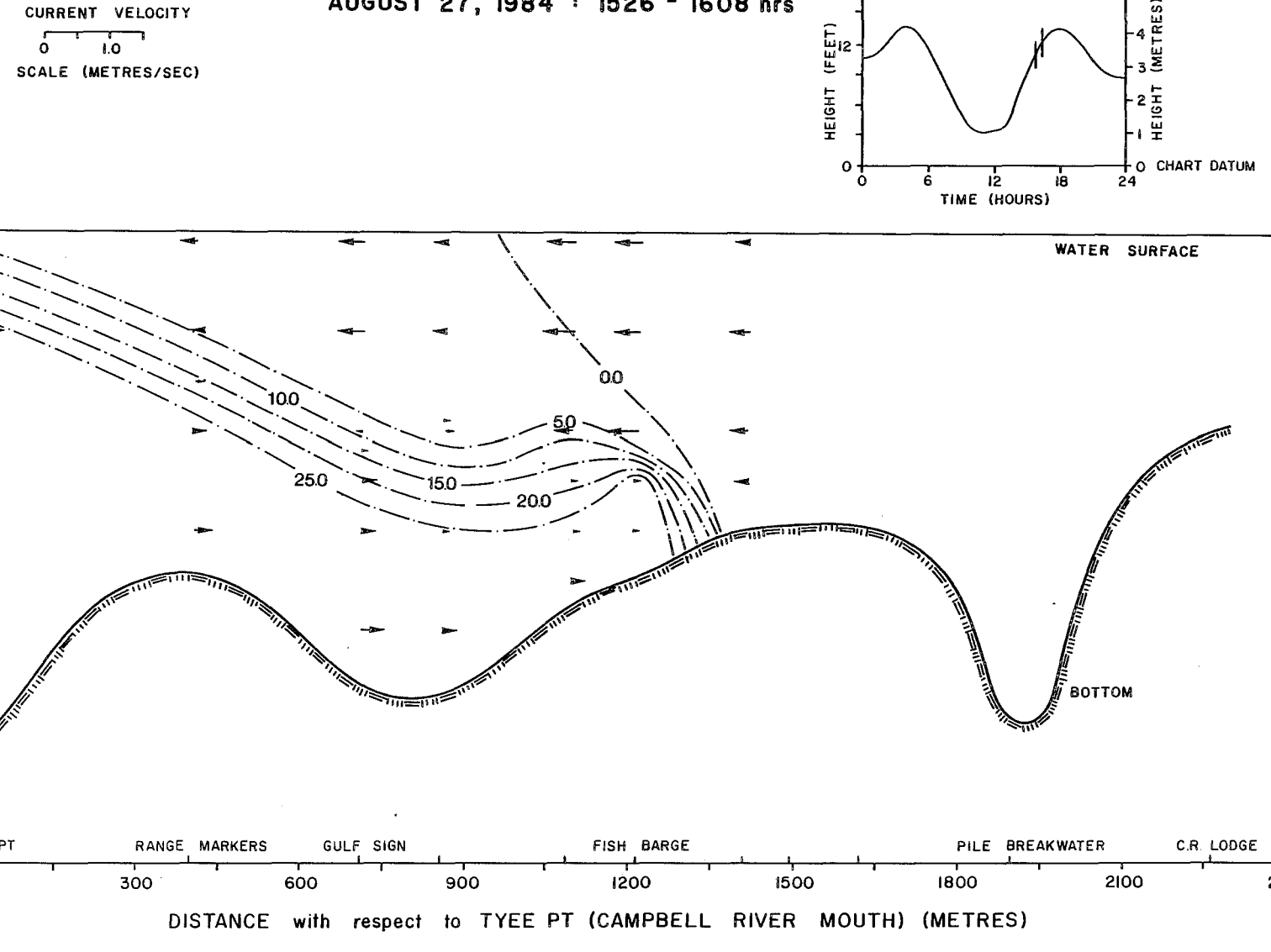

SALINITY AND CURRENT DISTRIBUTION
CAMPBELL RIVER ESTUARY

AUGUST 27, 1984 : 1621 - 1720 hrs

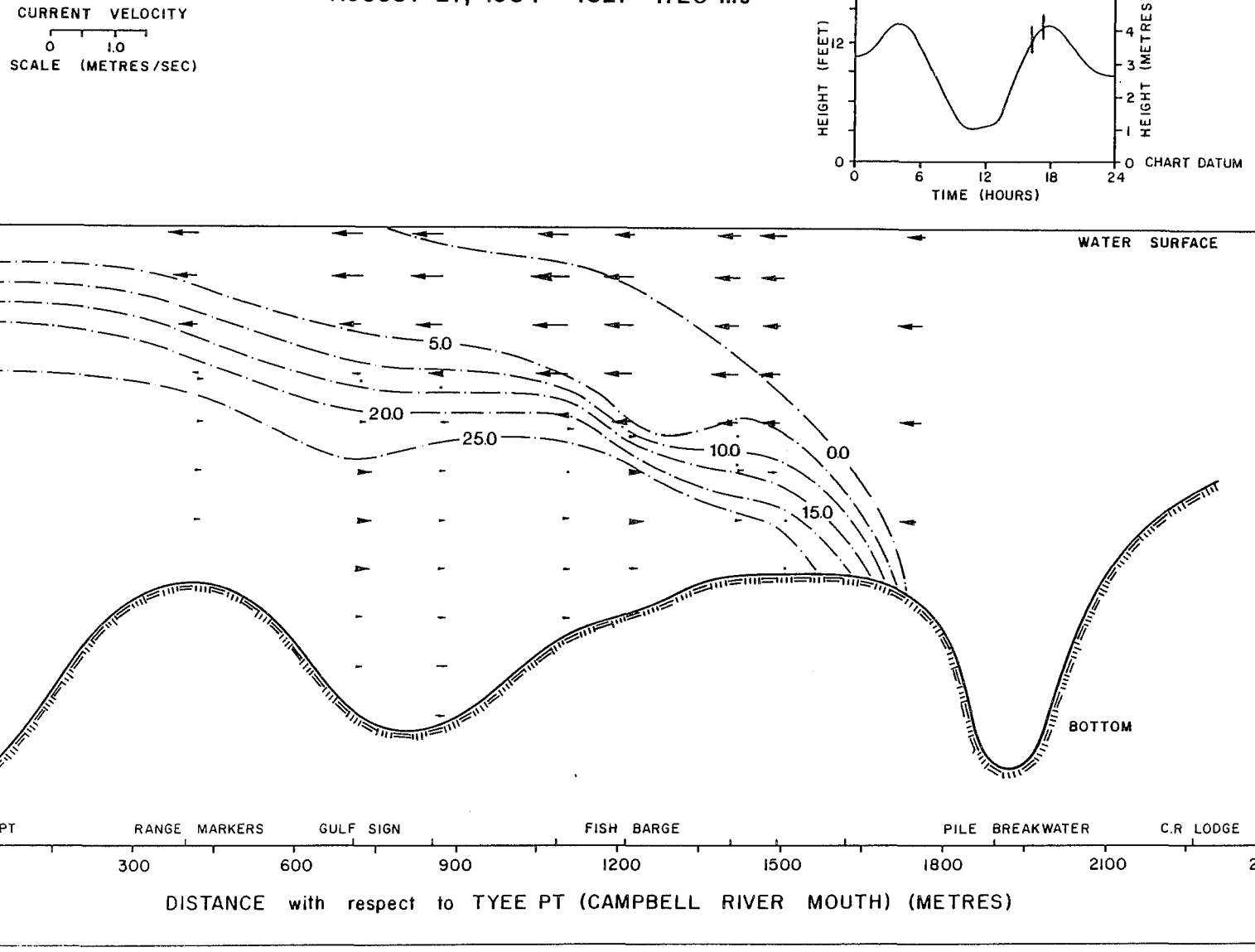

SALINITY AND CURRENT DISTRIBUTION
CAMPBELL RIVER ESTUARY

AUGUST 27, 1984 : 1745 - 1837 hrs

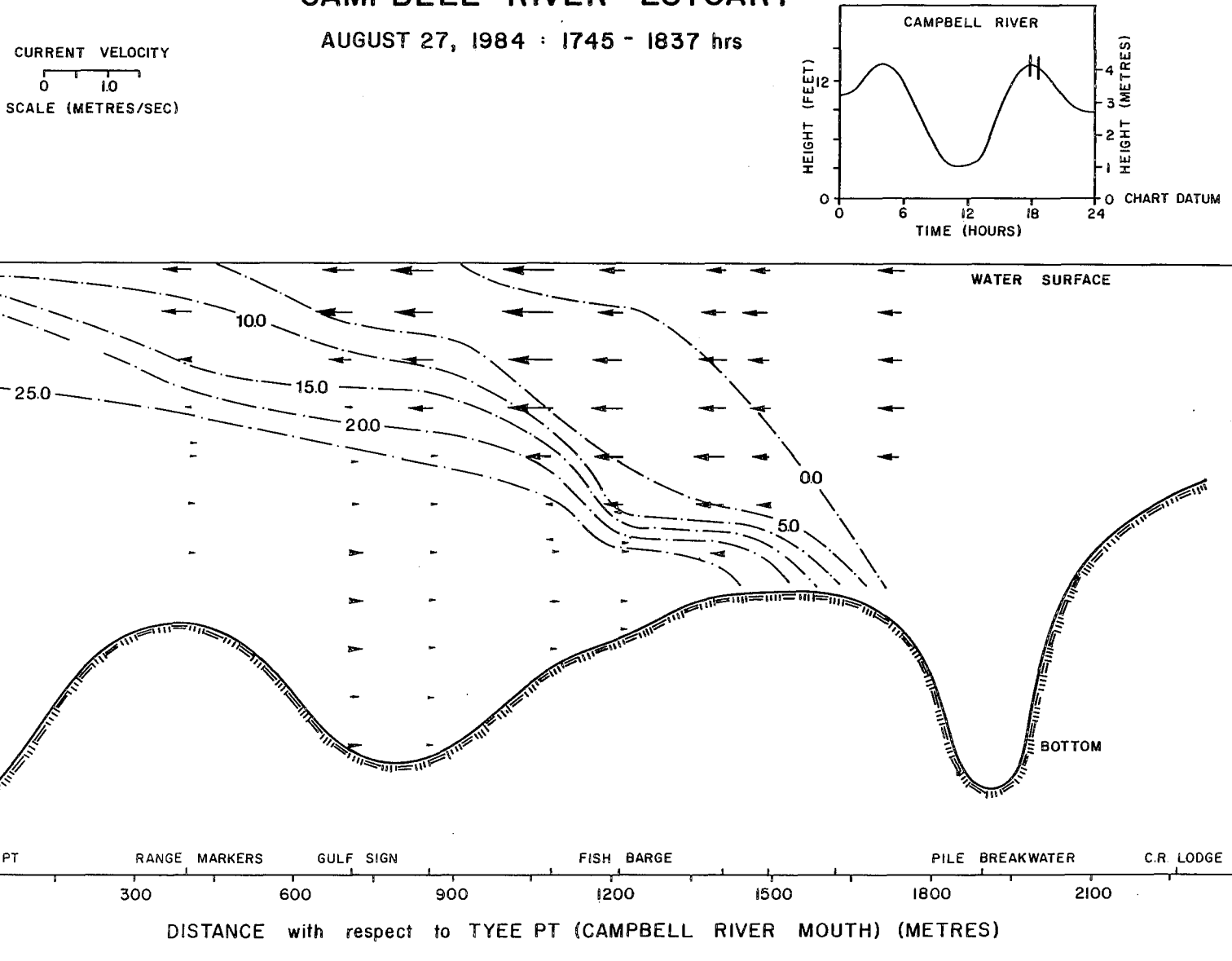

SALINITY AND CURRENT DISTRIBUTION
CAMPBELL RIVER ESTUARY

AUGUST 28, 1984 : 0735 - 0813 hrs

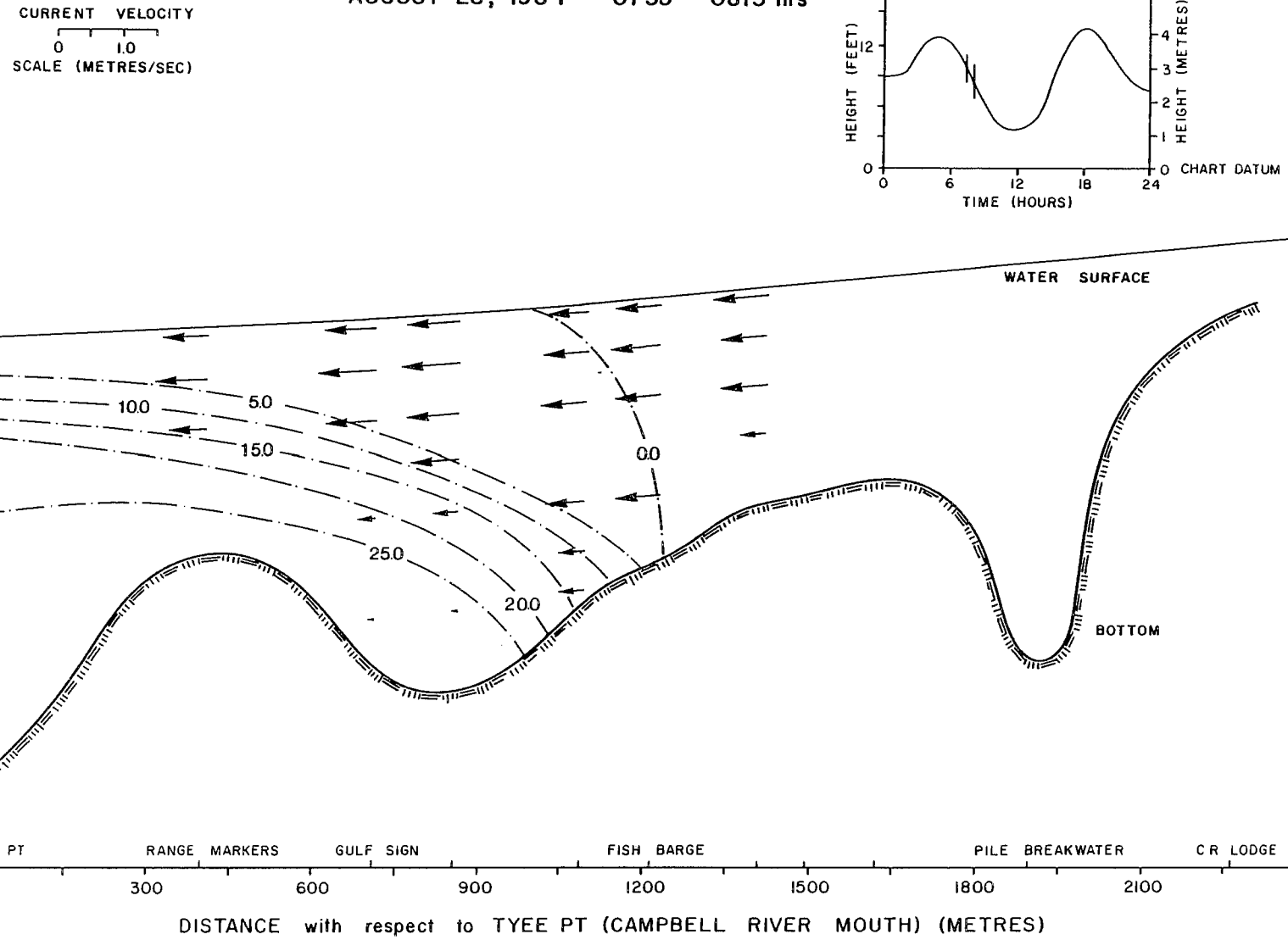

SALINITY AND CURRENT DISTRIBUTION
CAMPBELL RIVER ESTUARY

AUGUST 28, 1984 : 0823 - 0851 hrs

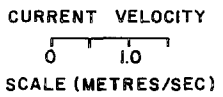

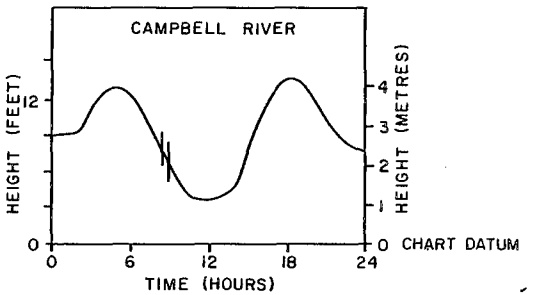

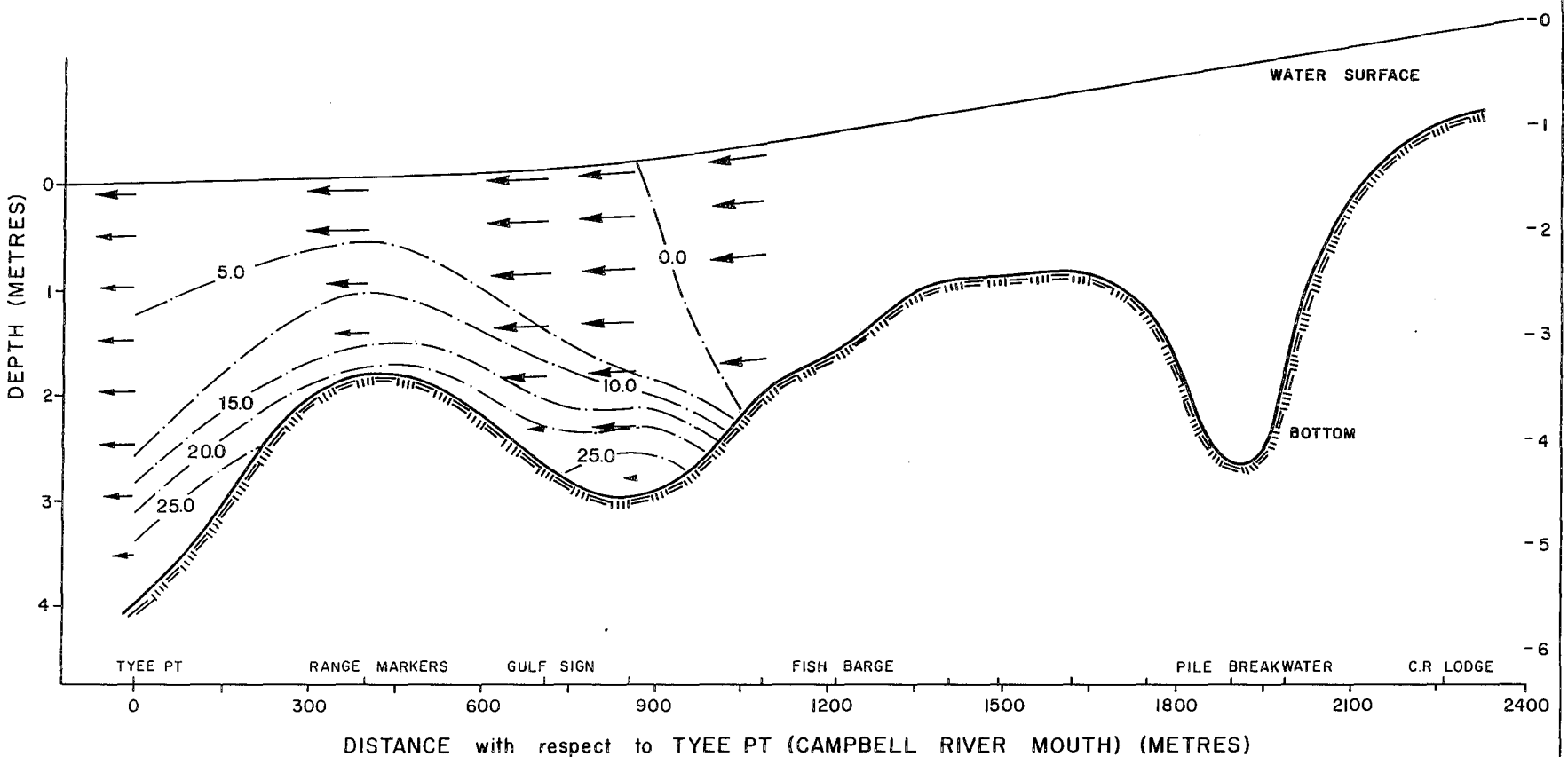

SALINITY AND CURRENT DISTRIBUTION
CAMPBELL RIVER ESTUARY

AUGUST 28, 1984 : 0902 - 0931 hrs

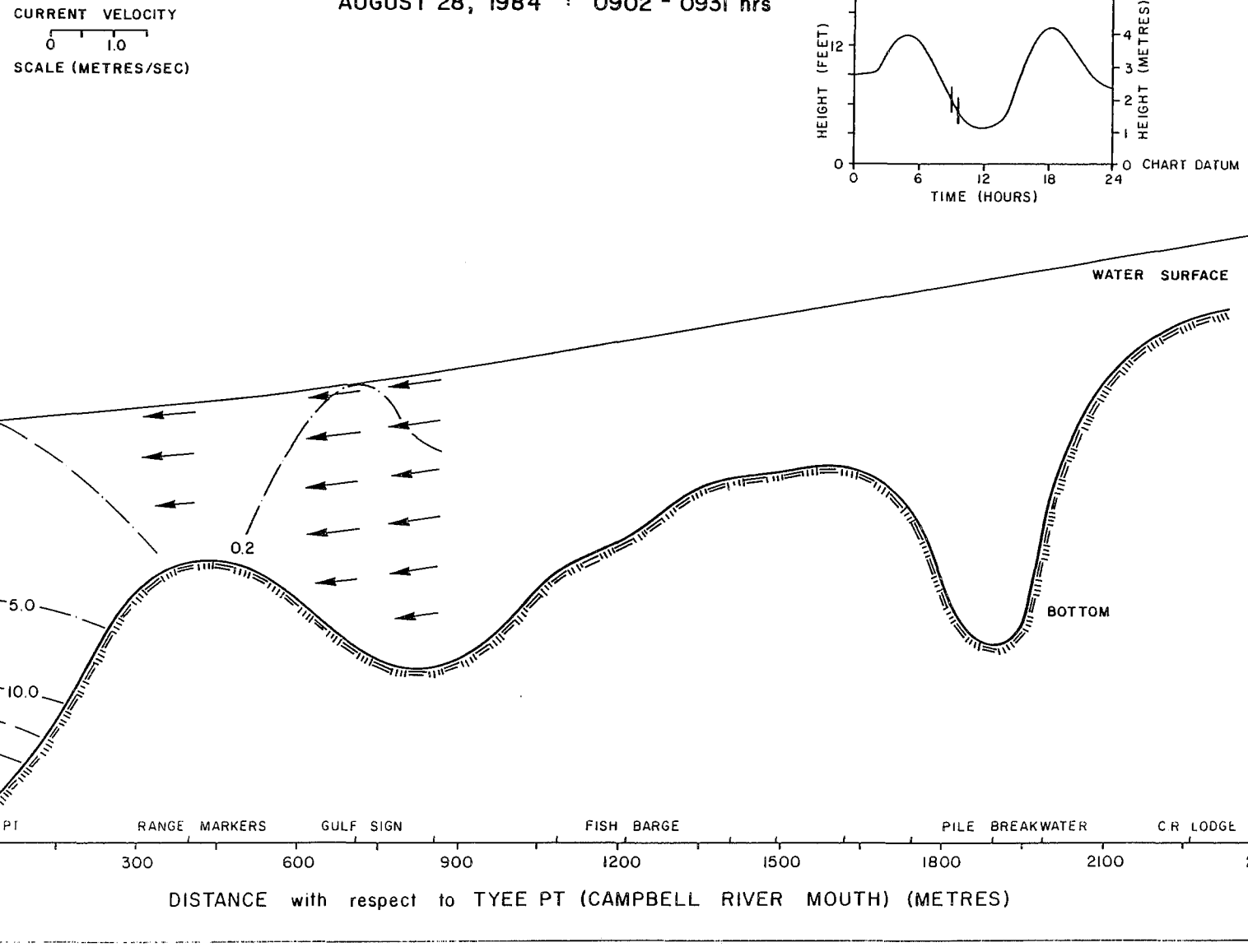

SALINITY AND CURRENT DISTRIBUTION
CAMPBELL RIVER ESTUARY

AUGUST 28, 1984 : 0946 - 1007 hrs

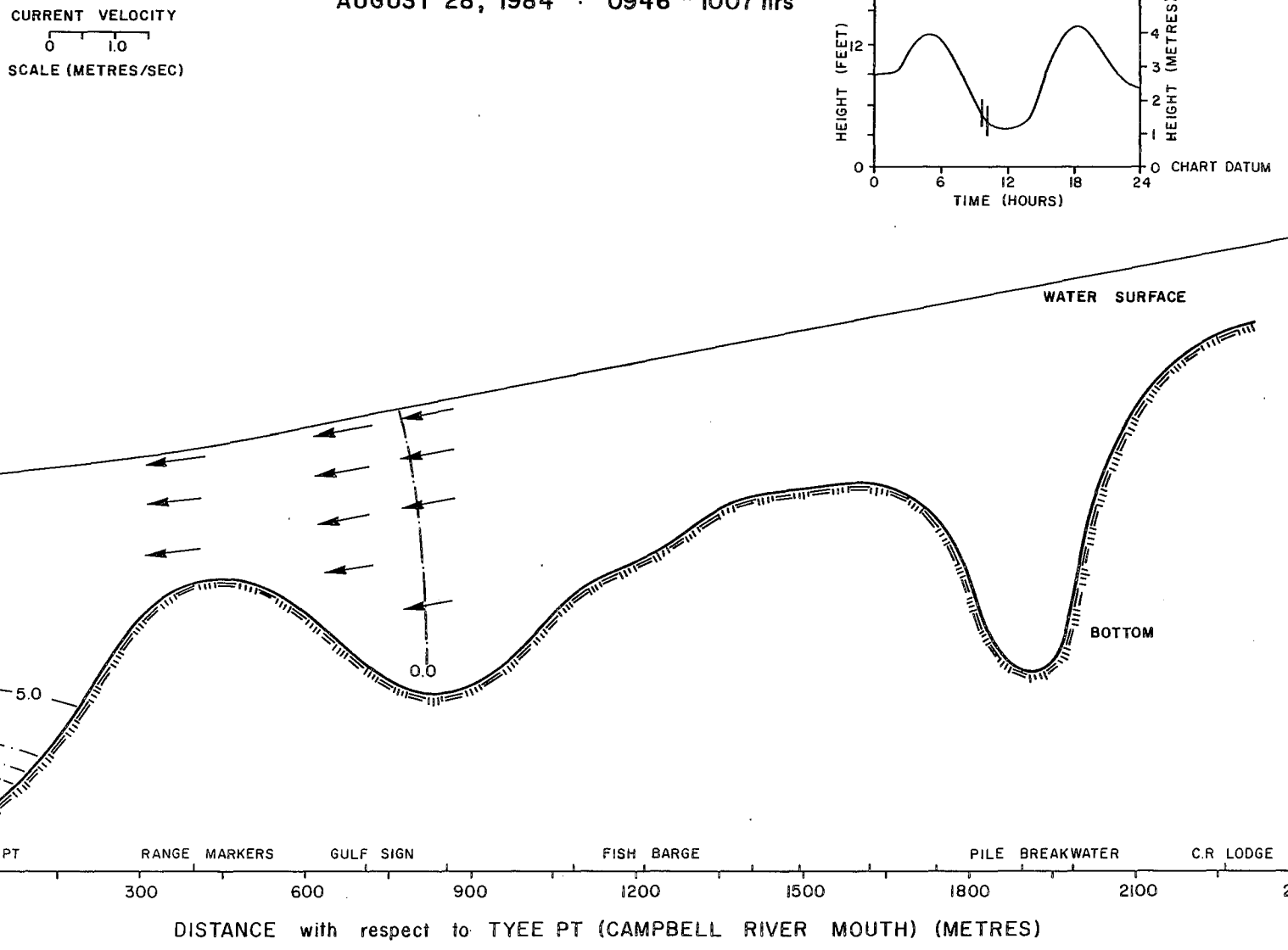

SALINITY AND CURRENT DISTRIBUTION
CAMPBELL RIVER ESTUARY

AUGUST 28, 1984 : 1018 - 1034 hrs

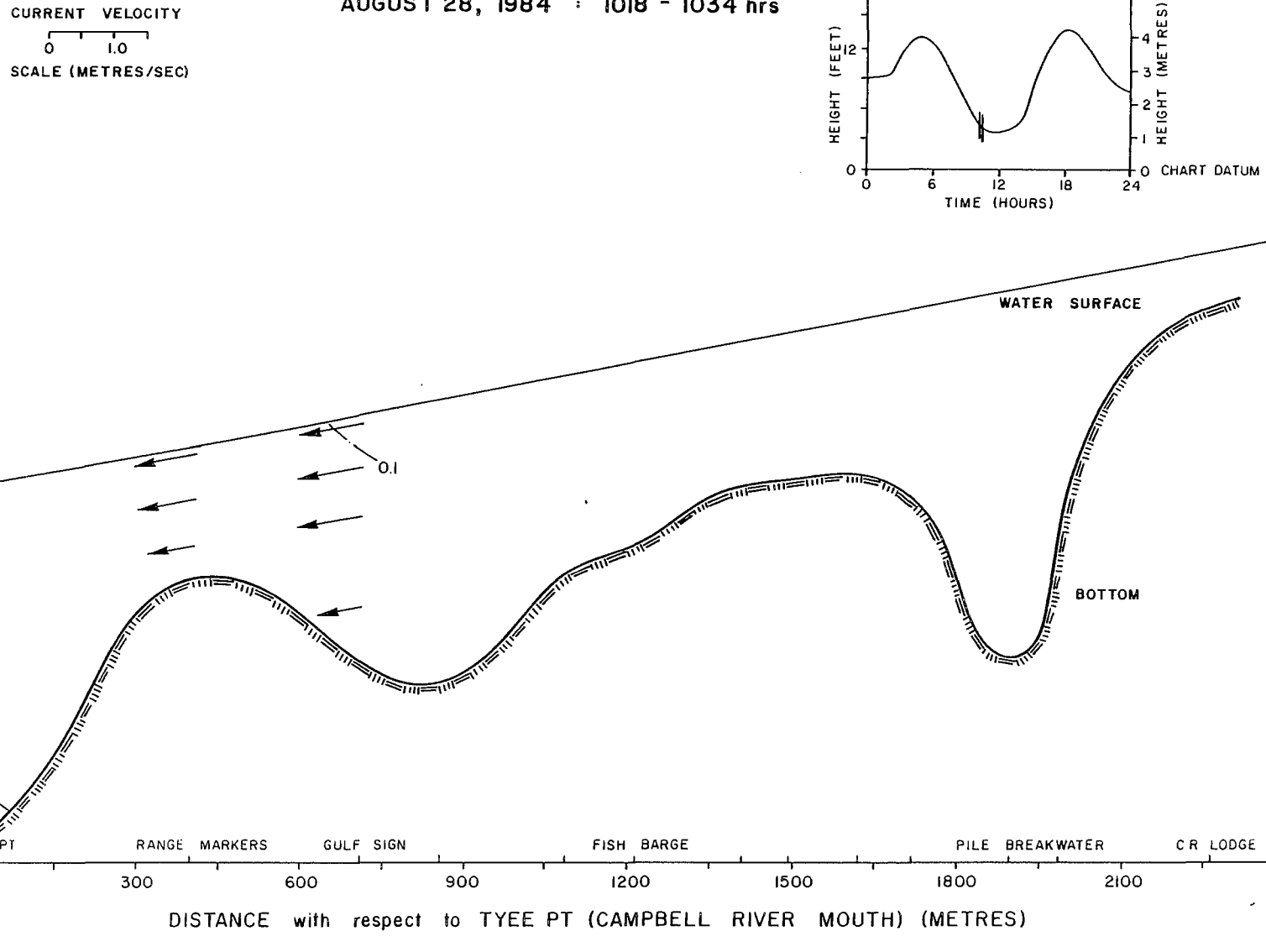

SALINITY AND CURRENT DISTRIBUTION
CAMPBELL RIVER ESTUARY

AUGUST 28, 1984 : 1043 - 1056 hrs

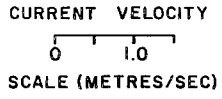

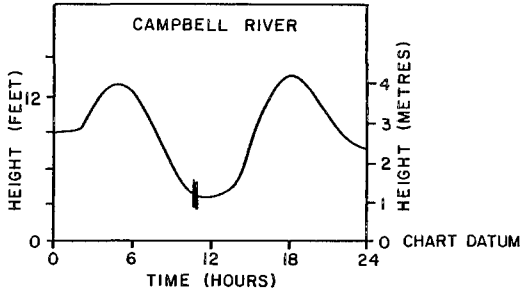

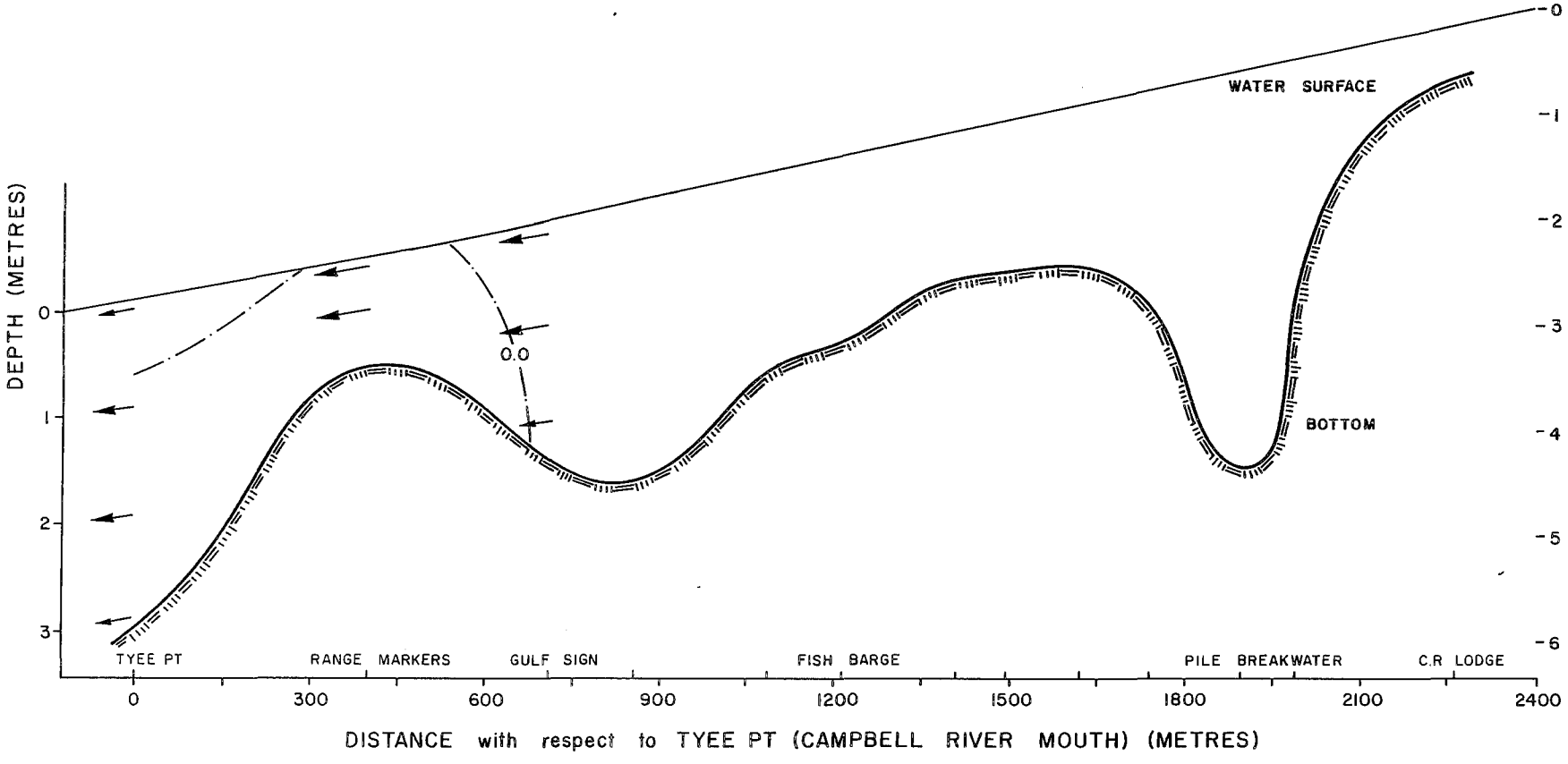

SALINITY AND CURRENT DISTRIBUTION
CAMPBELL RIVER ESTUARY

SEPTEMBER 10, 1984 : 1335 - 1356 hrs

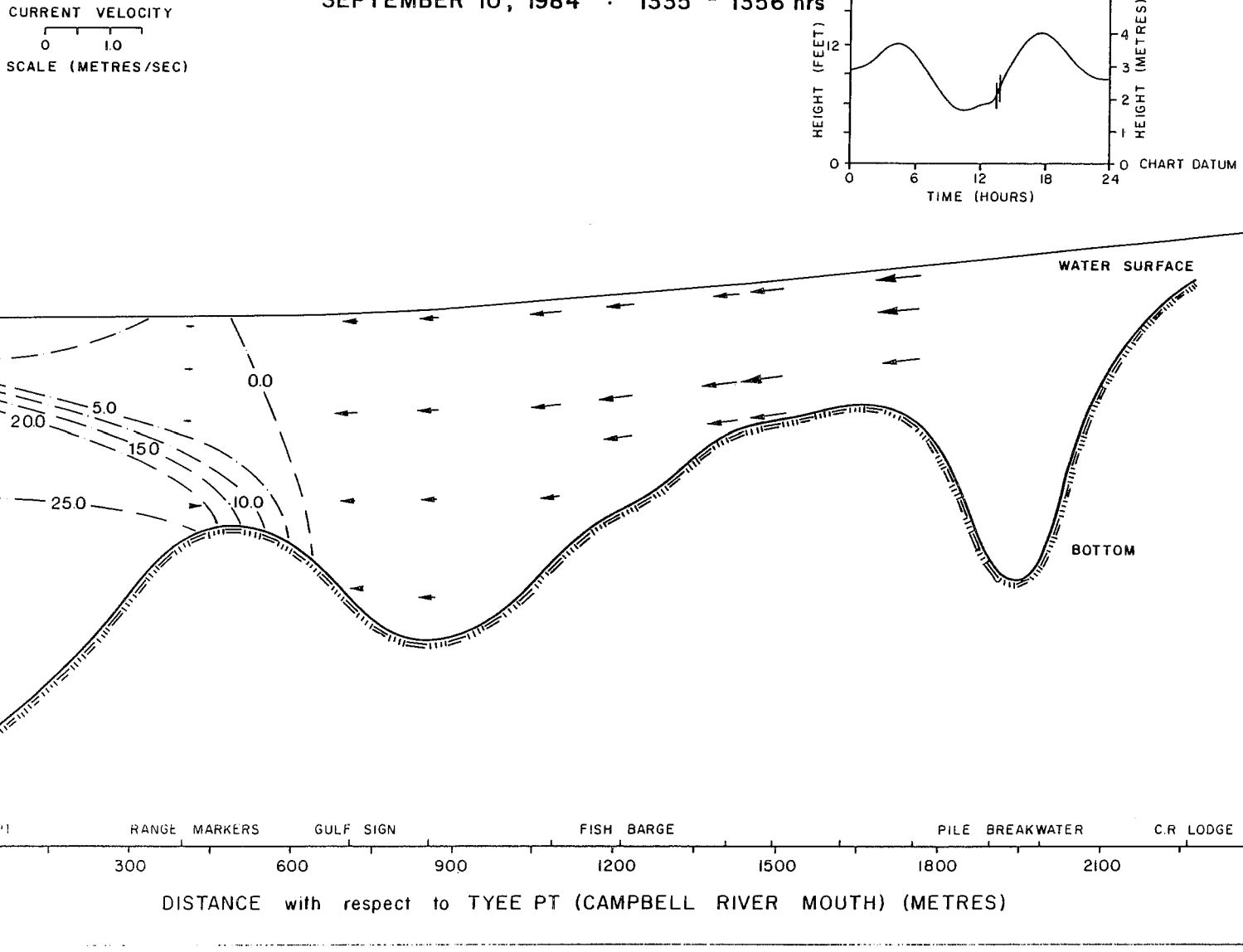

SALINITY AND CURRENT DISTRIBUTION
CAMPBELL RIVER ESTUARY

SEPTEMBER 10, 1984 : 1443 - 1528 hrs

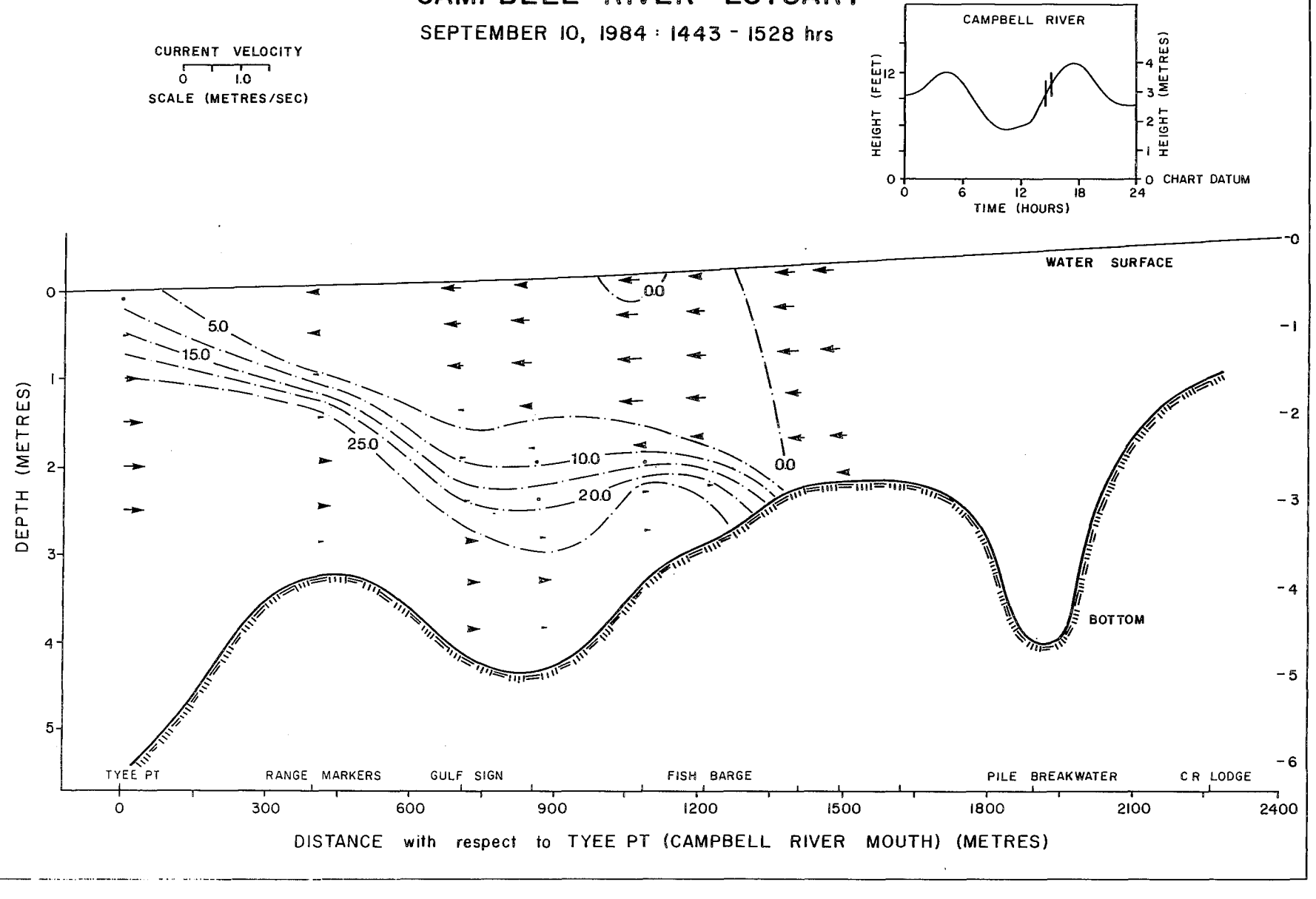

SALINITY AND CURRENT DISTRIBUTION
CAMPBELL RIVER ESTUARY

SEPTEMBER 10, 1984 : 1534 - 1614 hrs

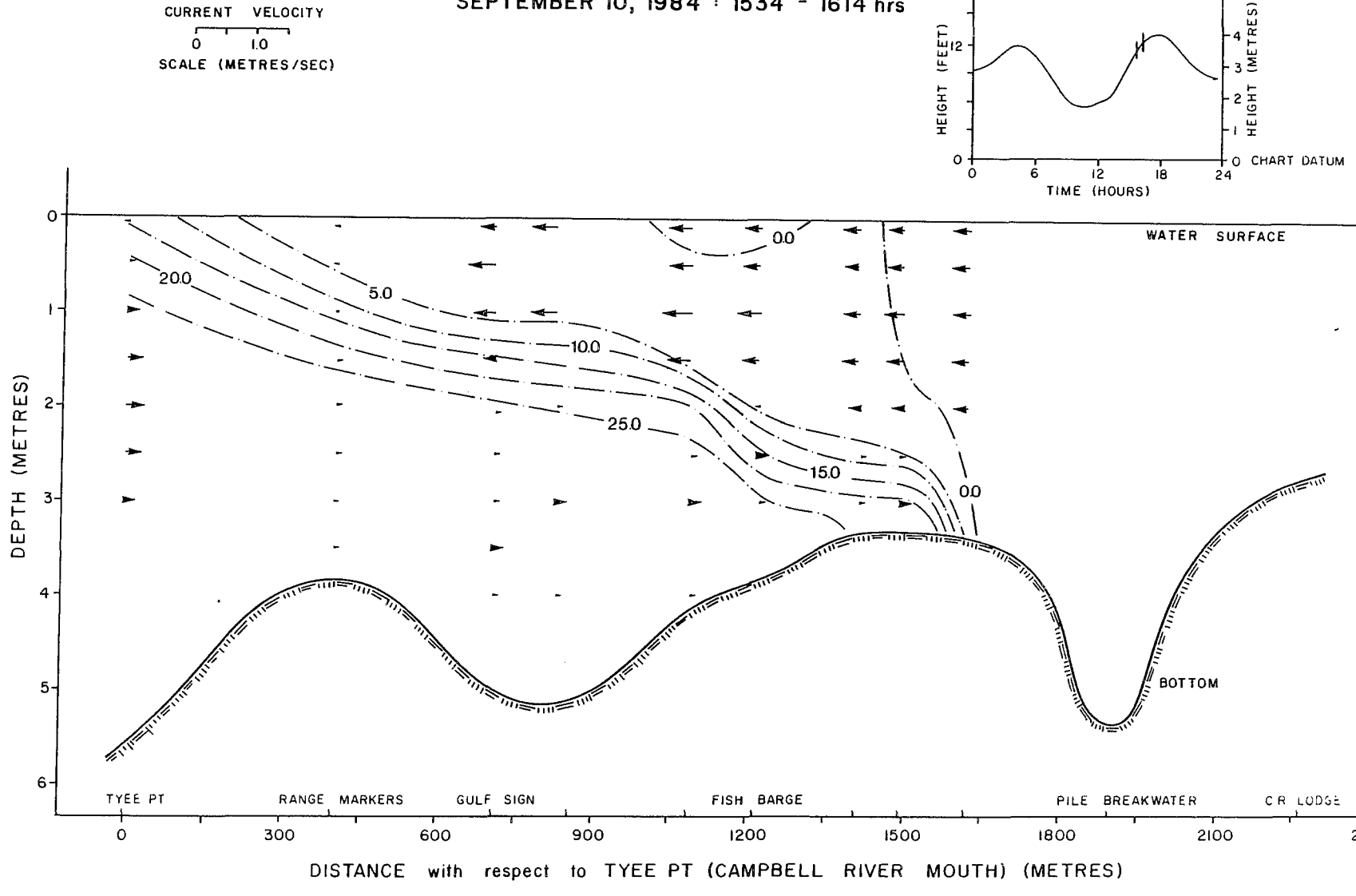

SALINITY AND CURRENT DISTRIBUTION
CAMPBELL RIVER ESTUARY

SEPTEMBER 10, 1984 : 1710 - 1806 hrs

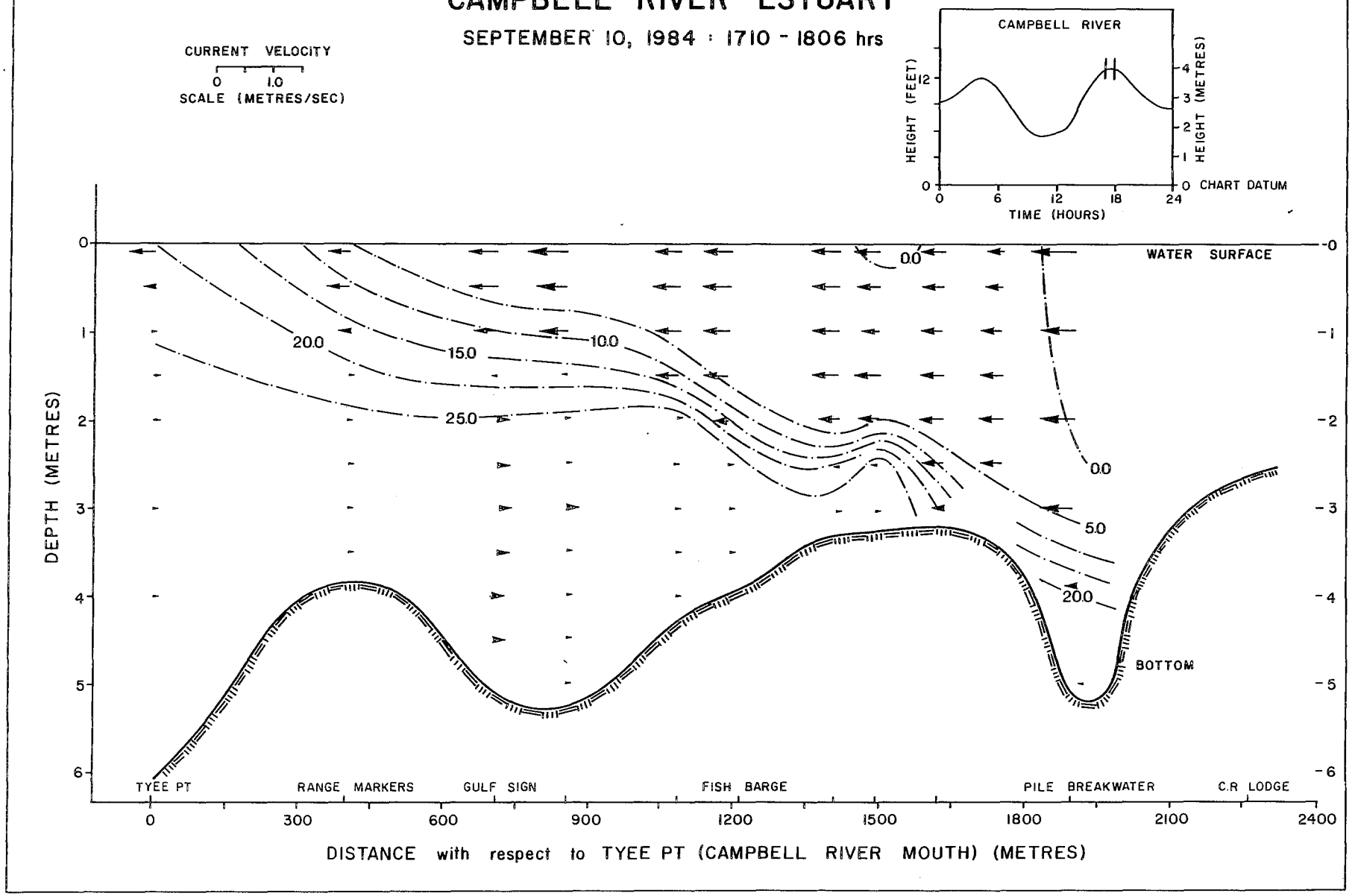

SALINITY AND CURRENT DISTRIBUTION
CAMPBELL RIVER ESTUARY

SEPTEMBER 10, 1984 : 1814 - 1836 hrs

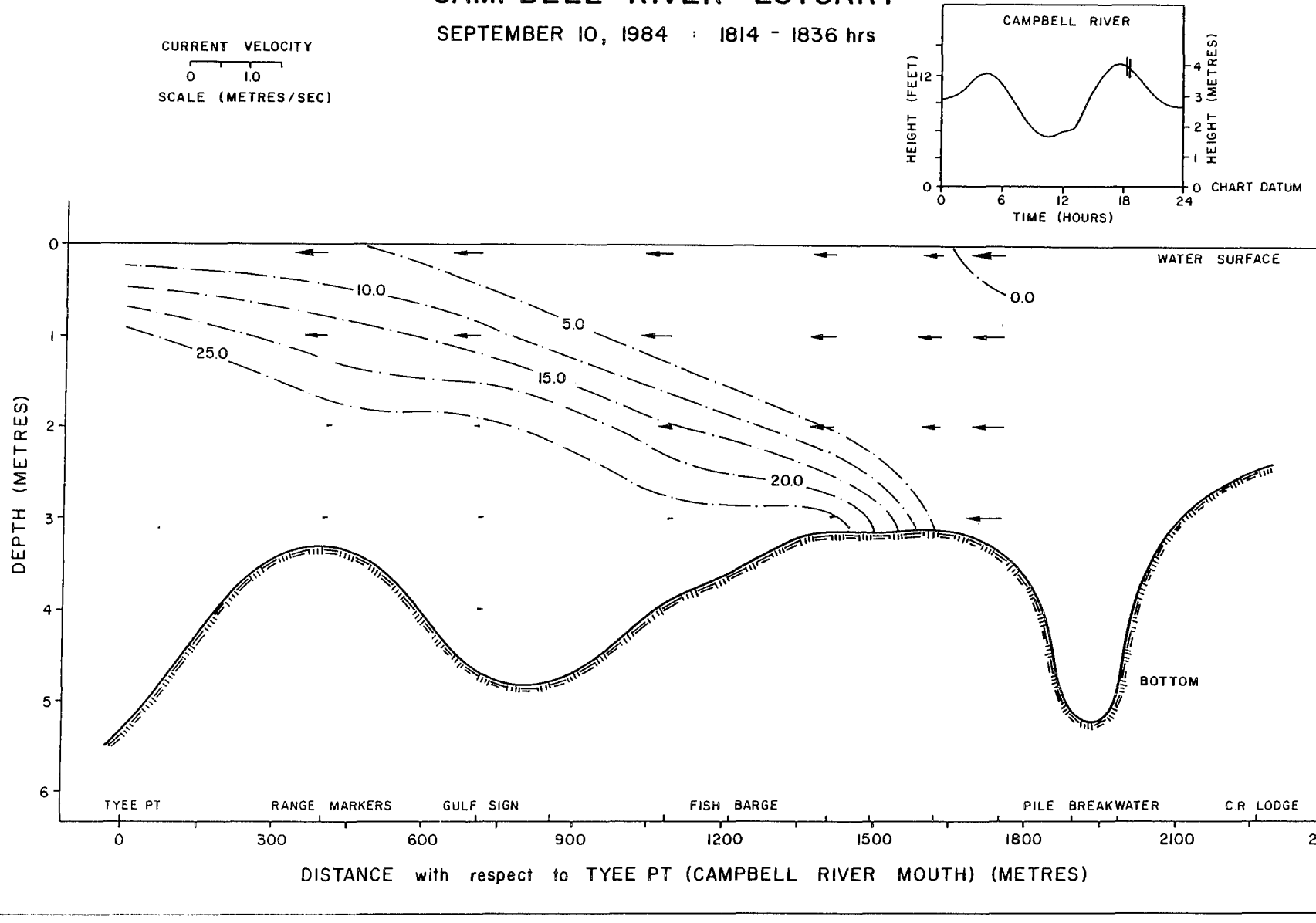

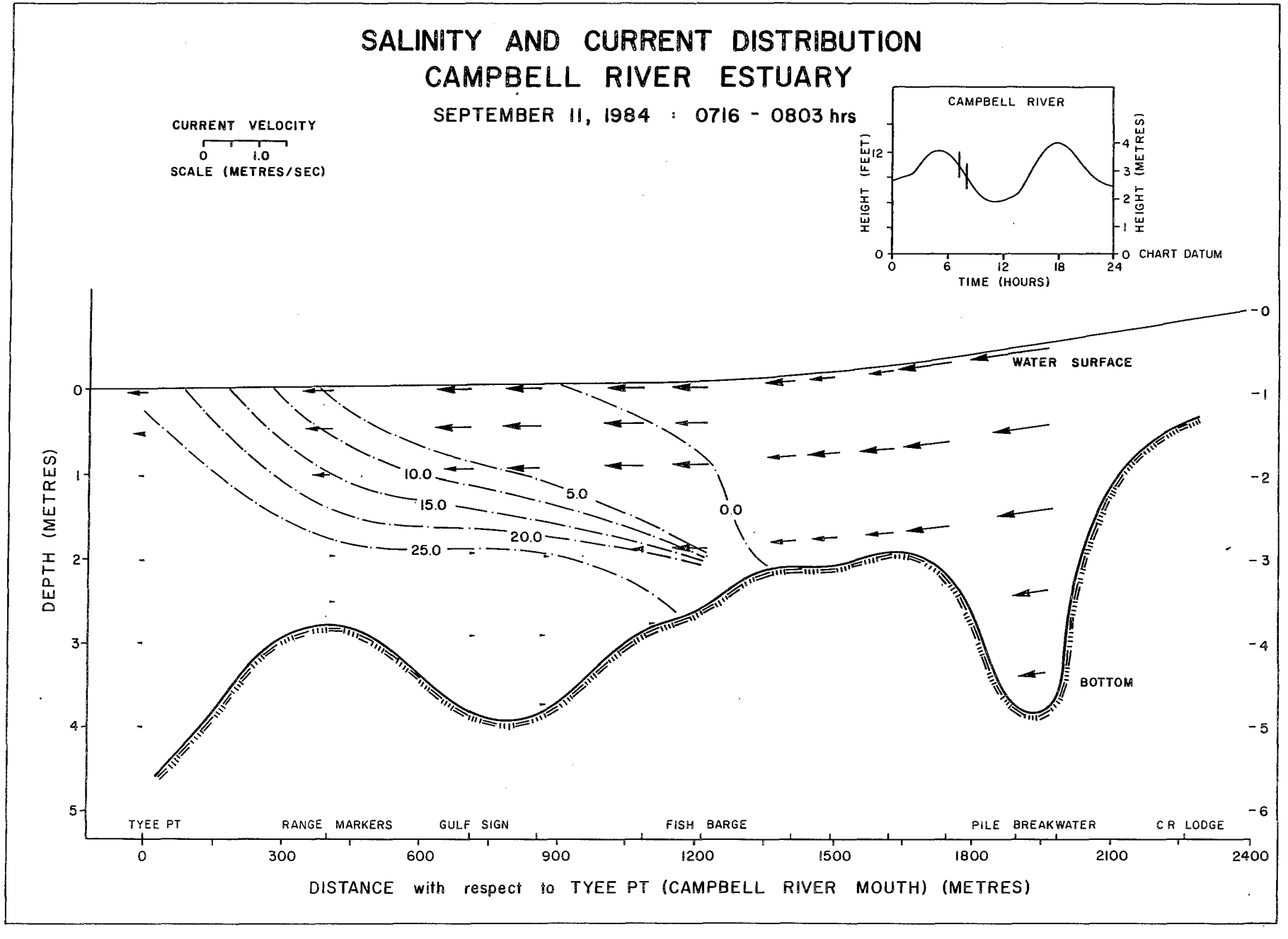
SALINITY AND CURRENT DISTRIBUTION
CAMPBELL RIVER ESTUARY
SEPTEMBER 11, 1984 : 0716 - 0803 hrs
CURRENT VELOCITY
0 1.0
SCALE (METRES/SEC)
CAMPBELL RIVER
HEIGHT (FEET)
HEIGHT (METRES)
0 CHART DATUM
TIME (HOURS)
WATER SURFACE
BOTTOM
10.0
15.0
20.0
25.0
5.0
0.0
DEPTH (METRES)
TYEE PT
RANGE MARKERS
GULF SIGN
FISH BARGE
PILE BREAKWATER
C R LODGE
DISTANCE with respect to TYEE PT (CAMPBELL RIVER MOUTH) (METRES)

SALINITY AND CURRENT DISTRIBUTION
CAMPBELL RIVER ESTUARY
SEPTEMBER 11, 1984 : 0925 - 0948 hrs

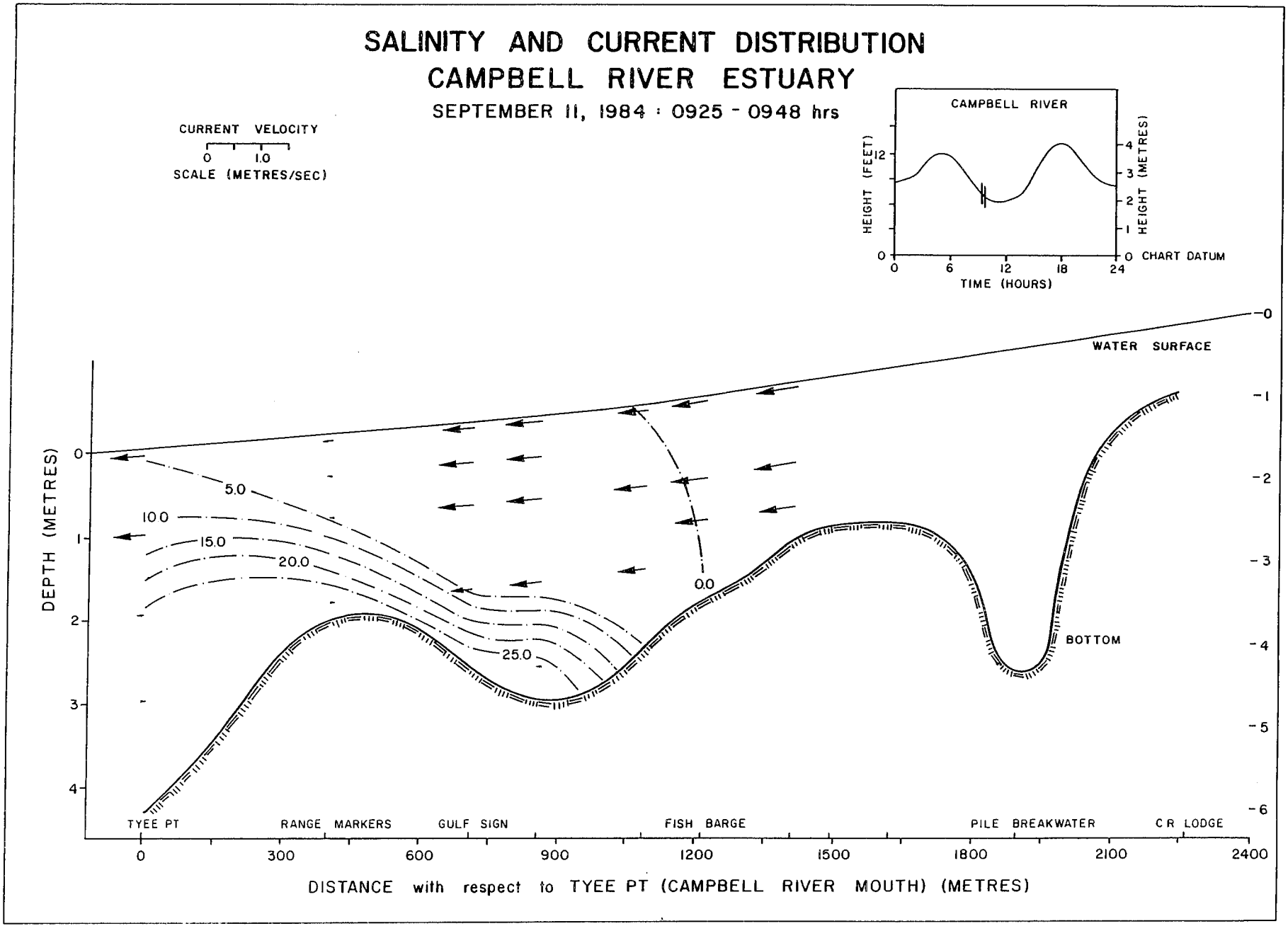

SALINITY AND CURRENT DISTRIBUTION
CAMPBELL RIVER ESTUARY

SEPTEMBER 11, 1984 : 1014 - 1036 hrs

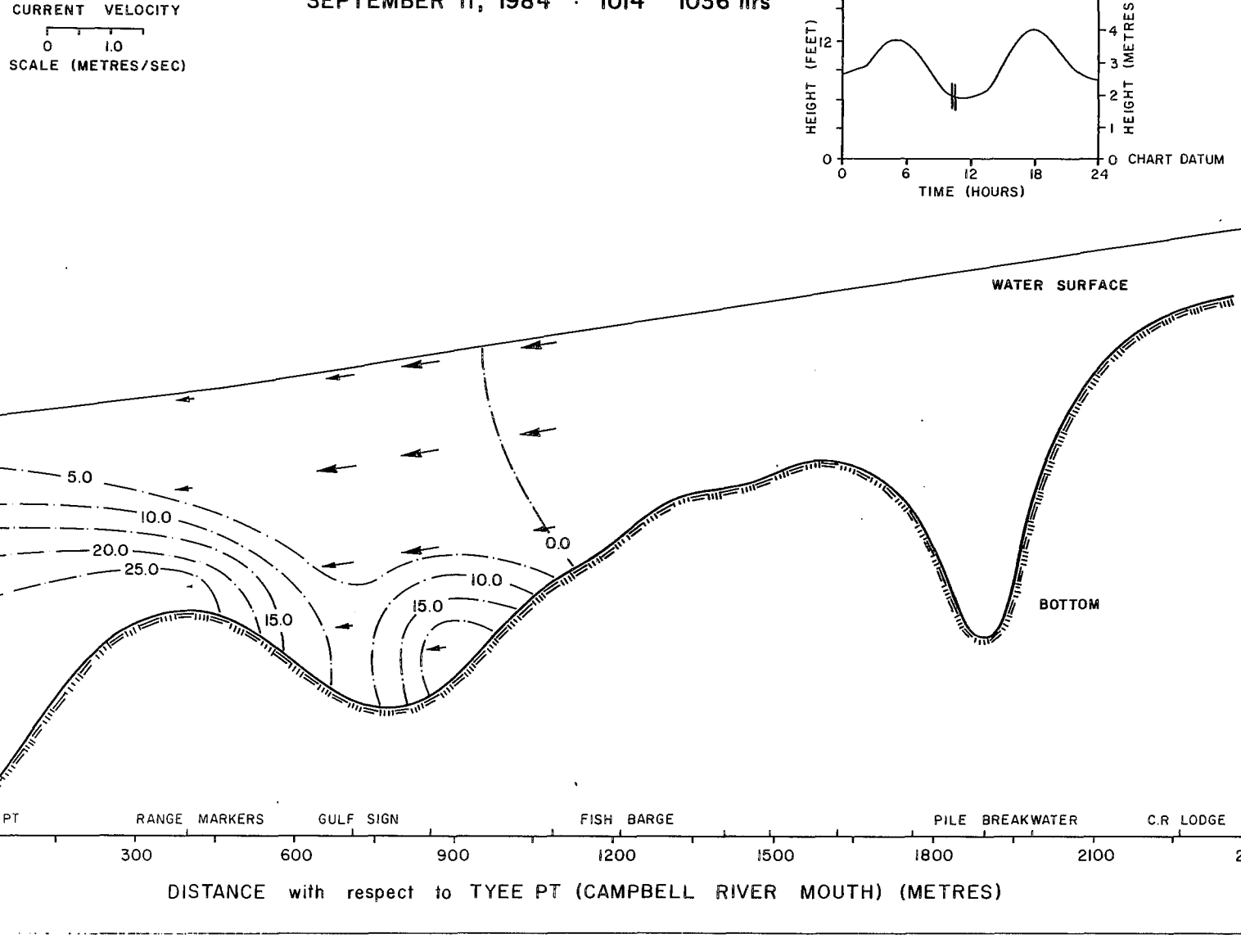

SALINITY AND CURRENT DISTRIBUTION
CAMPBELL RIVER ESTUARY

SEPTEMBER 11, 1984 : 1050 - 1104 hrs

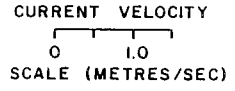

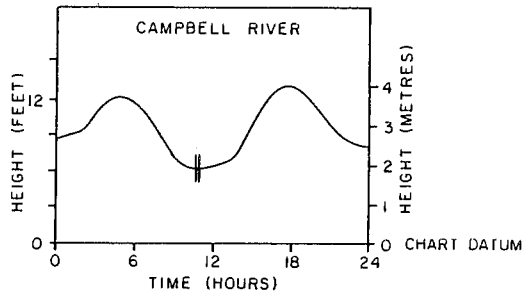

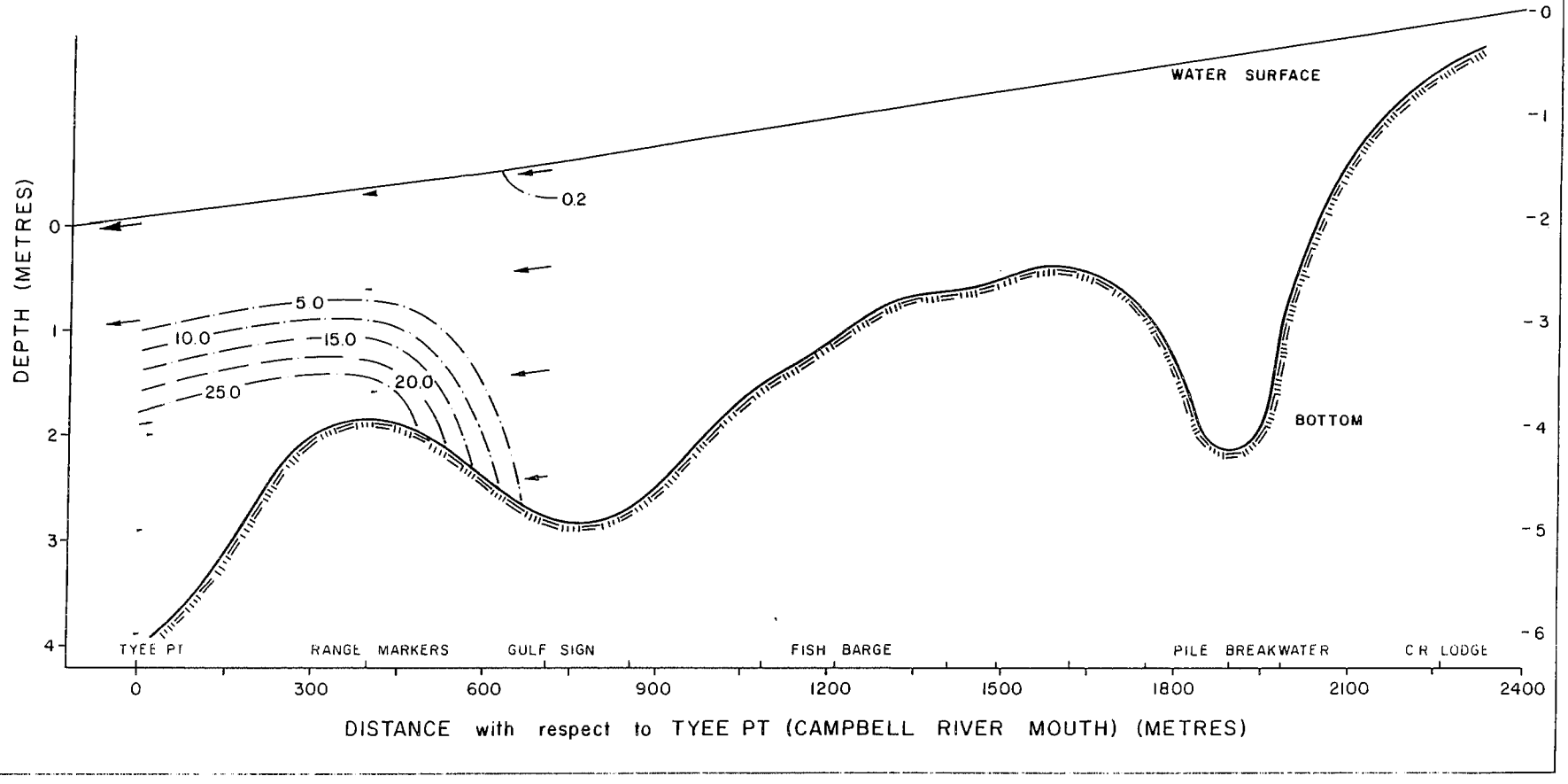

SALINITY AND CURRENT DISTRIBUTION
CAMPBELL RIVER ESTUARY

SEPTEMBER 24, 1984 : 1340 - 1402 hrs

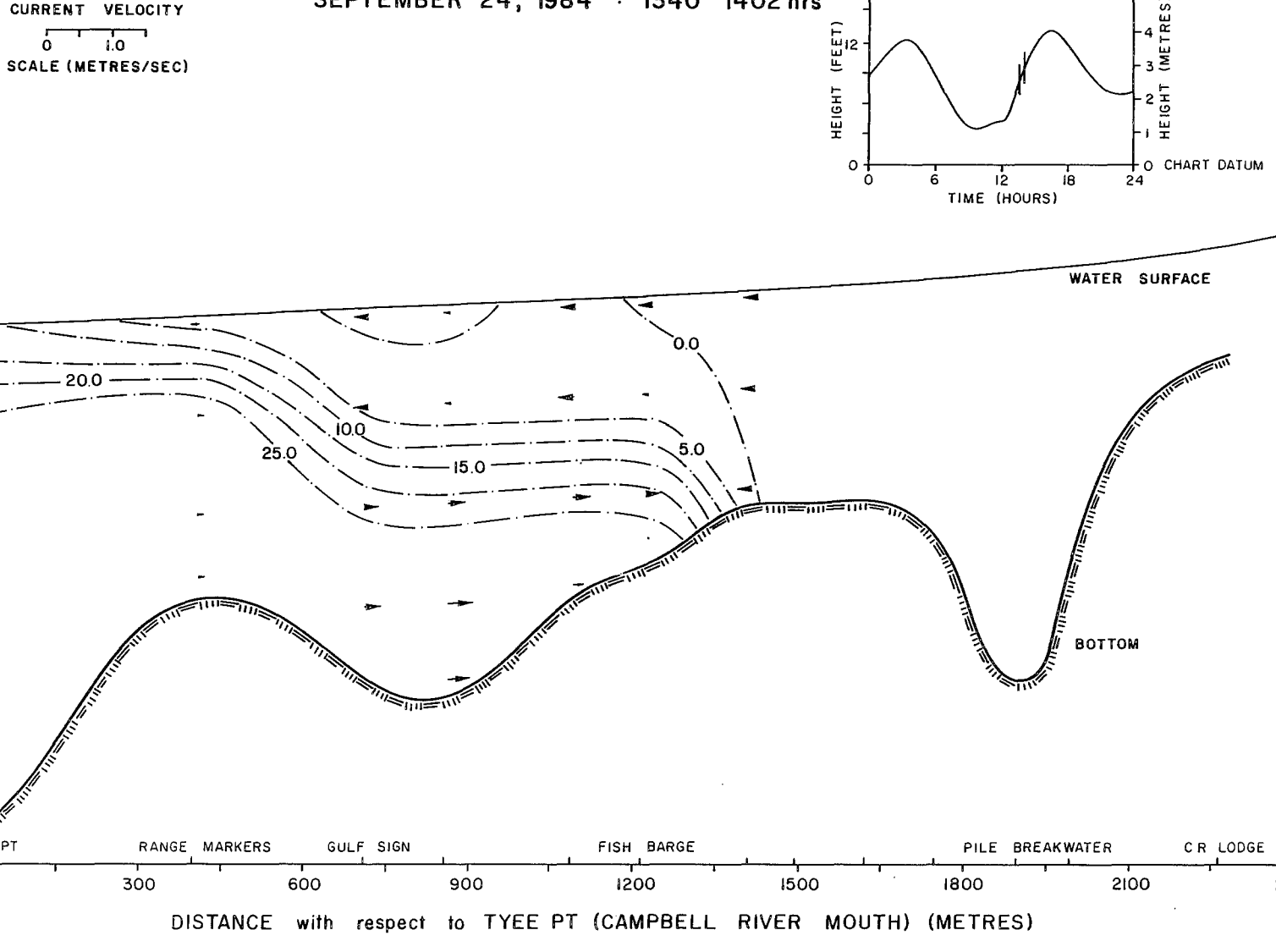

SALINITY AND CURRENT DISTRIBUTION
CAMPBELL RIVER ESTUARY

SEPTEMBER 24, 1984 : 1703 - 1755 hrs

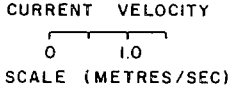

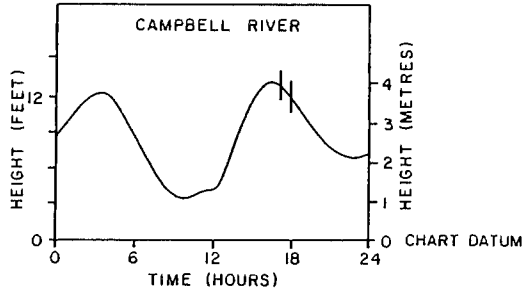

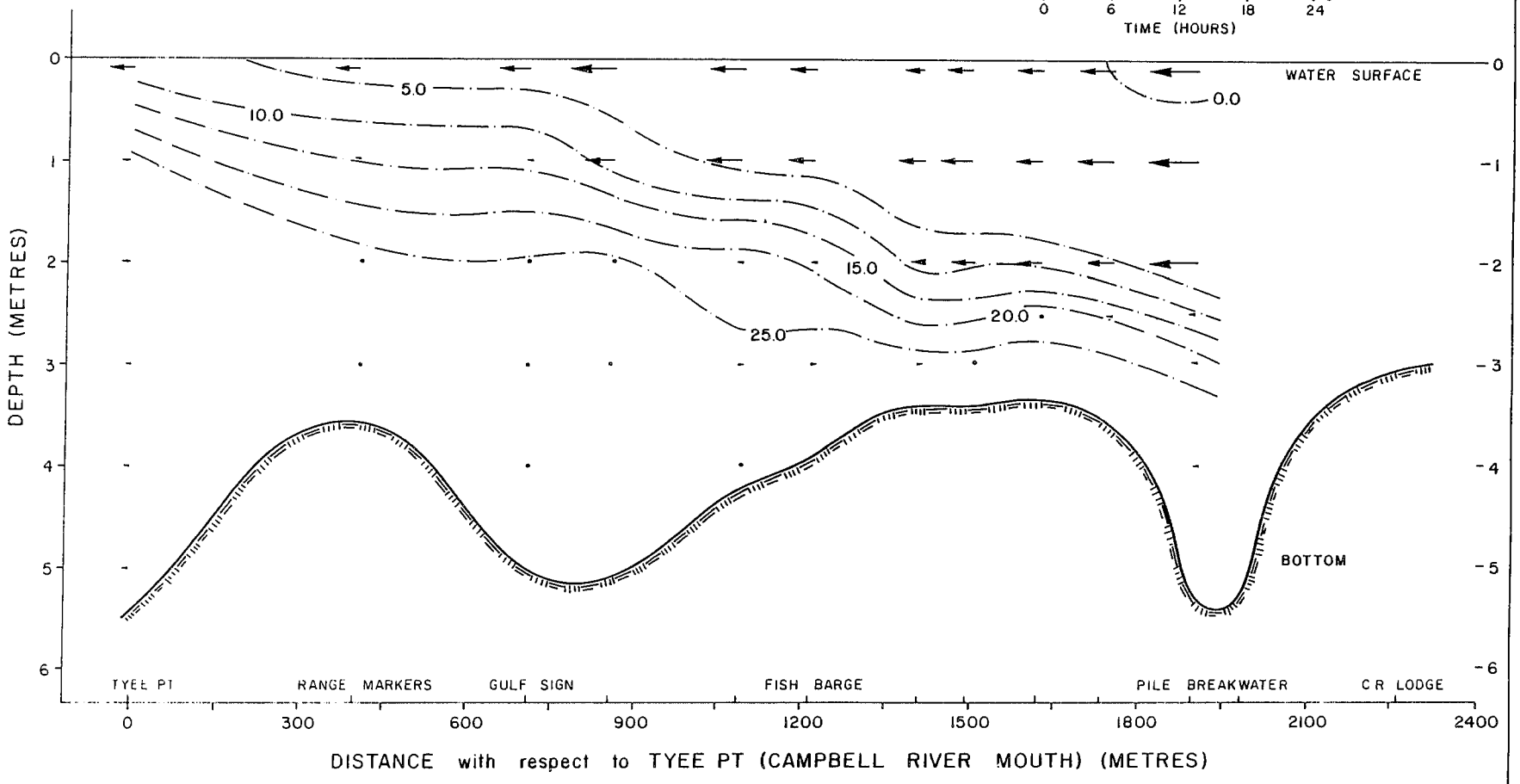

SALINITY AND CURRENT DISTRIBUTION
CAMPBELL RIVER ESTUARY

SEPTEMBER 25, 1984 : 0721 - 0752 hrs

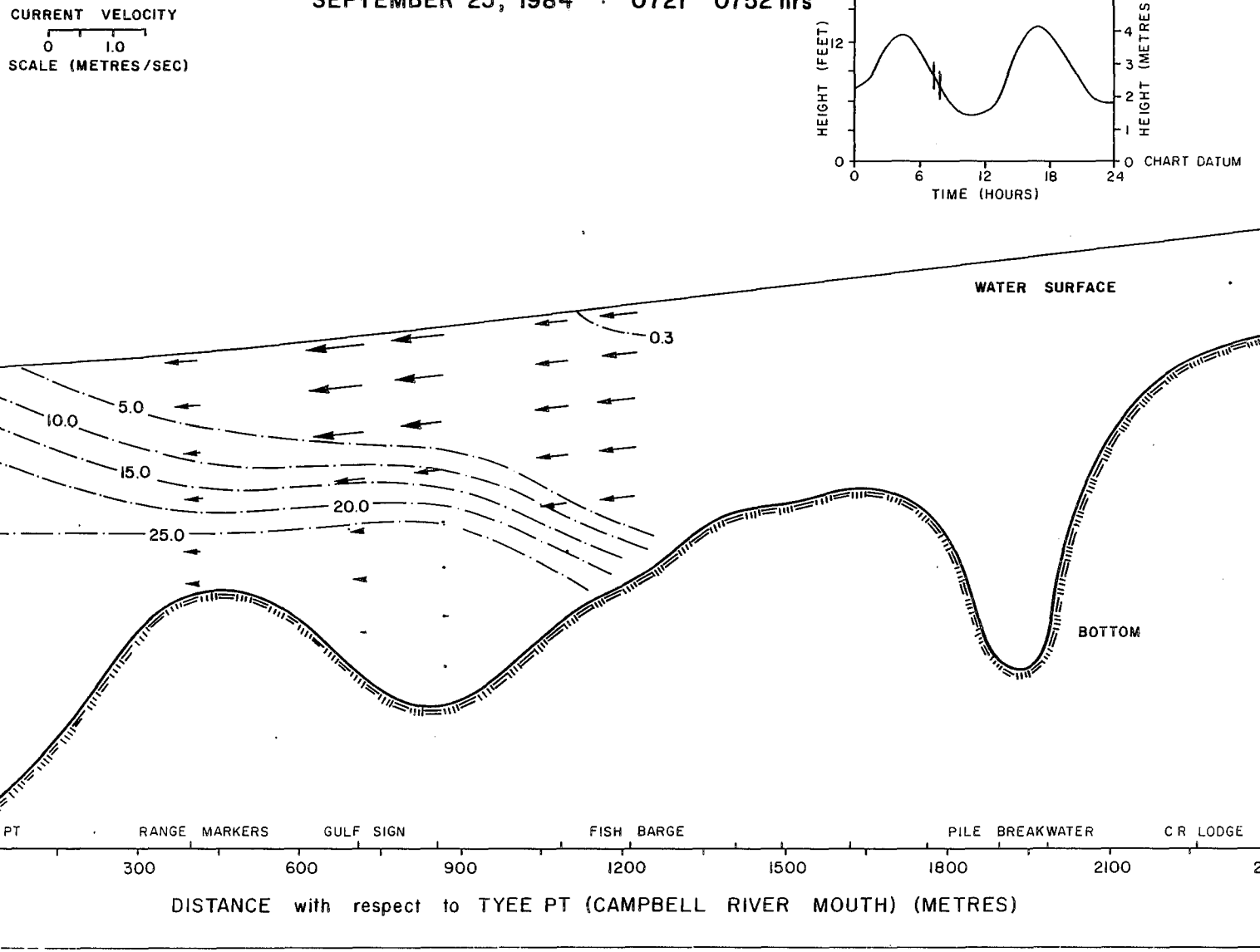

SALINITY AND CURRENT DISTRIBUTION
CAMPBELL RIVER ESTUARY

SEPTEMBER 25, 1984 : 1001 - 1024 hrs

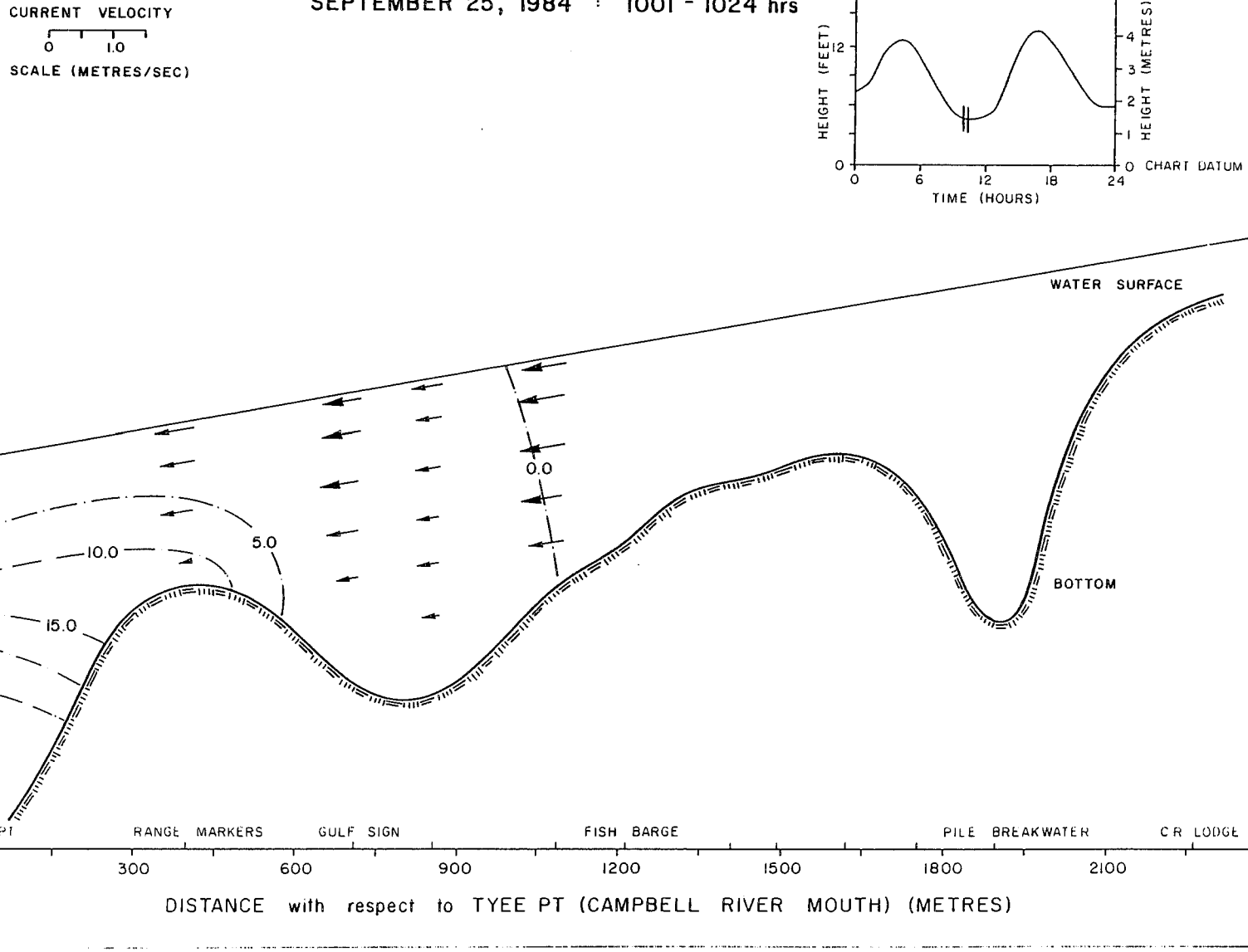

SALINITY AND CURRENT DISTRIBUTION
CAMPBELL RIVER ESTUARY

JANUARY 09, 1985 : 0831 - 0920 hrs

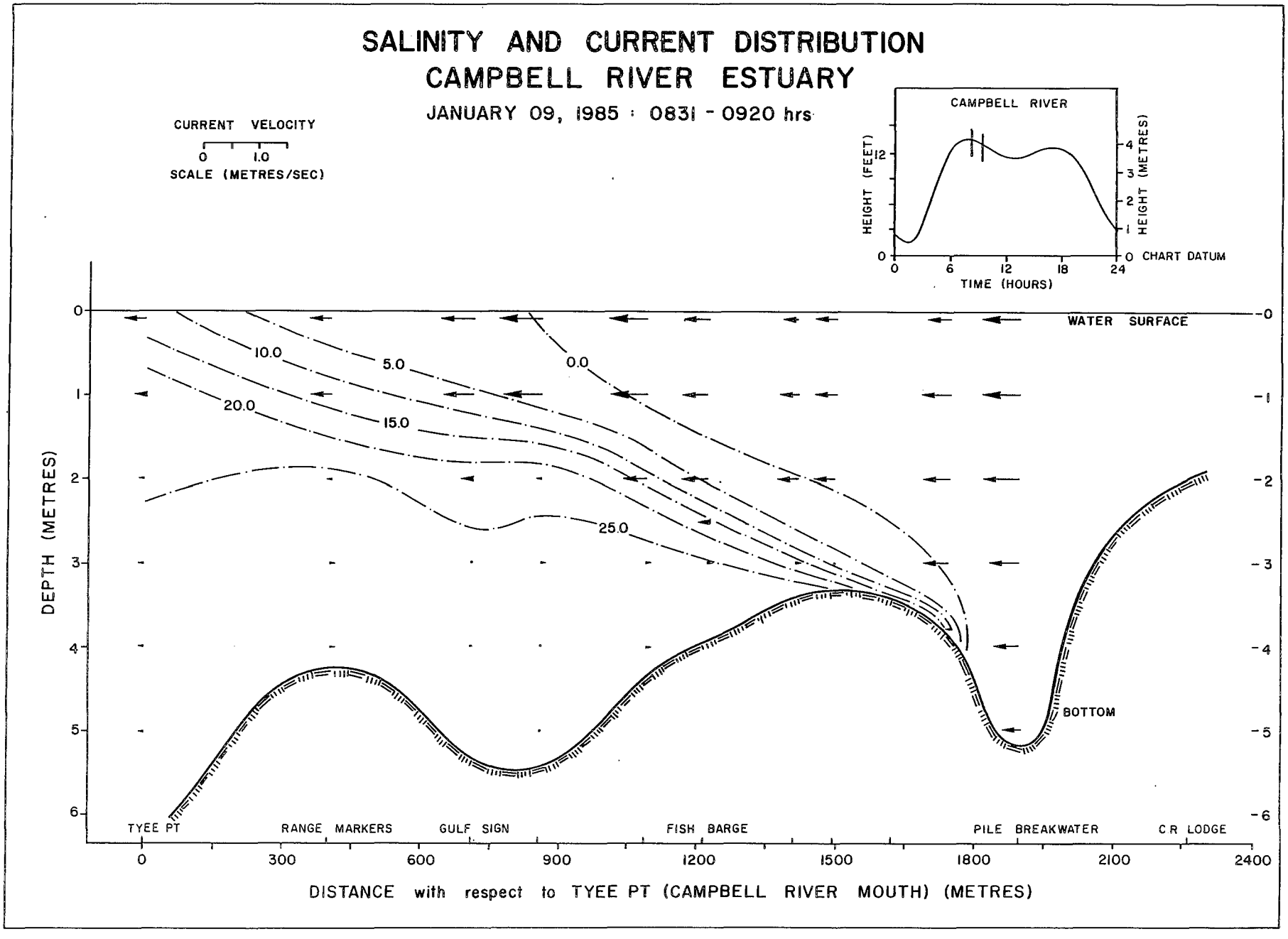

SALINITY AND CURRENT DISTRIBUTION
CAMPBELL RIVER ESTUARY

JANUARY 09, 1985 : 0940 - 1021 hrs

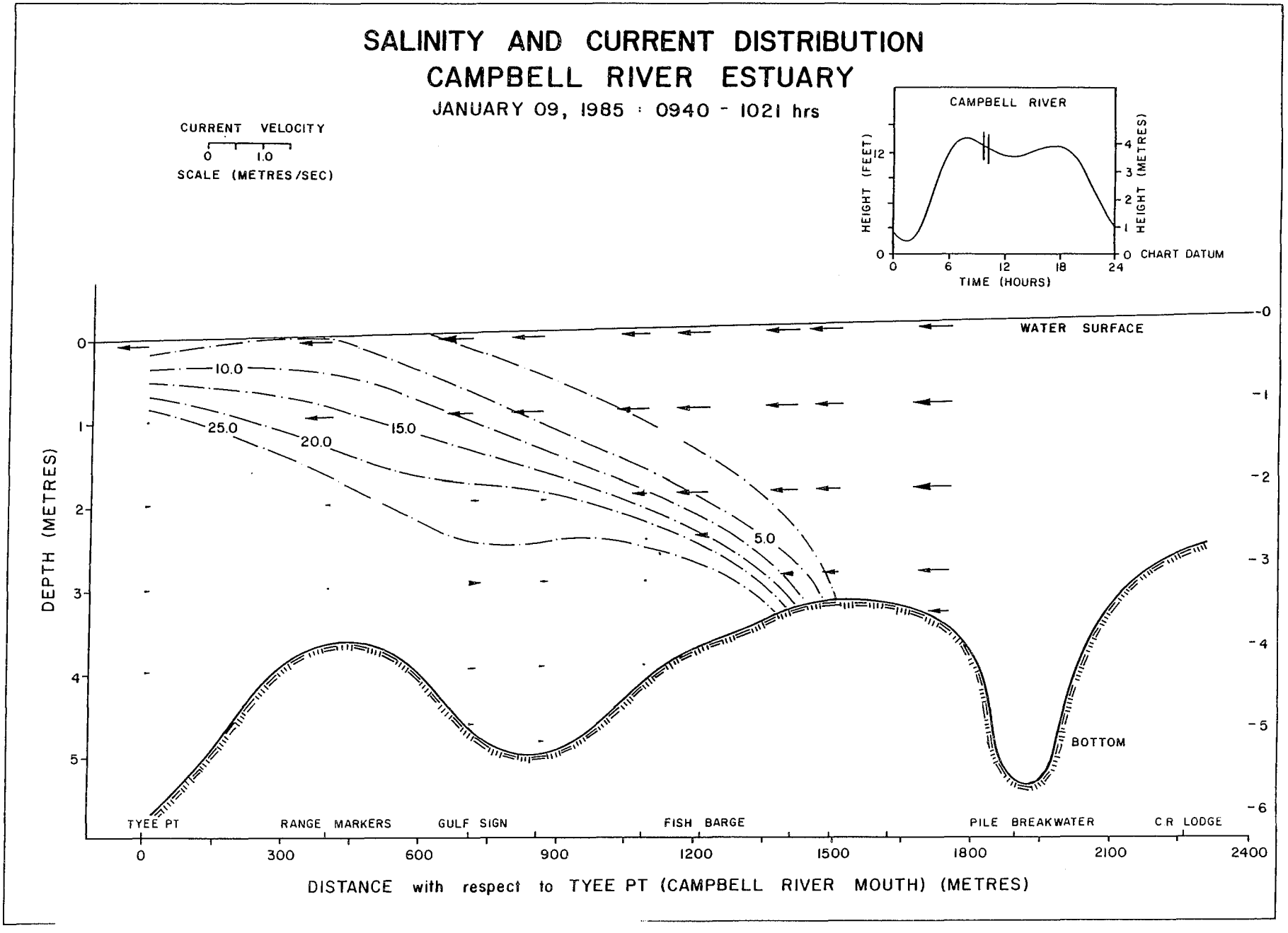

SALINITY AND CURRENT DISTRIBUTION
CAMPBELL RIVER ESTUARY

MAY 14, 1985 : 0746 - 0812 hrs

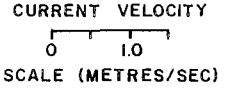

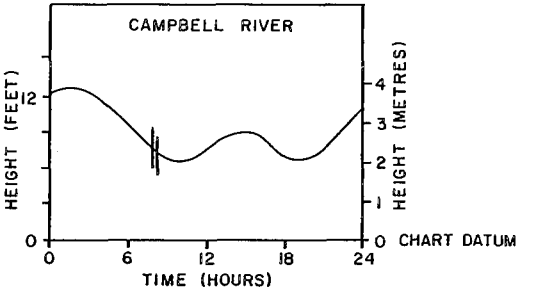

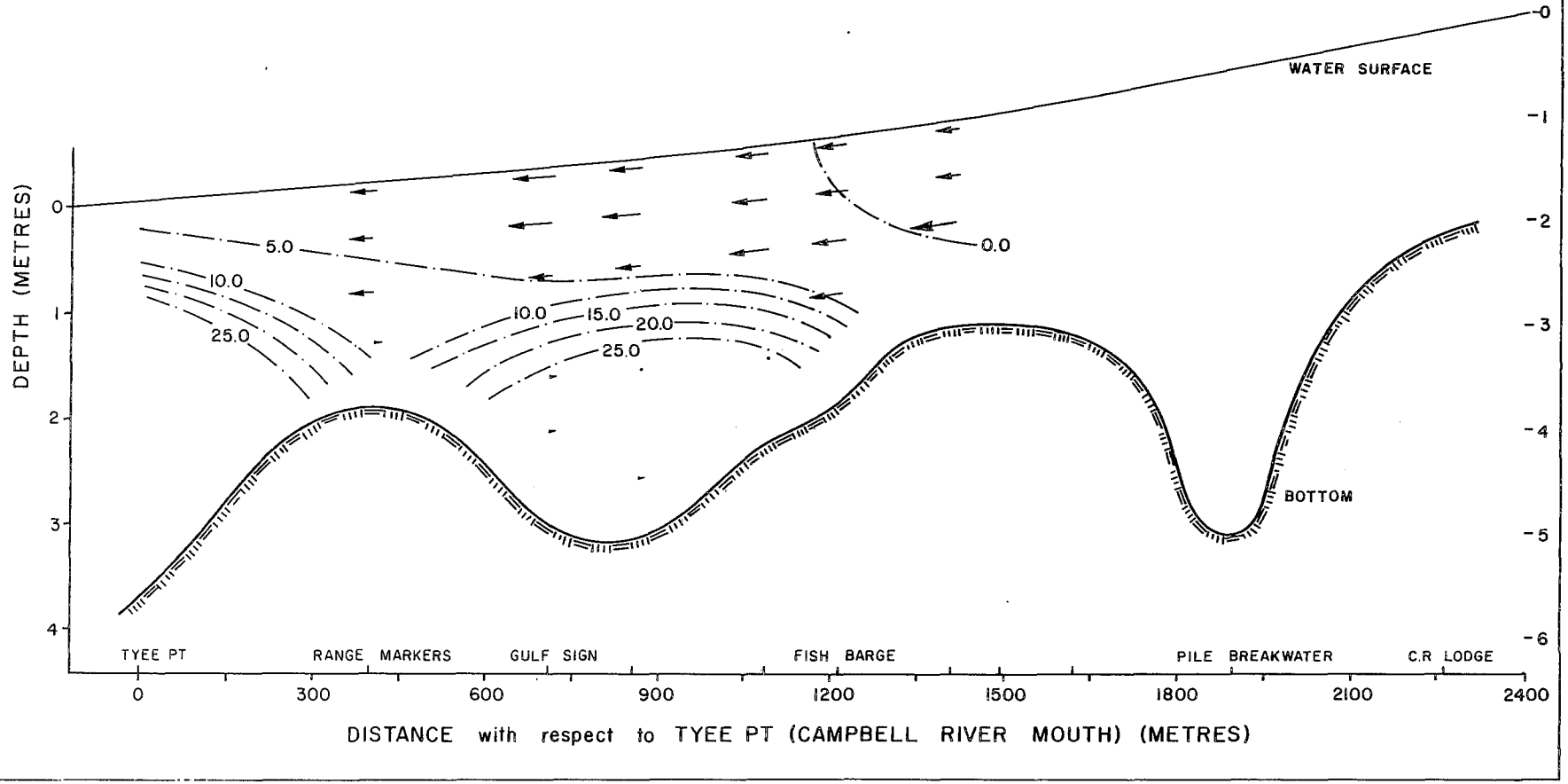

SALINITY AND CURRENT DISTRIBUTION
CAMPBELL RIVER ESTUARY

MAY 14, 1985 : 0905 - 0925 hrs

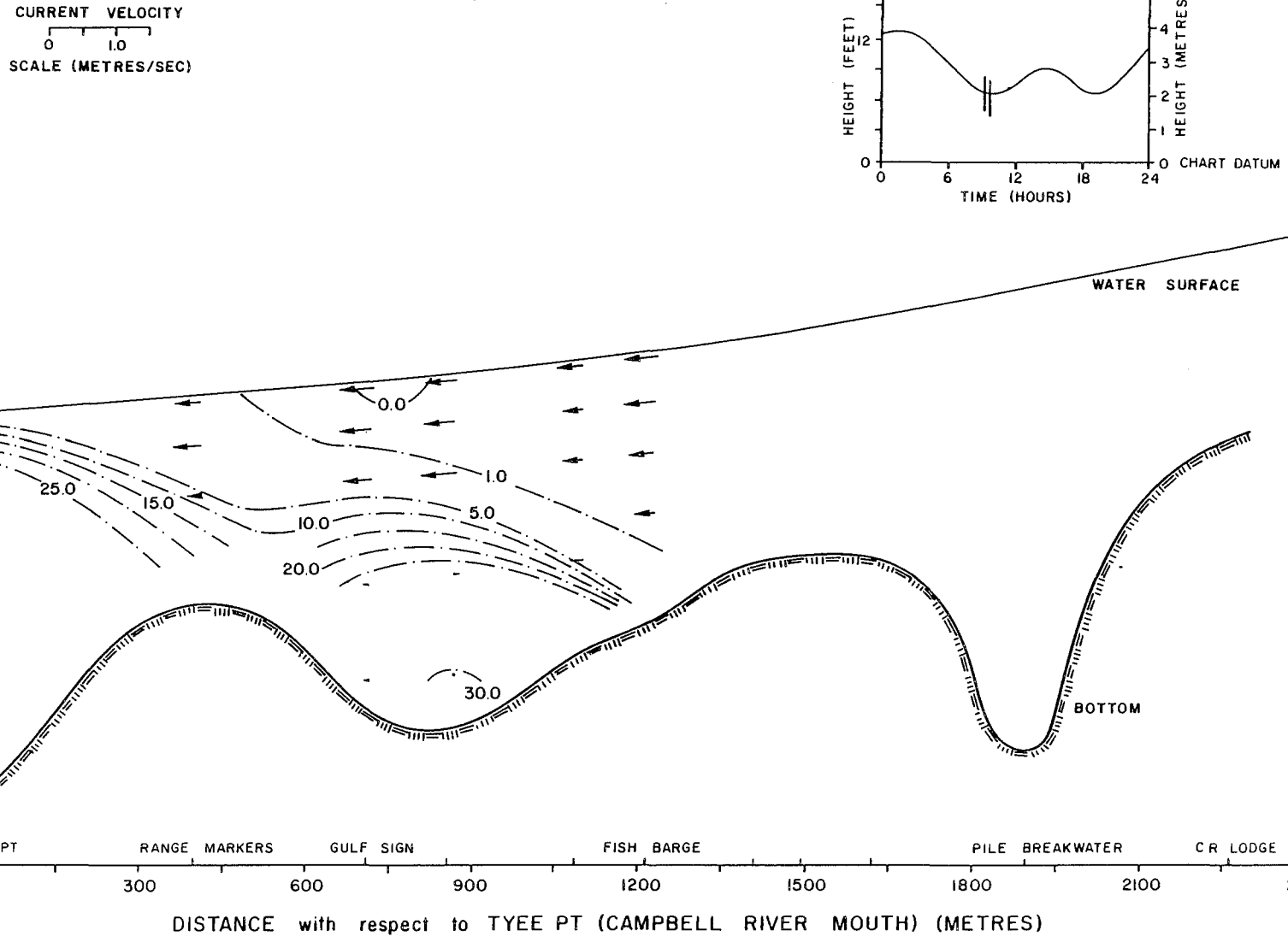

SALINITY AND CURRENT DISTRIBUTION
CAMPBELL RIVER ESTUARY
MAY 14, 1985 : 1033 - 1054 hrs

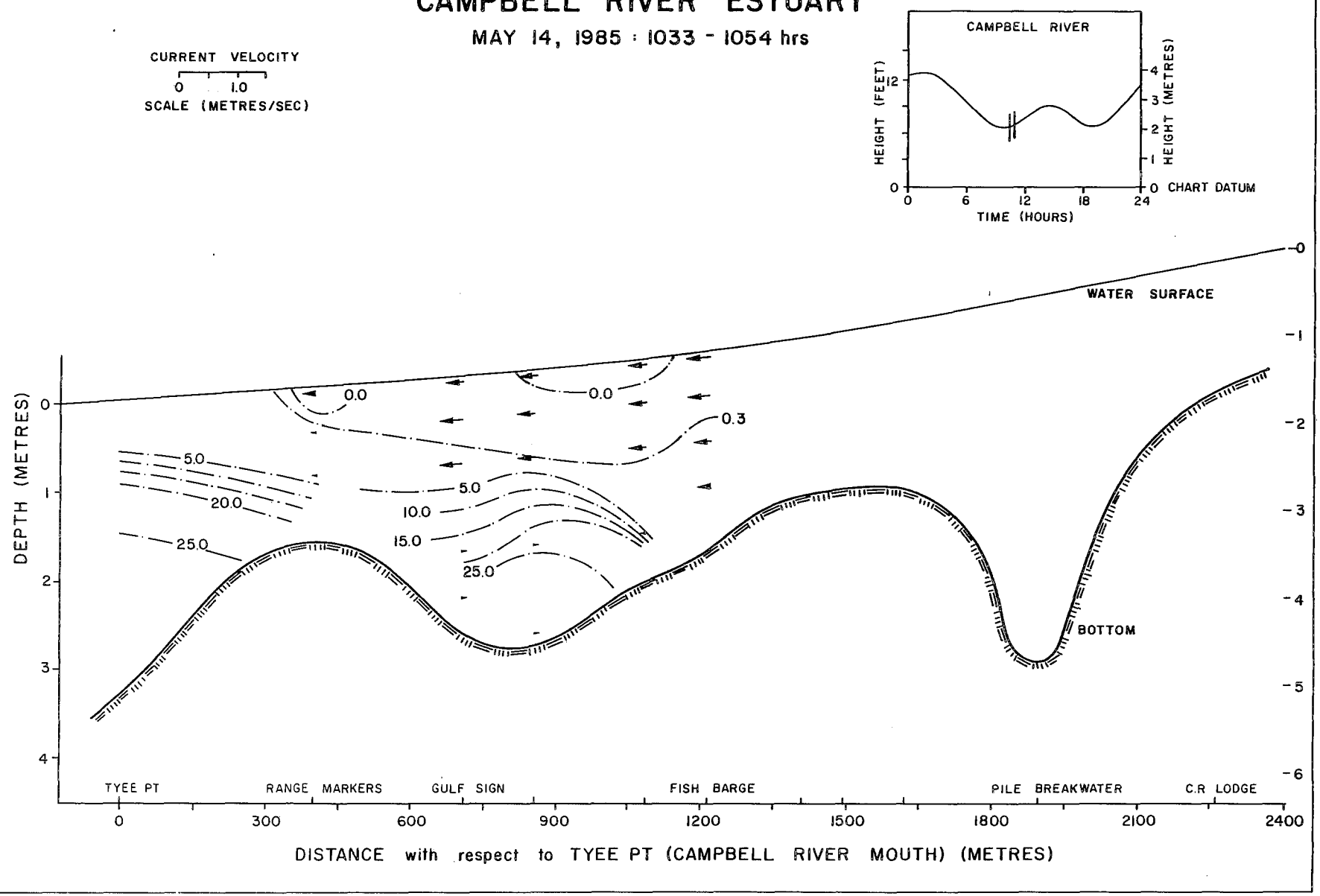

SALINITY AND CURRENT DISTRIBUTION
CAMPBELL RIVER ESTUARY

MAY 14, 1985 : 1250 - 1322 hrs

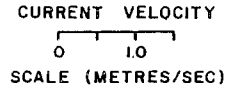

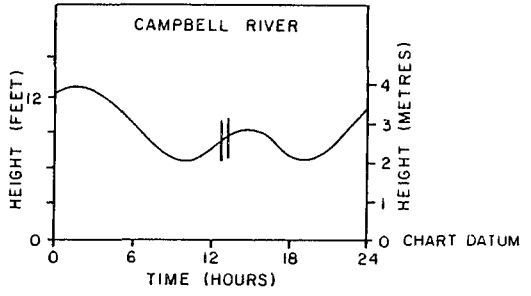

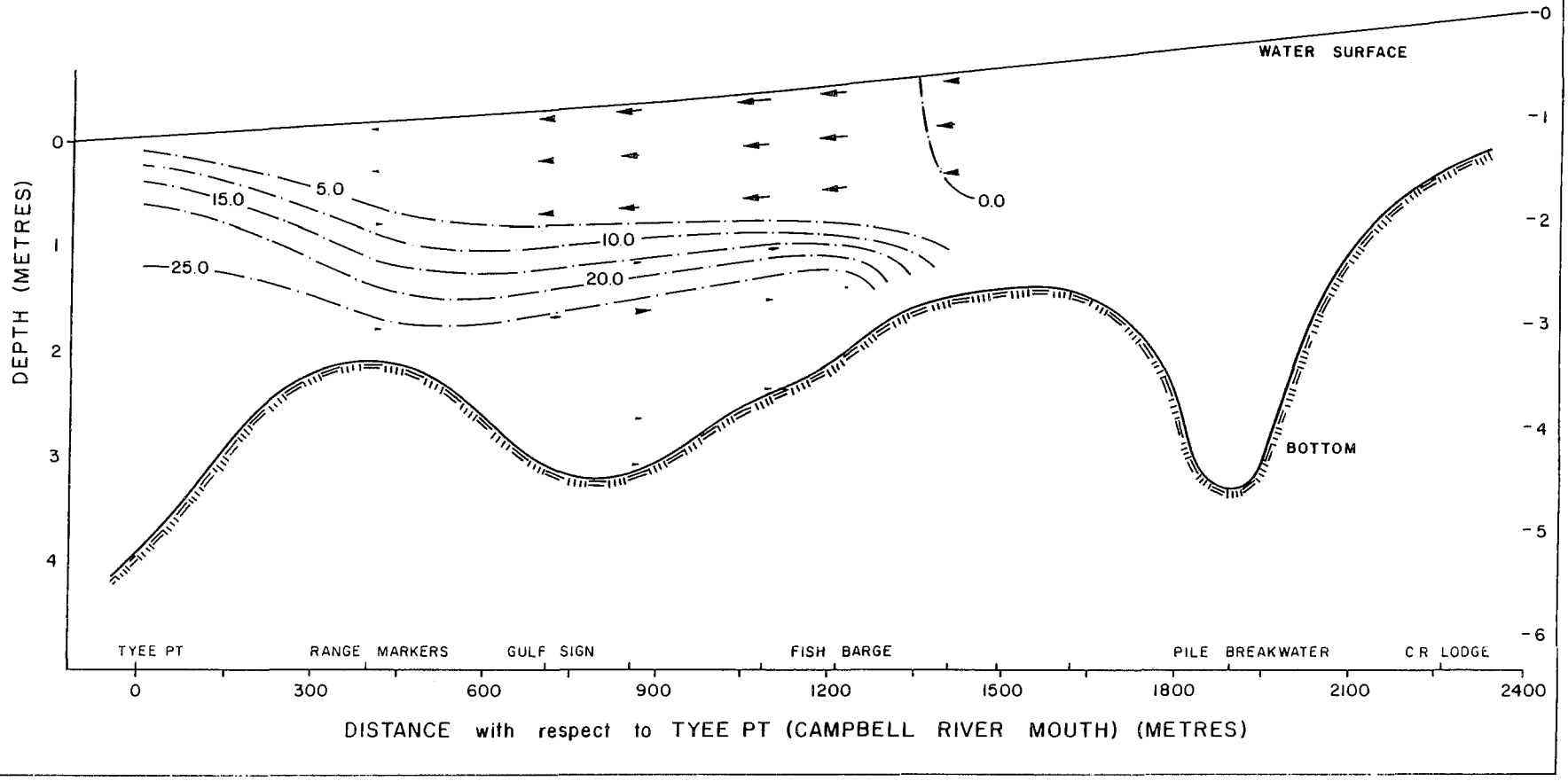

SALINITY AND CURRENT DISTRIBUTION
CAMPBELL RIVER ESTUARY

MAY 14, 1985 : 1340 - 1418 hrs

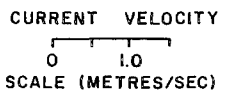

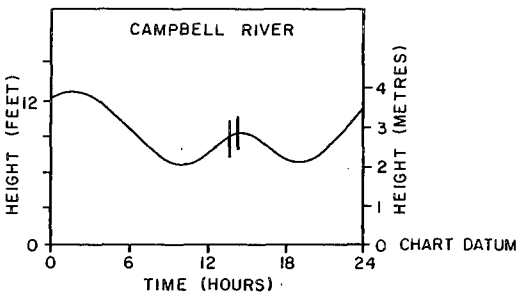

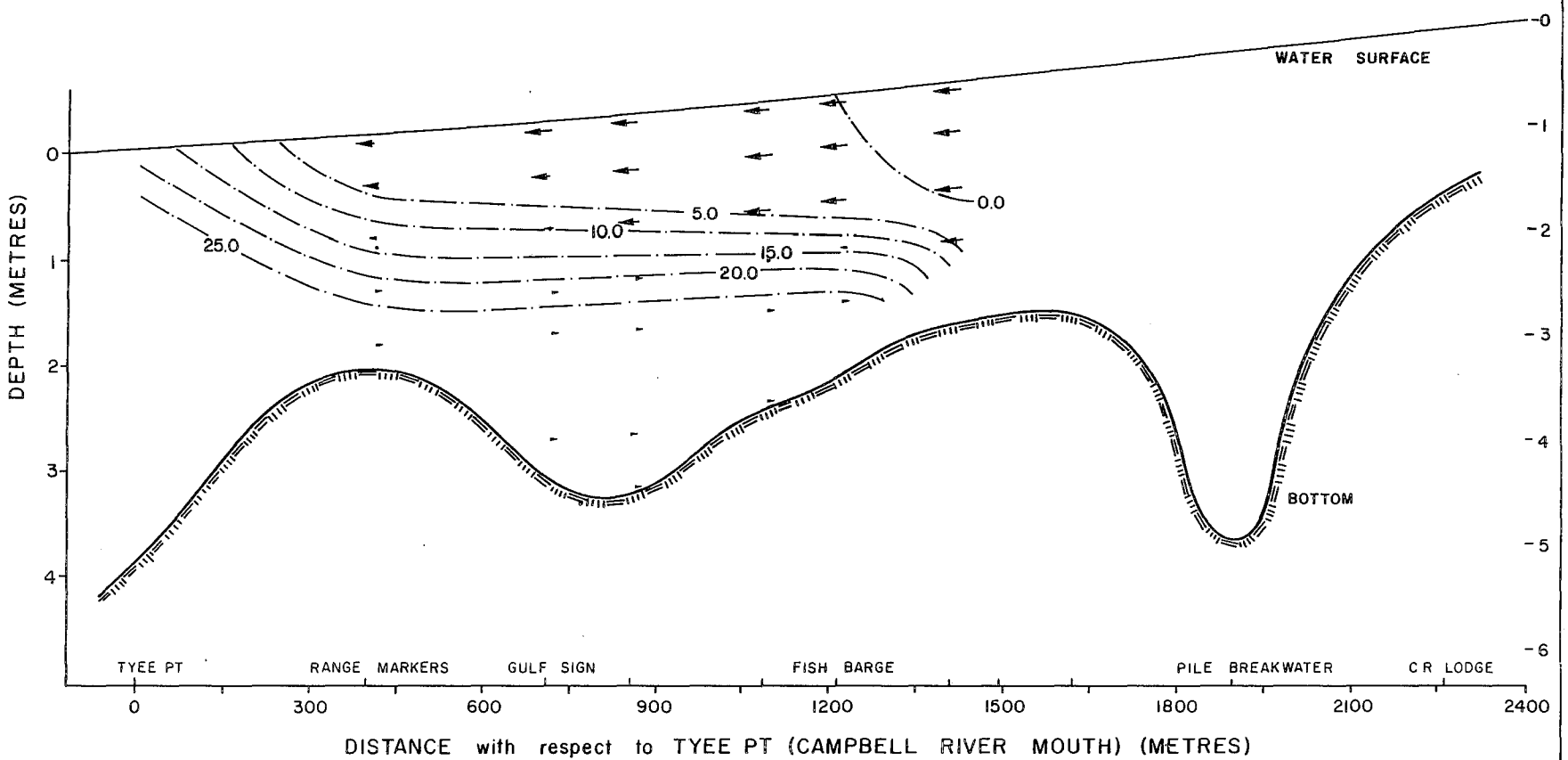

SALINITY AND CURRENT DISTRIBUTION
CAMPBELL RIVER ESTUARY

MAY 14, 1985 : 1427 - 1512 hrs

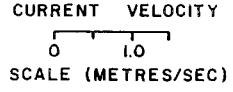

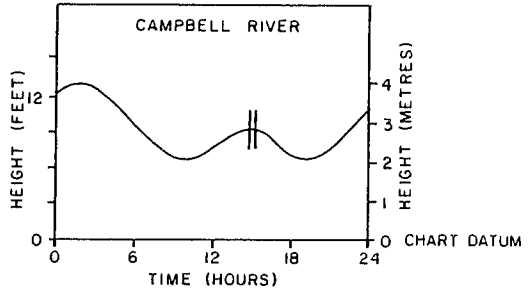

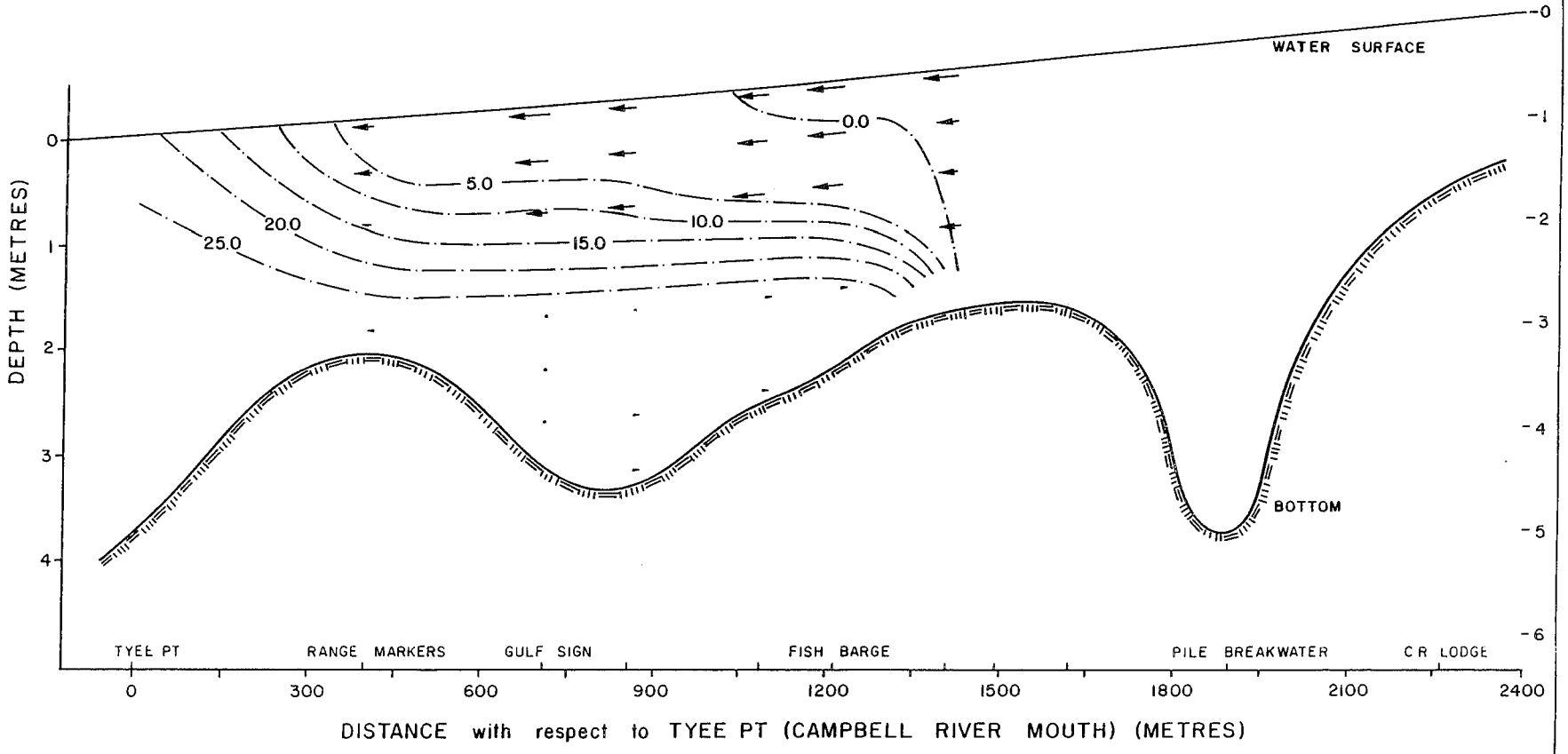

SALINITY AND CURRENT DISTRIBUTION
CAMPBELL RIVER ESTUARY
MAY 14, 1985 : 1557 - 1620 hrs

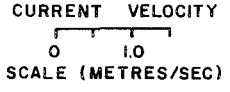

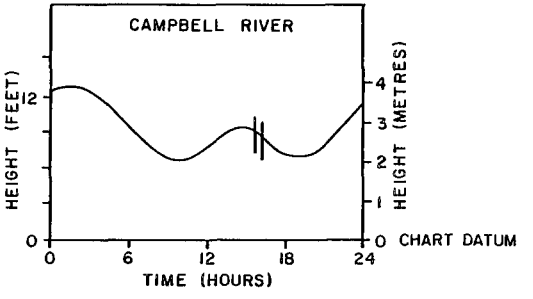

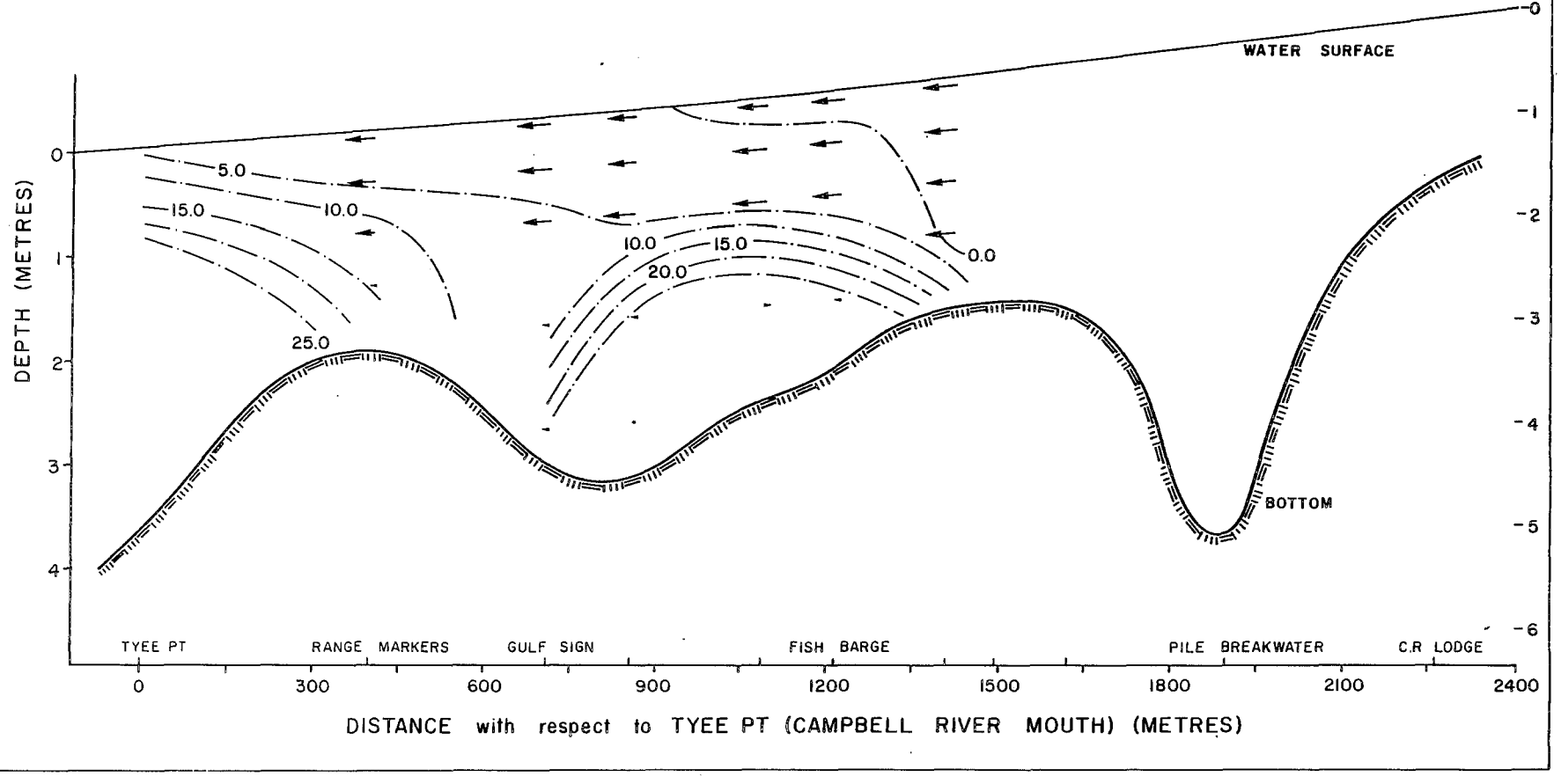

APPENDIX B

CAMPBELL RIVER MODEL
COMPUTED EXTREME LEVELS
July 8, 1982 Discharge at Hart Dam= 113 m^3/s
MAIN CHANNEL

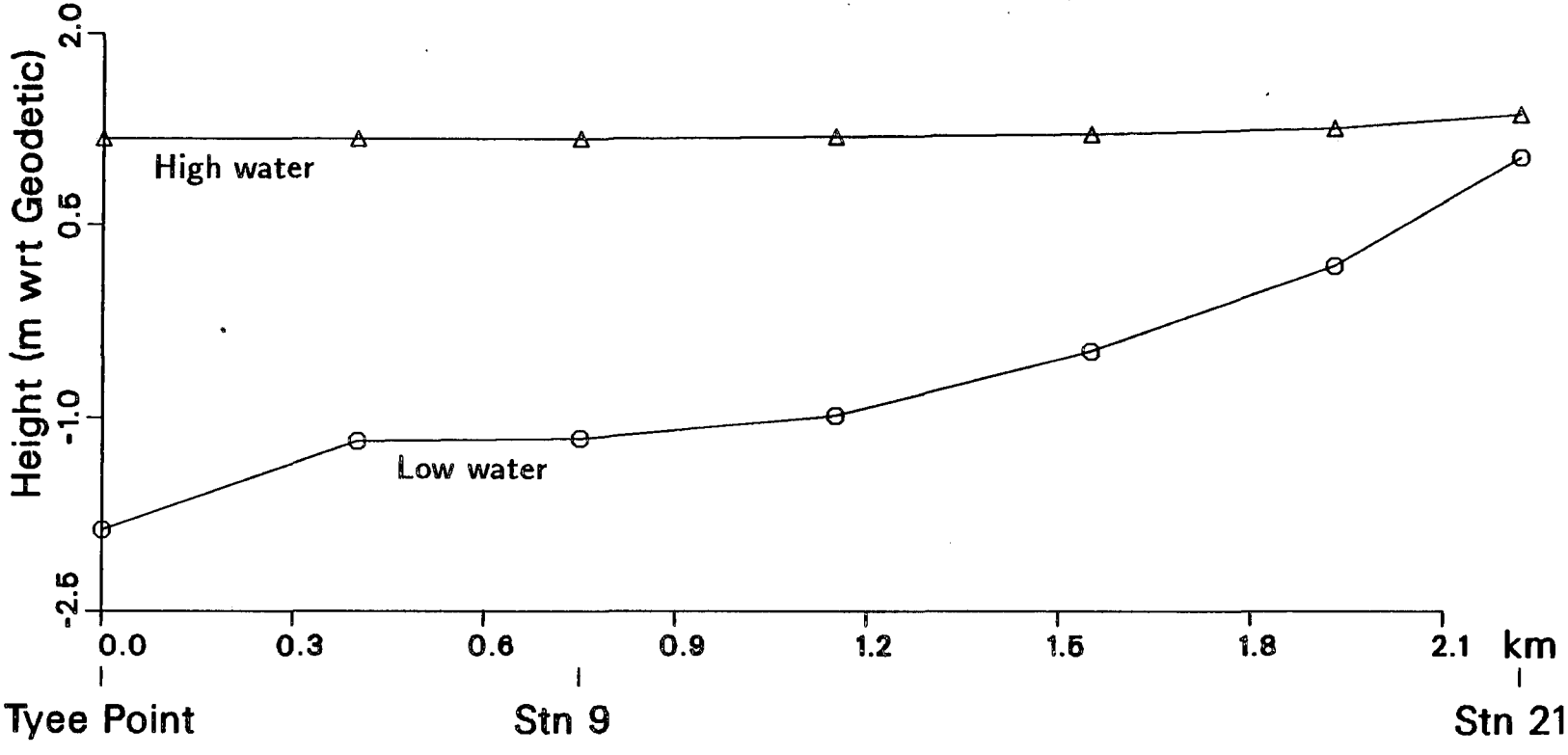

CAMPBELL RIVER MODEL
COMPUTED EXTREME LEVELS
July 8, 1982 Discharge at Hart Dam= 113 m^3/s

BAIKIE SLOUGH

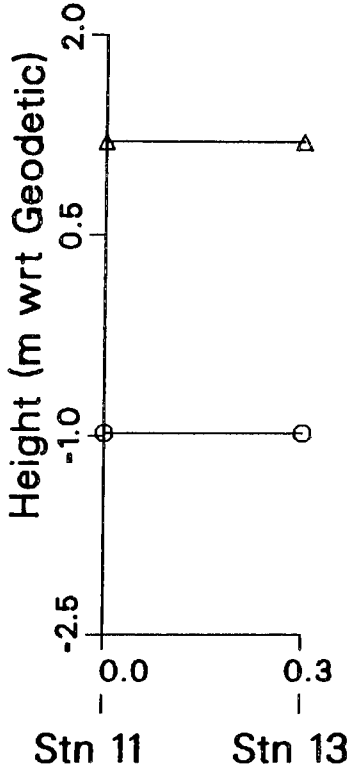

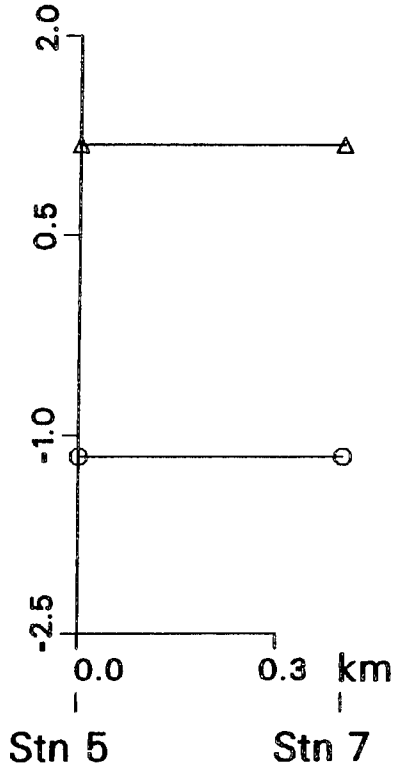

TYEE CHANNEL

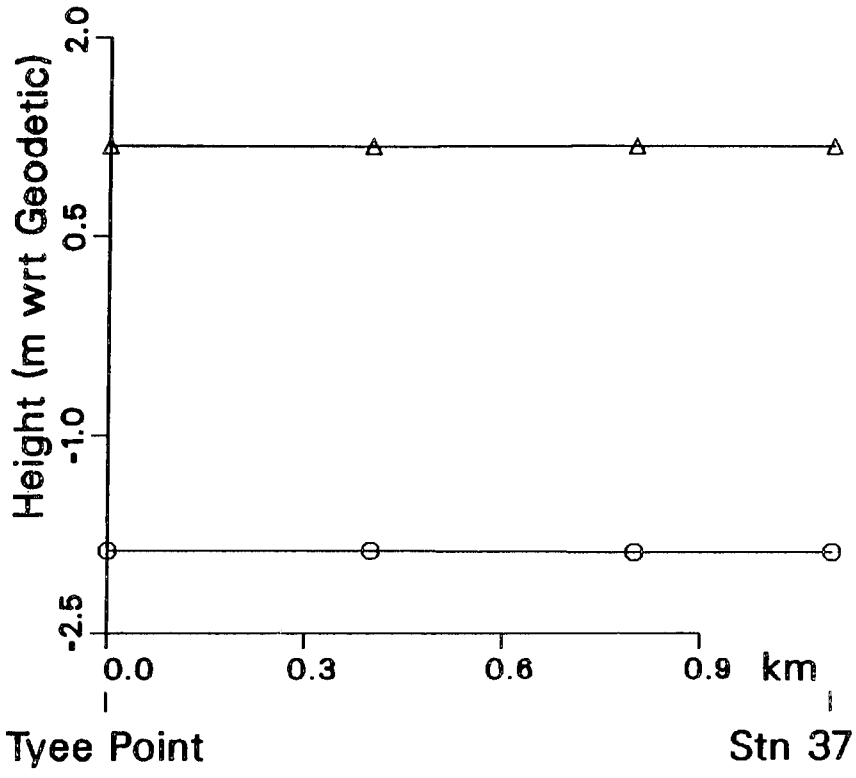

CAMPBELL RIVER MODEL
COMPUTED EXTREME LEVELS
Sept 10, 1984 Discharge at Hart Dam= 90 m^3/s
MAIN CHANNEL

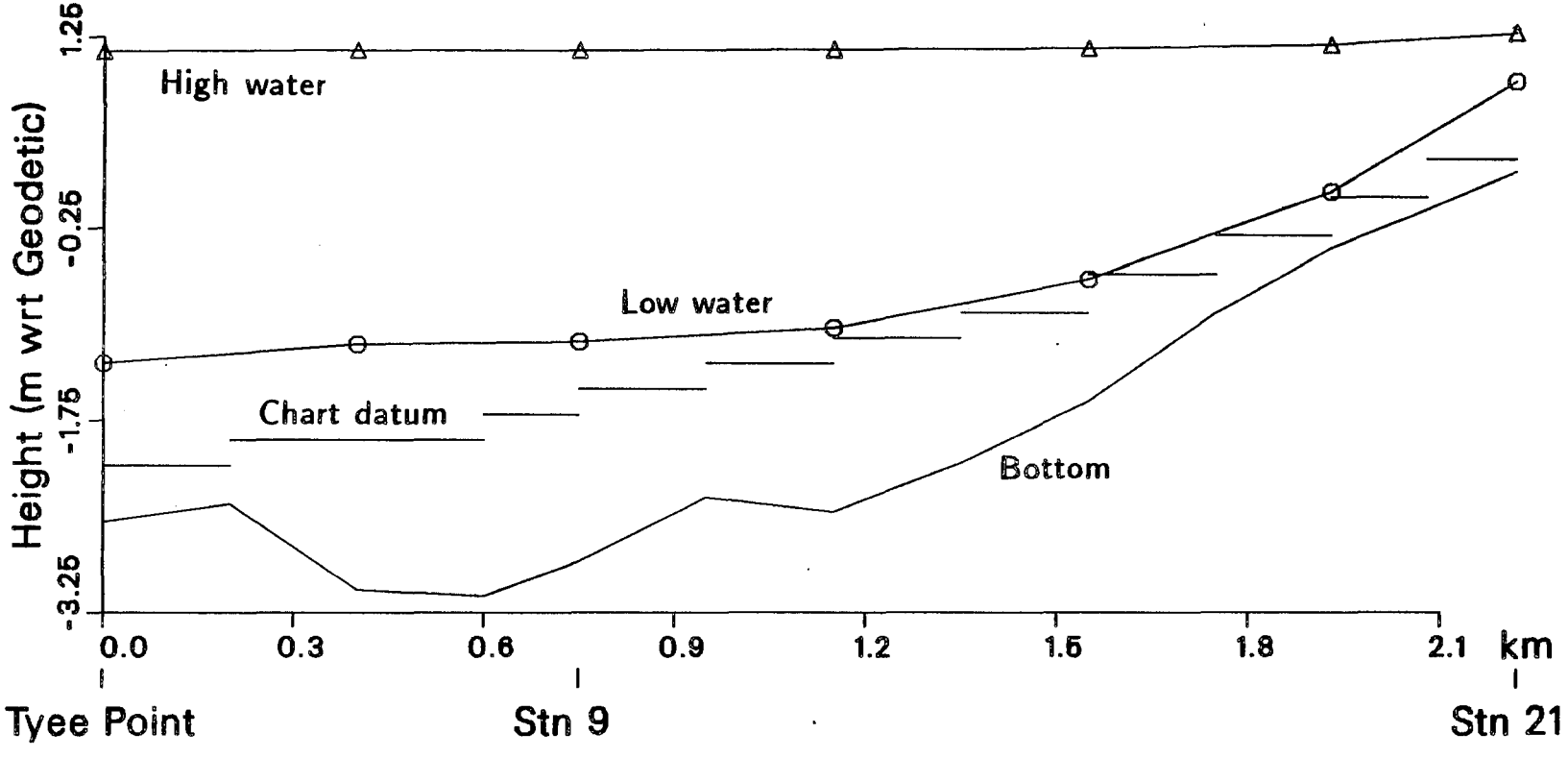

CAMPBELL RIVER MODEL
COMPUTED EXTREME LEVELS
Sept 10, 1984 Discharge at Hart Dam= 90 m^3/s

BAIKIE SLOUGH

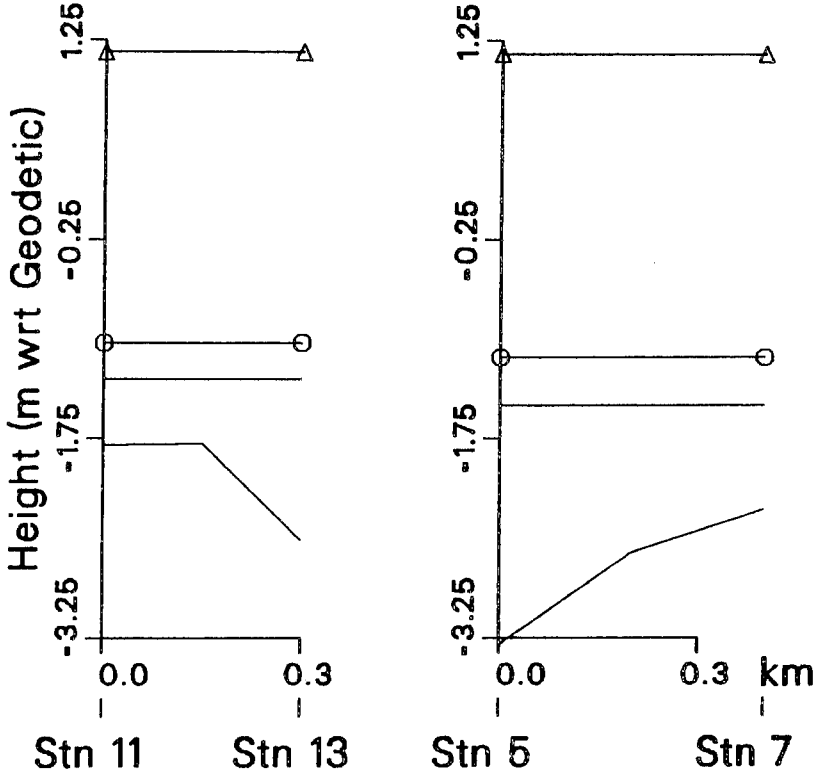

TYEE CHANNEL

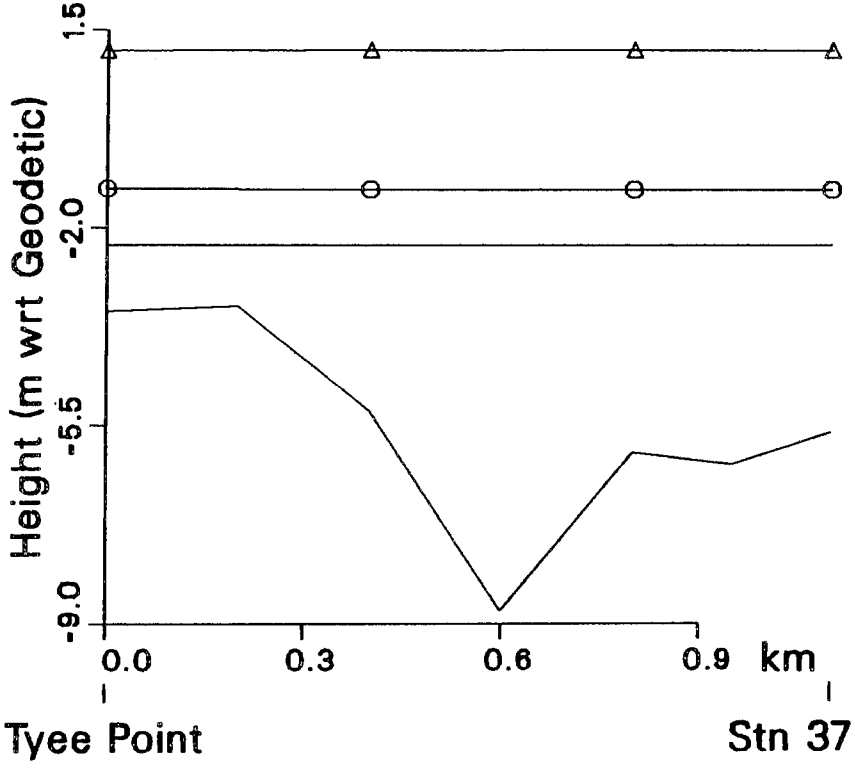

CAMPBELL RIVER MODEL
COMPUTED EXTREME LEVELS
June 12, 1986 Discharge at Hart Dam= 142 m^3/s
MAIN CHANNEL

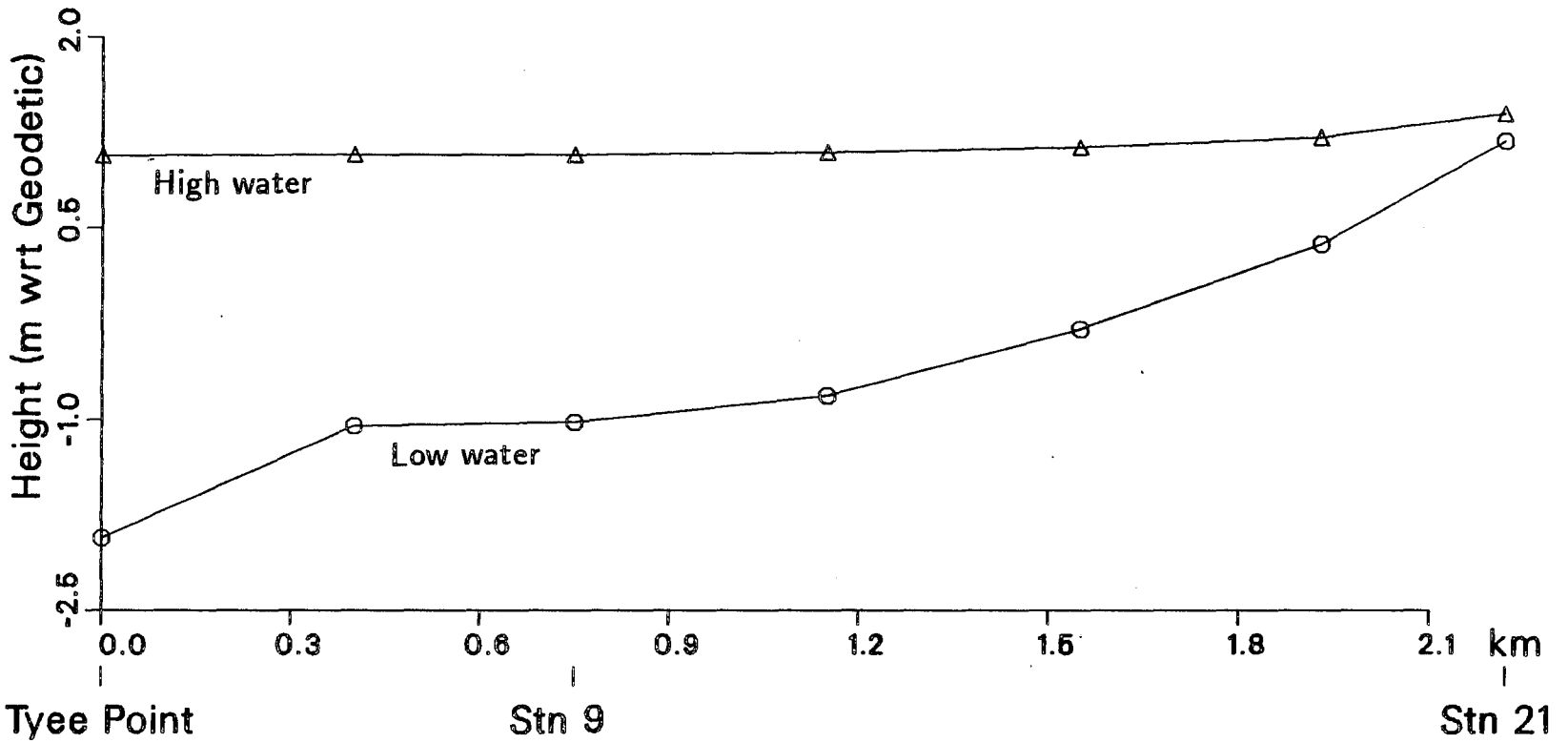

CAMPBELL RIVER MODEL
COMPUTED EXTREME LEVELS
June 12, 1986 Discharge at Hart Dam= 142 m^3/s

BAIKIE SLOUGH

TYEE CHANNEL

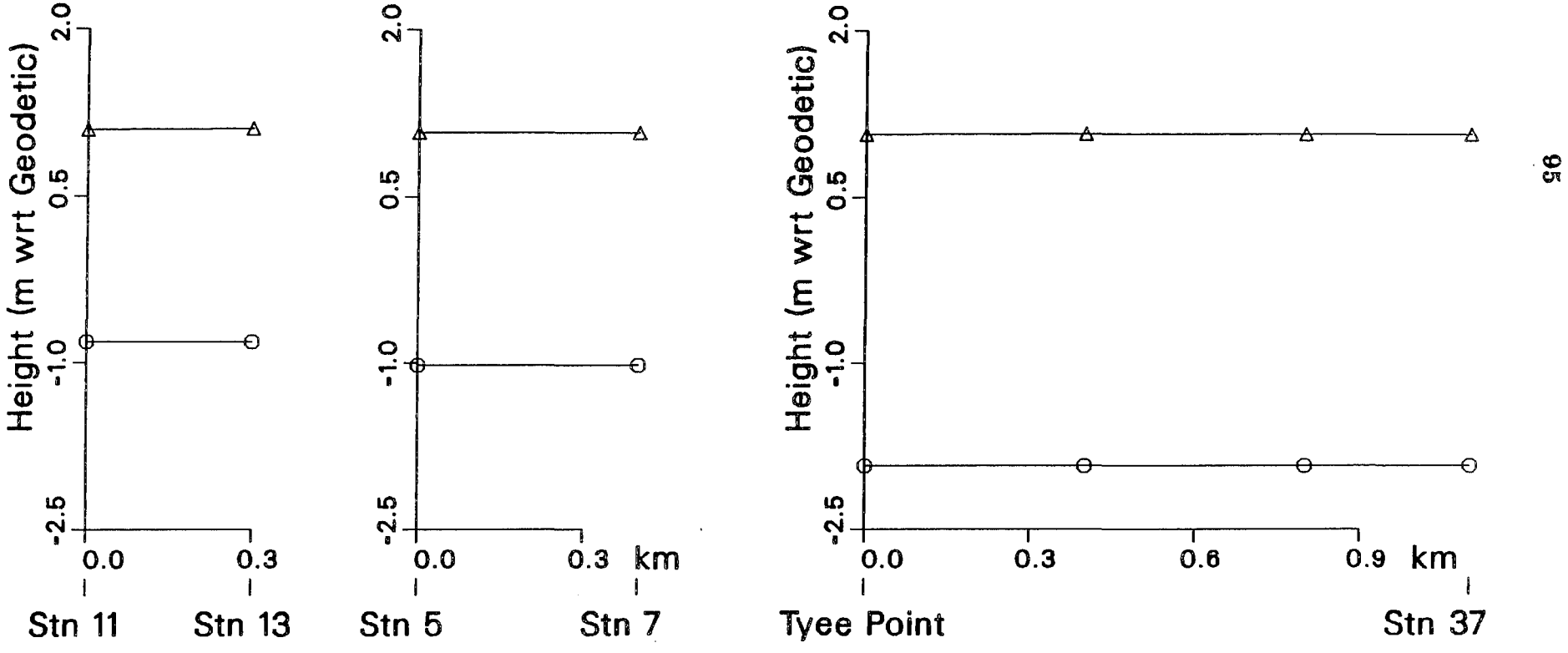

CAMPBELL RIVER MODEL
COMPUTED EXTREME LEVELS
Aug. 13, 1986 Discharge at Hart Dam= 58 m^3/s
MAIN CHANNEL

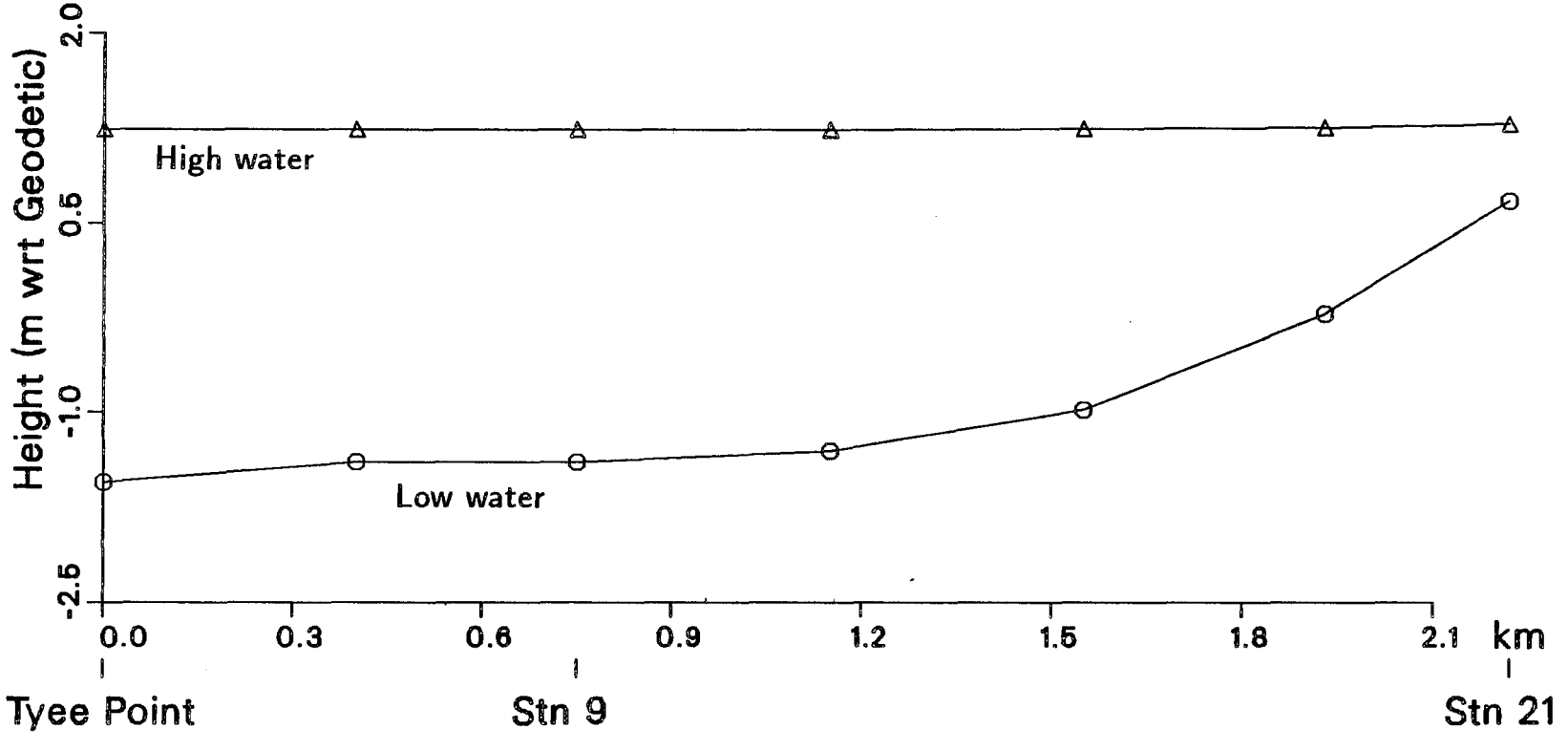

CAMPBELL RIVER MODEL
COMPUTED EXTREME LEVELS
Aug. 13, 1986 Discharge at Hart Dam= 58 m^3/s

BAIKIE SLOUGH

TYEE CHANNEL